Technical University of Crete
School of Production Engineering and Management
Turbomachines & Fluid Dynamics Laboratory (TurboLab – TUC)

Flow field simulation inside the centrifugal compressor of a small turbojet

By

Kastrisios Konstantinos

A dissertation submitted in partial fulfilment of the requirements for the degree of

Master of Science

Supervisor
Prof. Ioannis K. Nikolos

Chania, October 2021

Technical University of Crete

School of Production Engineering and Management

Turbomachines & Fluid Dynamics Laboratory (TurboLab – TUC)

Flow field simulation inside the centrifugal compressor of a small turbojet

By

Kastrisios Konstantinos

Approved by:

Dr. Ioannis K. Nikolos
Professor
Technical University of Crete,
School of Production Engineering
& Management

Dr. Anargiros Delis
Associate Professor
Technical University of Crete,
School of Production Engineering
& Management

Dr. Georgios Arabatzis
Assistant Professor
Technical University of Crete,
School of Production Engineering
& Management

Chania, October 2021

"Intentionally Left Blank"

Acknowledgements

I would like to express my deep gratitude to my supervisor, Professor I.K. Nikolos for his patient guidance, enthusiastic encouragement and useful critiques on this research work. Also, I would like to offer my special thanks to my colleague and friend Zografos P. who gave me the inspiration of this project, through his master thesis, helping with the measurements of the components. My grateful thanks are also extended to PhD Student Leloudas S. for his guidance and advice during the mesh analysis in ANSA. Also, I have to express my thanks to former student of our School Bilalis G., for the measurement of the impeller's geometry. Finally, I would like to thank the love of my life, my wife Dimitra, for her continuous support and encouragement throughout my study and dedicate this thesis to my new born son Chris, who gave me even more motivation to accomplish this goal.

Kastrisios Konstantinos

“Intentionally Left Blank

Abstract

The goal of the present thesis is to simulate the flow field inside a centrifugal compressor of a small turbojet engine for propulsion of high-performance small UAVs. Firstly, geometry measurements and 3D geometry definition of the AMT Olympus compressor components will be accomplished with the use of SOLIDWORKS (CAD Software). The compressor's model consists of the inlet duct, the duct casing, the impeller and the diffuser blades. The diffuser vanes are integrated in the casing. After creating the assembly, meshing will be accomplished with use of ANSA mesh generation software. The flow domain inside the impeller will be considered as rotating, with the rest being stationary. Finally, using an ANSYS CFX steady state analysis simulation, iso-contours are generated to depict the distribution of basic thermodynamic quantities through the compressor, such as pressure and temperature and results evaluation is accomplished. The simulated centrifugal compressor can then be used as a reference for a subsequent optimization of its geometry.

Table of Contents

Table of figures

Nomenclature

P	*Pressure*
T	*Temperature*
F	*Force*
A	*Cross Section Area*
D	*Diameter*
C_P	*Specific Heat Constant Pressure*
V	*Velocity*
$\dot{W}$	*Power*
Πc	*Pressure Ratio*
$\dot{Q}$	*Heat Transfer Rate*
Tsfc	*Thrust specific fuel consumption*
$\dot{m}$	*Mass Flow Rate*
φ	*Flow coefficient*
λ	*Head coefficient*
Ω	*Reaction*
Ψ	*Pressure coefficient*
σ	*Slip factor*
V	*Relative velocity*
r	*Radius*
C	*Absolute velocity*
W	*Tangential velocity*
MTE	*Micro Turbine Engine*
rpm	*Rotations Per Minute*

1. Introduction

This chapter is an overview of micro gas turbines, their use and their applications, with an emphasis at those for small aircraft propulsion. Additionally, technology background is provided, with basic analysis of the operational principles of micro engines, their advantages and an introduction to basic components and specifications that constitute a modern micro turbine. Finally, a short analysis of the operation of a centrifugal compressor (that the majority of micro jet engines use) is included, being the main objective of this thesis.

1.1 Micro gas turbine engines

The development of small engines or generally known as micro gas turbines, began from people who were interested in aviation model making. The first person involved in remote control research, who created the first drone, was Nikola Tesla. Since then, modeling has gone through many stages to the present day. In the first decades until the 1960s modelers had to solve the main problem of remote control of their models. For a long time, only a few people dealt with the issue of the engines of their models, despite the fact that turbine engines were well established as propulsion systems for large flying vehicles. In fact, most people believed that it was not possible to build a turbine in a "model" size. Additionally, it was also the fact that the market of modelers was not able to meet the economic requirements of such research, but also of the subsequent production.

Nowadays, these engines are treated equally to the larger aviation constructions. The dynamic development of these engines is caused not only by the interest of aviation modelers, but also by the utilization of micro turbojet engines in military applications for propulsion of Unmanned Aerial Vehicles (UAVs) or Unmanned Aerial Systems (UAS). The microturbines are miniatures of larger gas turbines engines (turbojet, turboprop, turbofan, or turboshaft). There is no specification for the definition of a micro jet engine, although generally engines that produce less than 1kN thrust and weigh less than 90kg (200lbs) are considered small, with various characteristics suitable for their mission [*Garett et al., 2019*]. Surely, they cannot compete with larger engines at thrust, but that doesn't make them less complex or impressive. Such engines have great energy capacity, compared to their total weight and this makes them ideal for use in small propulsion vehicles, like UAVs, model airplanes, and missiles.

Maximum Thrust of Various Engine Class

Engine class	Micro	Mini	Small	Medium	Large
Max Thrust (lb)	<10	10 to <100	100 to <1000	1000 to <10000	10000<
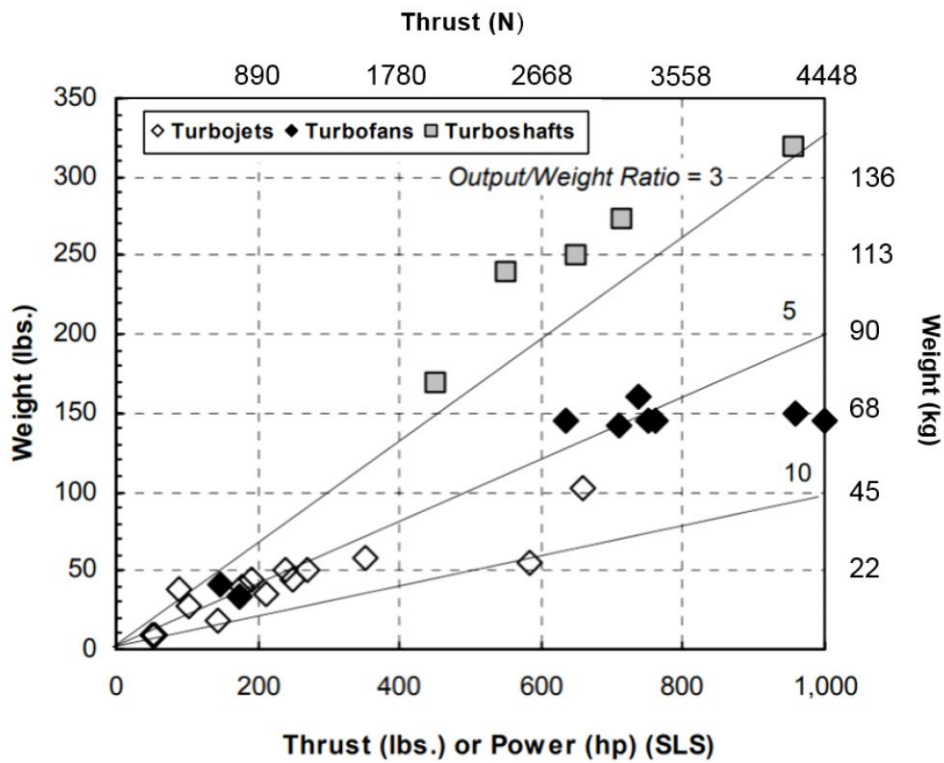
Figure 1: Existing gas turbine engines under 1000 lbs of thrust [J. Large & A. Pesyridis, 2019].

The idea of micro turbine engines application for the propulsion of small and medium sized professional military UAVs is at present highly developed. Today, lots of different UAVs are operating all over the world for all kinds of mission types, with small jet engines. Used mainly for military purposes, also increasingly in civil applications such as firefighting, reconnaissance, target acquisition and surveillance, UAVs or drones are controlled either by computers or by remote control [*Ivanov et al., 2016*].

Figure 2: X-56 by Lockheed Martin.

As on-going operational requirements expand, there is a need for smaller UAVs with increased mission profile capabilities in terms of speed and endurance [*Pesyridis et al., 2019*]. Typical UAVs are X-56A (Figure 1), built by Lockheed Martin and NASA, which uses two 90-pounds thrust JetCat P-400 turbojet engines, and the latest XQ-58 Valkyrie built by Kratos (Figure 2). Another common use for micro gas turbines is for auxiliary power units (APU), supplementing aircraft engines by providing additional power for non-propulsion functions when required. They are also used in small electrical power generation plants, as range extenders in hybrid vehicles applications, as micro-CHP (Combined Heat & Power), as portable power generators, as marine auxiliary power units and standby power units, etc.. Although there are many interesting applications for small gas turbines this thesis focuses on aircraft propulsion applications.

The market in UAVs is dominated currently by the United States and Israel. Especially USAF, deploying a wide variety of tactical UAVs and cruise missiles, funds the Advanced Turbine Technologies for Affordable Mission (ATTAM) program from 2019. Nine companies have been awarded ATTAM phase 1 contracts, relevant to small turbine engine development. Those include Boeing, Kratos Turbine Technologies, GE Aviation, Honeywell International, Lockheed Martin Aero, Northrop Grumman, Pratt & Whitney, Rolls-Royce Liberty Works, and Williams International. The participation of these companies shows that micro engines are a very promising technological field. Funds from the USAF, combined with manufacturing technologies such as 3D printing, are enabling improved performance for small jet engines [*Garett, 2019*]. USAF future plan for air combats is to have a parent stealth aircraft like F-35 and wingman UAVs that will be controlled by the former, to accomplish tasks like scouting or

absorb enemy attack; this is one of the main reasons that USAF shows so much interest for small jet engines. Other companies manufacturing small jet engines are King Tech Turbines International, JetCat, Jet Breetle, WREN Turbines, and AMT Turbines. A detailed market research analysis is presented in Chapter 2.

Figure 3: XQ-58 Valkyrie.

The latest years, small jet engine development has been focused on fuel efficiency, reducing emissions to environment, and reducing the noise they produce. These goals are associated with the latest component designs, fuel types and flow behavior. Designers must also achieve efficiency and power goals and this is an extra challenge of doing it to a much smaller scale, which brings more problems for materials and components. As an additional challenge, the economic requirements (to keep the cost low) do not allow designs incorporating highly complex and expensive technologies. Also, in these applications there is a strong limitation in size and weight. For example, turbojet performance is directly associated with mass flow rate and exhaust gas velocity; however mass flow rate is almost predefined for a given engine inlet diameter. A small and compact design with simple components is a crucial design objective [*Fuchs, 2016*].

Figure 4: The family of King-Tech Turbines.

1.2 Technology background

The **Brayton** or **Joule** cycle was proposed by George Brayton for the reciprocating diesel engine he designed at 1870. Despite this fact, nowadays it is applicable only in thermal turbomachines. The ideal (reversible) cycle consists of four processes:

1. Isentropic compression (in a compressor)

2. Constant pressure heat addition

3. Isentropic expansion (in a turbine)

4. Constant pressure heat rejection

The most common application of the cycle is in open-cycle thermal turbomachines, being open to the atmosphere and using an internal combustion chamber for providing heat; the other application is in closed-cycle turbomachines, where heat exchangers are used for heating and cooling the gas, which recirculates inside the closed system (Figure 5). The cycle is represented in temperature – specific entropy (T-s) and pressure - specific volume (p-v) diagrams, as shown in Figure 6.
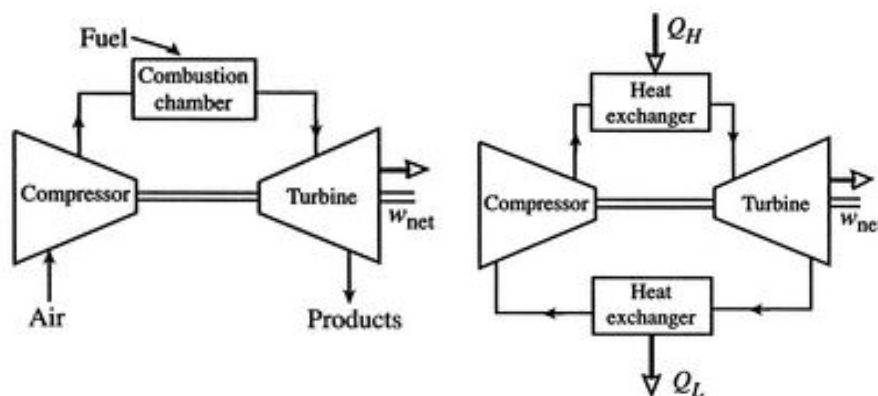
Figure 5: Open and closed cycle operation [B. Zohuri, 2017].
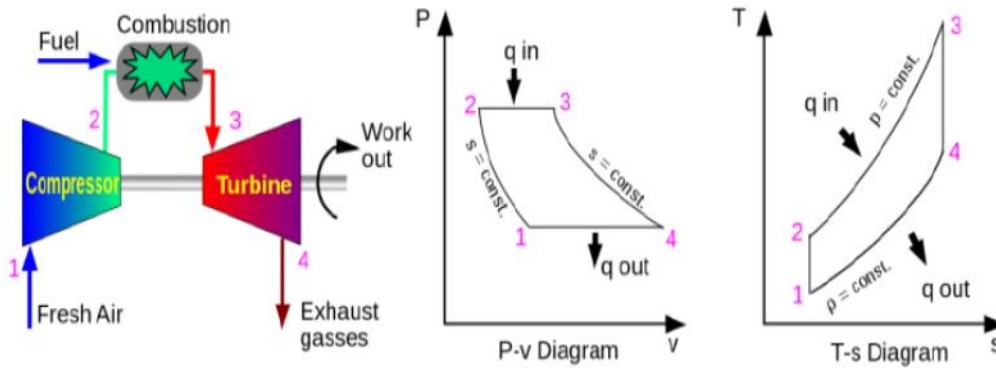
Figure 6: Ideal Brayton Cycle P-v and T-s diagrams [B. Zohuri, 2017].

A jet engine is a type of an internal combustion engine that contains five major parts: an inlet, a compressor, a combustor, a turbine and a nozzle. A basic turbojet configuration consists of an inlet duct (usually an S-duct), where air at free stream velocity is decelerated and directed into a compressor [*Hunecke, 1997*]. The air is compressed across the compressor stages, where pressure and temperature increase, and enters into the combustion chamber. Fuel is injected into the combustion chamber, combined with the high-pressure air, and the air-fuel mixture is burned. The hot and high-pressure gas from the combustion chamber is forced to flow through the turbine blades, resulting in rotation of the shaft which connects the turbine with the compressor. From here the exhaust gas (having adequate specific enthalpy) is accelerated through an outlet nozzle, where it is accelerated. The high velocity exhaust gas is at a much greater speed than the free stream velocity and therefore produces thrust. The work of the engine is the change at the kinetic energy and especially axial momentum, between the flow that enters and the flow that exits the jet engine.

Considering a calorically perfect gas (for zero mechanical friction in the rotating shaft of the jet engine), the following equations indicate the rate of energy transfer for each of the above components:

$$\dot{W}_c = \dot{m}c_p(T_2 - T_1) \tag{1.2.1}$$

$$\dot{W}_t = \dot{m}c_p(T_3 - T_4) \tag{1.2.2}$$

$$\dot{Q}_{in} = \dot{m}c_p(T_3 - T_2) \tag{1.2.3}$$

$$\dot{Q}_{out} = \dot{m}c_p(T_4 - T_1) \tag{1.2.4}$$

$$\dot{W}_t = \dot{W}_c \tag{1.2.5}$$

According to the momentum theorem, the thrust force created by a turbojet is equal to the mass flow rate of the exhaust gas multiplied by its velocity relative to the free stream velocity

of air entering the jet engine. The more fuel that is consumed by the engine, the more thrust is created, assuming constant efficiency [*Alonzo et al., 2018*].

$$F = \dot{m}(V_{exit} - V_{inlet})$$ (1.2.6)

The micro gas turbines for distributed power generation applications mostly operate with the **recuperated Brayton** cycle. The recuperator is a heat exchanger that preheats compressed air before it enters the combustion chamber by recovering heat from exhaust gas, reducing thus fuel consumption and exploiting the energy of the exhaust gases. A recuperated cycle diagram is presented in Figure 7.
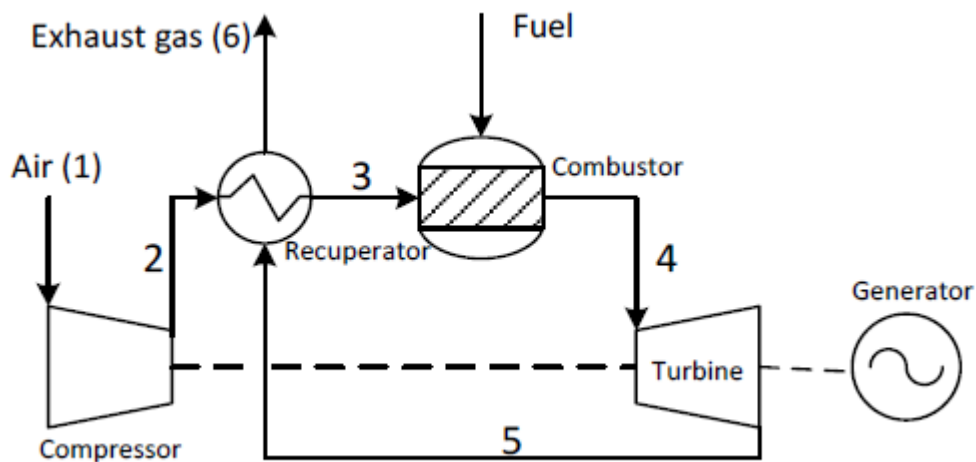
Figure 7: Single shaft recuperator engine.

The physics between smaller and larger turbomachines are essentially the same (Brayton Cycle), but it is also difficult to miniaturize many gas-turbine technologies, because they are not simply a size reduction of larger engines. For instance, over the past decades larger gas-turbines have been able to generate more and more power by burning fuel at higher temperatures and using cooling systems to keep turbine blades from melting; this is very difficult to replicate on micro turbines, due to difficulties at designing and constructing at a much smaller scale, including the processing of the materials [*Garett, 2019*].
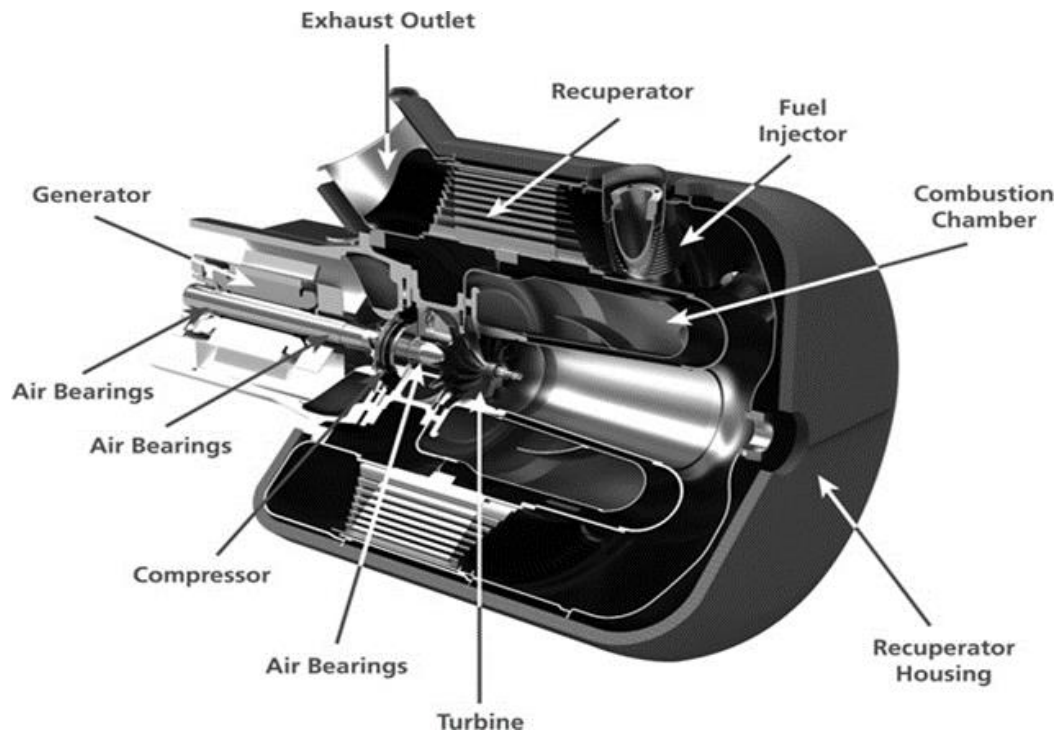
Figure 8: A microturbine with a recuperator component.

There is no official classification for micro engines but it is possible to categorize them depending on some basic characteristics and applications they have been utilized to. Microturbines operate at very high rotational speed between 35,000-180,000 rpm, for idle and maximum thrust. Small **turbojets** can be categorized in those who use a radial or centrifugal compressor and a radial or axial turbine and those that use an axial compressor and an axial turbine, which are still less used and more experimental. However, it seems that this kind of engines will be dominating the micro turbojet applications in the next years. Micro turbojets have been mainly applied on UAVs, but its design and construction emerged from the corresponding needs of airplane modelers. An engine with axial compressor (Figure 9), manufactured by Bladon firm, equipped with integral electric generators, was applied to the battery charging of an experimental Jaguar C-X75 hybrid car during 2010.
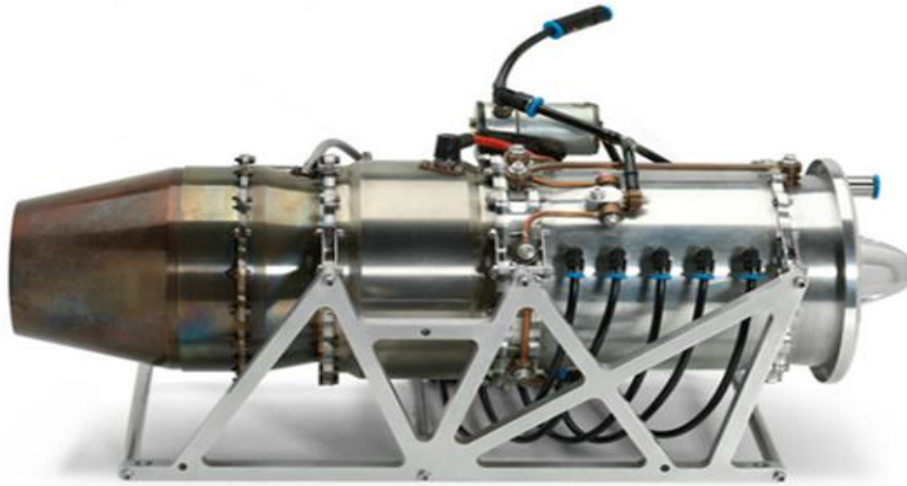
Figure 9: Experimental engine with axial compressor for a hybrid car.

Small **turboshafts**, applied for propulsion using of the mechanical power delivered to the engine shaft or spool, are also suitable for distributed generation applications, because of their advantages, such as high specific power, multi-fuel operation, low maintenance costs, ability to provide reliable and stable power, and parallel connection to serve larger loads and low pollutant emissions [*Environmental Protection Energy, 2008*]. Small turboshafts are more complex than turbojets since they usually utilize the recuperator component. In this case there are two kinds of construction: the single and the dual shaft engines.

In the single shaft configuration, the compressor and the generator are mounted on the same shaft and the turbine drives them both by generating power. In the dual shaft, the hot gases from the combustion chamber partially expand inside the high-pressure turbine and generate power for the compressor. Afterwards, the exhaust gases exit from the high-pressure turbine and fully expand on the free turbine to produce power for the generator. In this configuration the rotating speed of the free turbine remains constant. Some designs incorporate a gearbox to reduce the shaft speed and transmit the power to the generator, increasing although the weight and complexity of the engine, due to the gearbox and its lubricating system [*Bakalis, 2019*]. Dual shaft configurations are also used for propulsion of helicopter drones. **Turboprop's** difference from turboshaft is that the turboprop uses some of the exhaust gas energy not only for the separate free turbine, which drives the propeller, but also to produce additional thrust (Figure 10).
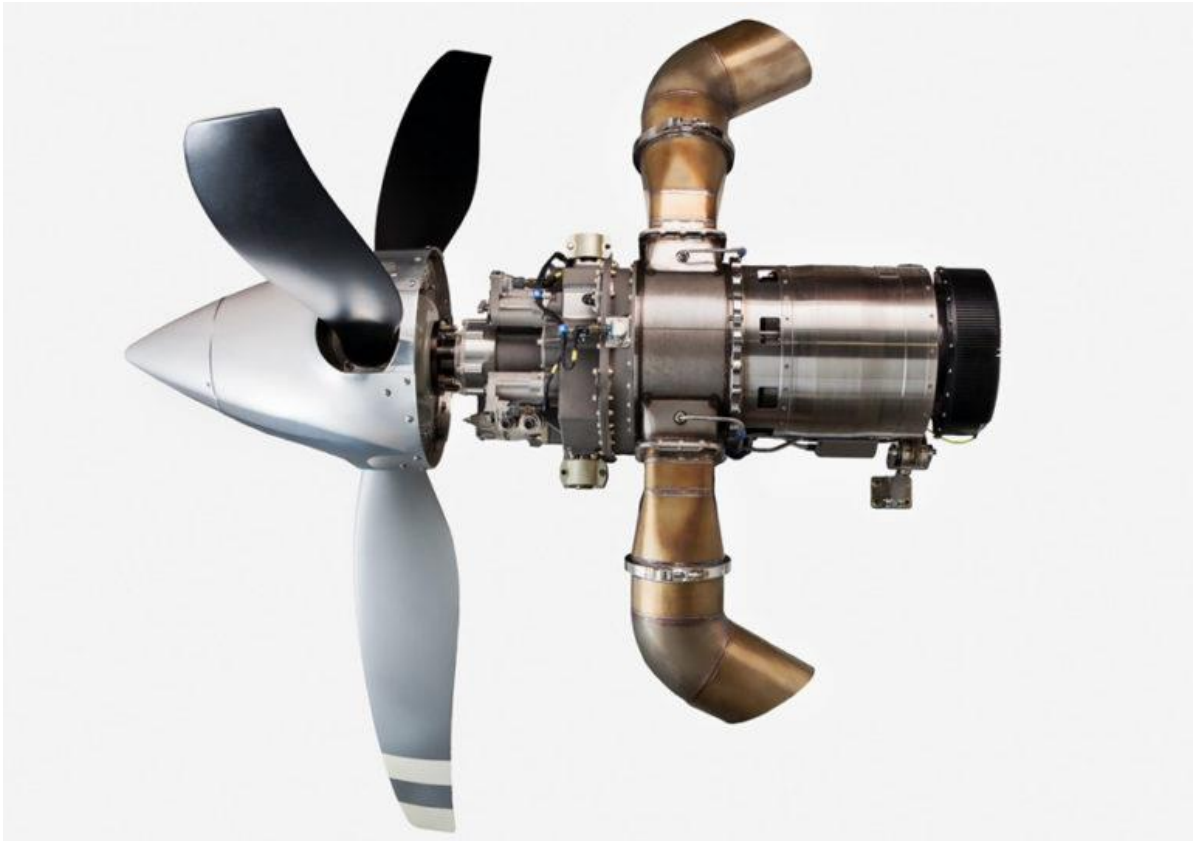
Figure 10: Turboprop engine TP100 for ultralight air vehicles [aviaexpo.com].

1.3 Components and basic specification of micro jet engines

Despite the fact that this thesis' main objective is the simulation of the flow field into a centrifugal compressor, is deemed appropriate to give a brief overview of the major components and specifications of a small jet engine, to have a better understanding of how they interact with each other and a total view of their operation. The components of a micro jet engine are similar with those of the larger ones, of course at a much smaller scale.

The **compressor**, whose goal is to increase the pressure enough for the combustion, has two types: the radial or centrifugal and the axial one. The centrifugal type is mostly applied at small gas turbines. The average pressure ratio values are from 1.2 to 4.6 depending on the size of the engine and the power demand. Professional compressors are manufactured with the use of advanced CAD software, CNC machining and 3D printing methods, usually from aluminum, a fact that solved many problems existed on the past with the precision of the manufacturing due to the small size requirement [*J. Dutczak, 2016*]. Detailed analysis about the centrifugal compressor and its operation will be given in section 1.5.

Turbines like compressors can be either radial or axial (Figure 11). Small gas turbines usually use single stage axial turbines. The purpose of the turbine is to drive the compressor and accessories, by taking part of the energy produced by the combustion chamber to create torque rotation. A turbine stage consists of a stator (Inlet Guide Vanes – IGV) and a rotor, vice

versa the compressor stage. Stator blades are airfoils with their leading edges facing the combustion chamber [*Hunecke, 1997*]. Their purpose is to convert a part of the gas energy exit from the combustion chamber to kinetic energy and accelerate the gas towards the entrance to the rotor blades. The goal for the flow is to be axial at the exit of the turbine with as little swirl as possible. The maximum exhaust gas temperature of a micro engine is limited by the thermal load at the turbine rotor, with values between 700 and 1000 °C. Due to high temperatures, pressures and rotational speeds, high centrifugal forces and stresses are created in the turbine blades. Therefore, nickel-based alloys, such as Inconel, are used for the turbine. These materials must also have high resistance of creep due to their continuous use under these conditions (high rotational speed – high temperature). Small jet turbines also suffer from relatively larger turbine blade tip clearances. That gap between the end of the turbine blade and the inside wall of the engine is a leakage point for pressure, meaning losses in power and efficiency [*Turbine Engine Division, 2019*]. A lot of research is in progress for the turbines used in micro engines, because its design is critical and affects the thrust creation.
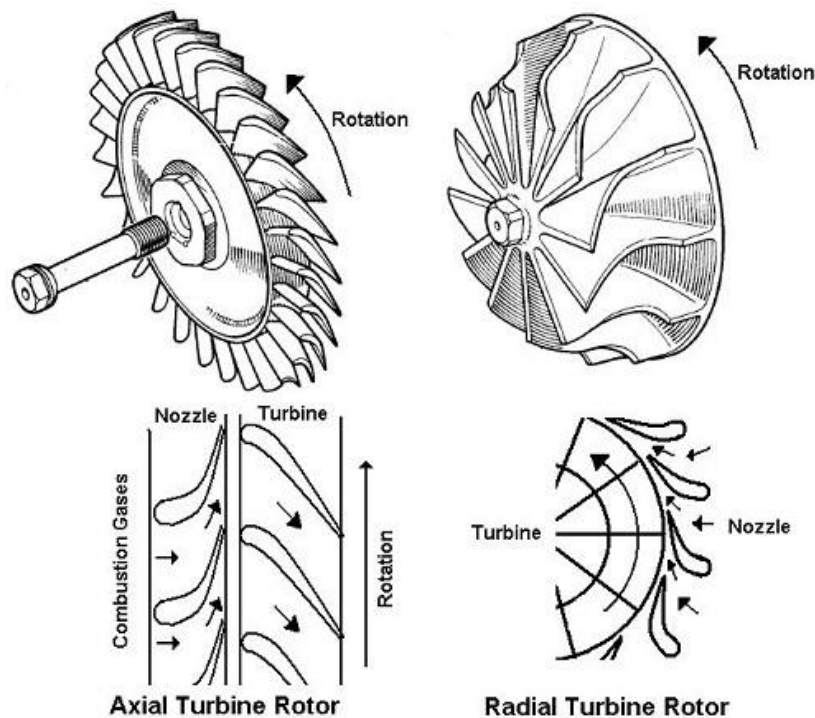
Figure 11: Axial flow and radial flow turbines
[http://www.gasturbineworld.co.uk/microturbineguide.html].

The **combustion chamber** is the section where heat is added in the cycle by burning fuel. The main goal is to receive air in ideal conditions from the compressor and transmit it to the turbine in much higher temperature, to be exploited for thrust creation. Higher-pressure air will produce more energy from the air-fuel mixture, so the diffuser section of the compressor decelerates the airflow in order to increase pressure before entering the combustion chamber. The stoichiometric air to fuel ratio is critical to achieve combustion. This ratio defines the amount of air consumed by the engine compared to the amount of fuel

consumed. Combustion chamber is divided in three zones: the primary, the secondary and the dilution zone. The primary zone, which is the first after the compressor, ignites through a spark plug the gas mixture. A homogenous mixing of fuel and air is important and therefore the fuel has to be atomized. After that, the atomized fuel is mixed with air. A flammable mixture has been created and can be burned. In the secondary zone more air is injected to cool the heated gases and the combustion process is completed. The dilution zone is where any remaining air is injected to achieve temperatures suitable for entry into the turbine stage. Due to the short dimensions of the combustor (especially in small gas turbines), the residence time of the air fuel mixture in the chamber is very short. A simple and fast fuel atomization and vaporization process is thus necessary. Almost all available combustion chambers for small engines use vaporizer sticks [*Fuchs et al., 2016*]. Conditions that constitute an effective combustion stage design include: continuous uniform combustion with no hot spots, sufficient mixing of air-fuel and low-pressure losses. Combustion chambers in micro engines can be either of annular type, wrapped around the hot end of the engine, or a single can type mounted to one side of the rotating axis [http://www.gasturbineworld.co.uk/microturbineguide.html]. The single annular combustion chamber with flame tube made of Inconel alloy (nickel based super alloy for very high temperatures) is usually used; combining lighter, less complex, economical design and allows manufacture of smaller diameter engine [*Dutczak et al., 2016*]. Micro engines use generally fuel based on kerosene, premium paraffin, Jet-A1 or diesel fuels. Fuel-oil mixture is also used to lubricate the bearings of the engine. The oil-fuel ratio depends on the individual construction of the engine and the type of fuel applied, its range spanning from 1.5 to 5.0%. In general, the higher amount of lubricating oil is added to a kerosene-based lighter fuel [*Dutczak et al., 2016*]. Combustor design is the most complex among micro jet engine components, hence the design of effective and efficient combustor is indispensable for the performance of the engine.
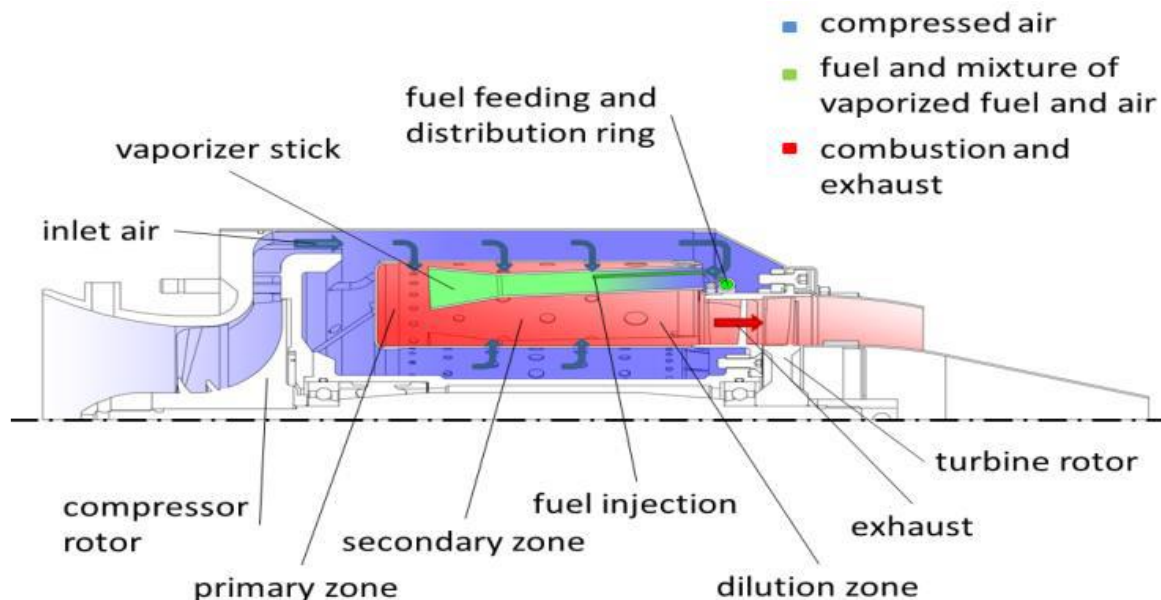

Figure 12: Schematic overview of a small jet engine combustion chamber [Fuchs, 2016].

The **nozzle's** purpose is to transform part of the remaining thermal energy of the exhaust gases into kinetic energy, to produce thrust. The flow through the nozzle is an expansion that leads to acceleration of the gases and, as a result, into increase of their kinetic energy and

decrease of pressure. A nozzle can be a converging one or a converging-diverging, and these types are commonly used in aircrafts. Converging nozzles are used for aircraft flying at subsonic speeds and converging-diverging nozzles are used to achieve supersonic jet flows (and thus supersonic aircraft speeds), which are typically used in fighter aircrafts. The smaller cross-section of a nozzle is known as the throat. Small jet engines are using a very simple converging nozzle design with minimal reduction in cross sectional area across the nozzle, in order to avoid choked flow at the exit [*Giacometti, 2007*]. Another important goal is to minimize the noise, which is very crucial for UAVS and avoid the creation of shockwaves.

Another interesting object for micro turbines is their **starting system**. Three main types are currently used: the air starting system, the propane-butane (gas) and the kerosene system. The air system uses air of the free stream and makes the engine lighter without use of a starter motor (Figure 13). The auto-start system (Gas or Kerosene) requires the use of an integral electric starter motor. The propane-butane mixture for engine starting is the most widespread method due to the good evaporating properties of the mixture at a low ambient temperature, making the easy flammable air-fuel mixture. After reaching a temperature about 100°C auto-start system changes the fuel to kerosene that is the main fuel. Also, micro turbines are equipped with a digital electronic **engine control unit** that enables proper starting and operation of the engine. Another important factor of performance that characterizes the turbine is the **spool time** up and down, which is the time of the engine thrust response to the rapid throttle opening from idle speed (minimum rpm) to maximum thrust (maximum rpm) and vice versa *[J. Dutczak, 2016]*.
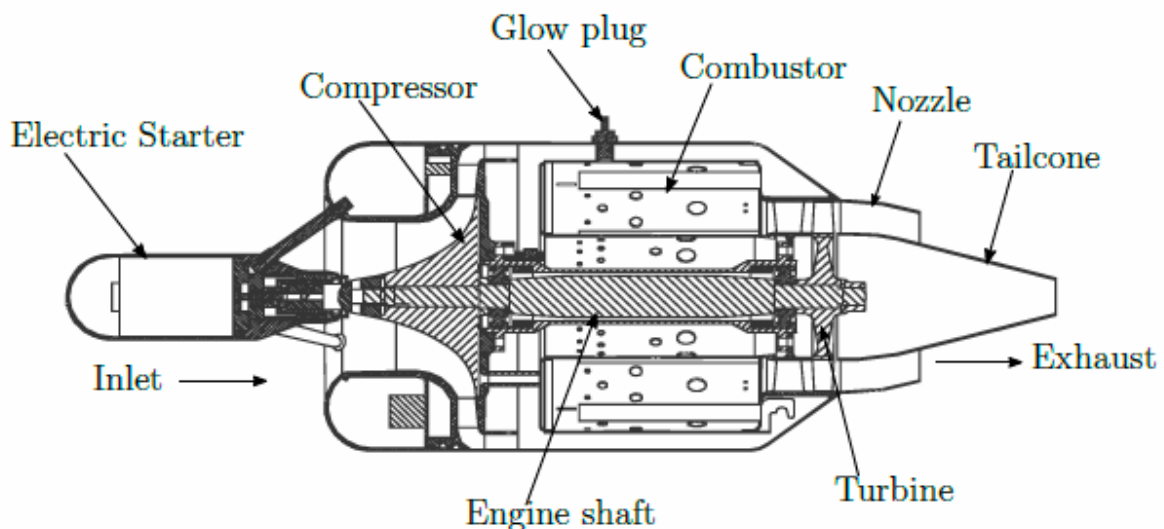

Figure 13: Schematic figure of BMT 120 KS micro engine [Kringe, 2013].

1.4 Advantages and engineering challenges of micro gas turbines

The main advantages of MTEs for every type of application can be summarized as follows [*Hartman, 2014 & Micro Gas Turbine Technology Summary, 2018*]:

1. High thrust to weight ratio, which is very important for UAVs and micro air vehicles.
2. Operation with various type of fuels. Most of micro turbines for aircraft propulsion use propane as a fuel to start the engine, due to its easy ignition, and then use kerosene for the rest of the process. Also, natural gas, biogas, diesel, biodiesel, kerosene etc. are used for micro gas turbines.
3. Micro gas turbines can be combined with one or more generation sources and make hybrid systems that have higher efficiencies compared to simple systems.
4. Parallel modular type configurations, which allows easier maintenance and replacement of a faulty engine.
5. Low emissions, cooperating also with renewable sources of energy, such as photovoltaic systems, wind turbines or combined with high temperature fuel cells, to supply electrical power with very high efficiency [*Bakalis, 2019*].
6. Small size, so a smaller installation area requirement.
7. As a thermal engine they reject heat to the environment and this energy is available in the hot exhaust gases and can be used for hot water production, space heating purposes etc., which is a main difference from piston engines.

Although MTEs have many advantages, there is a number of operational and practical issues of miniaturizing larger engines that affect the overall efficiency of MTEs and present a significant engineering challenge. The main issues are engine internal heat transfer, geometrical and mechanical constraints and limitations, large compressor and turbine tip losses and Reynolds number [*Soares et al., 2007*].

➢ **Heat transfer** is usually negligible in larger turbines between hot and cold components; however it is significantly larger in smaller turbines. The engine internal heat transfer influences the engine power output and thermal efficiency. Despite that MTEs high power to weight presents significant advantages, the higher surface to volume ratio creates heat transfer complexities in the engine. Large temperature difference between compressor and turbine combining with the small size of the engine results in a higher heat transfer, reducing thus the efficiency of them [*Verstraete et al., 2006*].

➢ **Low Reynolds** number is also a limiting factor for the overall efficiency of MTEs and especially compressor's stage and is a major designing challenge between small and larger gas turbines. Low Re is related to the small size of the engine, resulting in high viscous forces in the engine. These high viscous forces can slow down the air-fuel mixing and can cause significant losses of pressure and temperature, reducing combustion residence time, efficiency and power output of the engine. In addition, low Reynolds can create flow separation and transition from laminar to turbulent flow on the compressor, affecting the pressure ratio and the compressor's efficiency [*Oppong et al., 2017*].

➢ The **manufacturing accuracy** is very difficult to succeed for micro gas turbines, comparing to the manufacturing accuracy of larger engines. In addition, geometric constraints from the design and materials limitations are inherent with this inaccuracy. As a result, the smaller engines have relative higher surface roughness from the construction processes, leading to higher skin friction losses at the components. For a specific Reynolds number, the losses due to skin friction increase as the size of the components decreases [*Pesyridis, 2019*]. Furthermore, due to short compressor and turbine blade heights, micro turbines suffer from higher tip clearance losses. The higher the tip clearance the lower the component efficiency [*Oppong et al., 2017*].

1.5 Operation of a centrifugal compressor

In this section a brief overview of centrifugal compressor's operation is presented, since the main scope of the current thesis is the flow field simulation of such a type of component, of a small turbojet engine. Centrifugal compressors are mainly used in small gas turbines and turbochargers. In such applications a low mass flow rate and a high-pressure ratio are required. The advantage of a centrifugal compressor is that it can provide more pressure rise per stage than the axial compressor. Thus, for small engines where a light weight configuration is desired, it is a better option to use a centrifugal compressor to avoid a large number of stages, which an axial compressor would require to succeed the desired pressure ratio. The simplicity of its construction and the lower cost than multistage axial compressors have, are major advantages of the centrifugal compressors, for use in micro jet engines.

A centrifugal compressor consists of two main parts: the rotor or impeller and the stator or the diffuser. Figure 14 presents a schematic diagram of a centrifugal compressor and consists of an inlet pipe, an impeller tied to the rotating shaft, a vaneless or vaned diffuser, a volute casing and the shaft with its seal.

1. Inlet pipe, 2. Impeller, 3a. Vaneless diffuser, 3b. Vaned diffuser, 4. Volute casing, 5. Shaft, 6. Sealing.
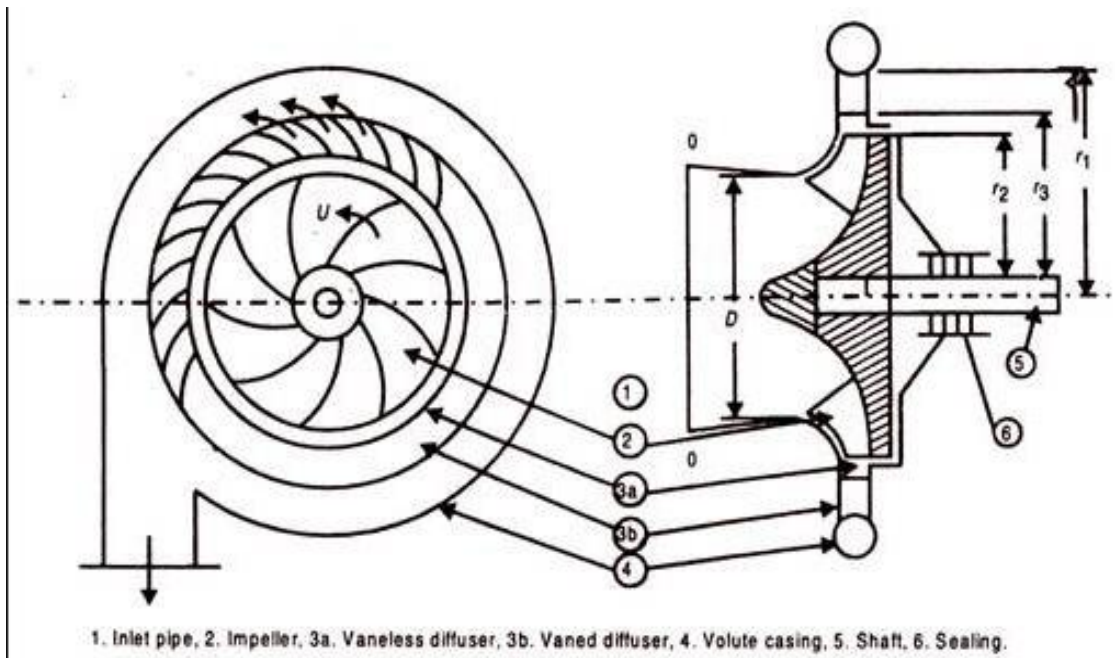
*Figure 14: Schematic diagram of a centrifugal compressor.*
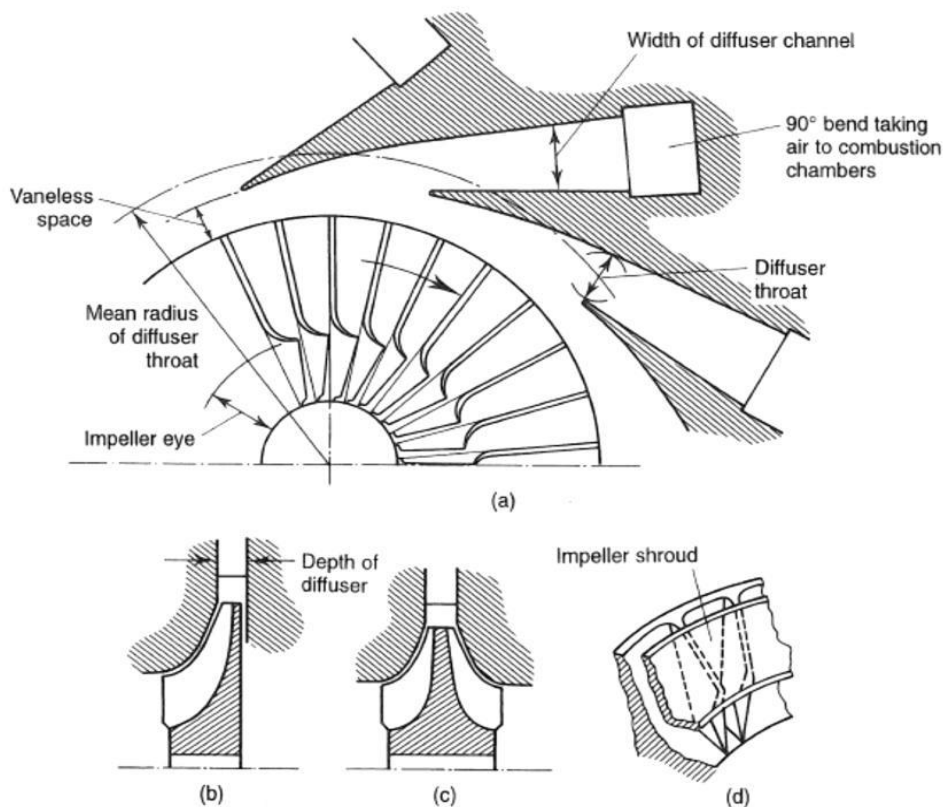
Figure 15: Impeller's eye, shroud and depth of diffuser [J. Hartman, 2014].

During operation, atmospheric air enters the centrifugal compressor at the eye. The inlet pipe directs air for smooth entry into the eye of the impeller. Air enters at the axial direction with an absolute velocity vector C_1. Pre-whirl may be applied to the inlet flow by adding a tangential component to C_1 so as to adjust the operational mass flow rate with negligible variation in shaft speed or pressure ratio [*Mohseni et al., 2012*].

The flow spreads along the blade channels until it reaches the impeller tip at r_2. The air now leaves the blades with an absolute velocity vector $\vec{C}_2$ and a relative velocity vector $\vec{W}_2$. The relative velocity vectors are acquired by subtracting the impeller velocity vectors $\vec{U}$ from the absolute velocity vectors, $\vec{C}$ or vice versa. The tangential component of the exit velocity C_{u2} would ideally be equal to the impeller's tip velocity U_2 plus the tangential component of the exit relative velocity W_{u2}. However, due to slip, the magnitude of C_{u2} is reduced by the amount ΔC_u [*Bosman, 2012*].
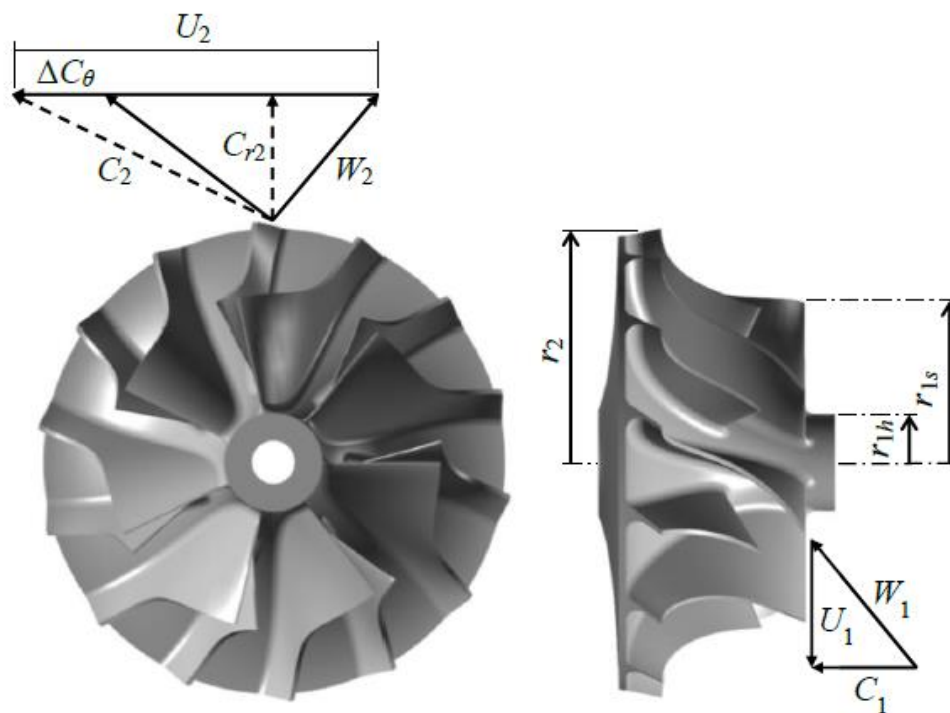

Figure 16: Velocity diagrams for centrifugal compressor impeller [Bosman, 2012].

As the air leaves the impeller at the tip, it enters the diffuser. At this point, the total pressure of the fluid has a high dynamic pressure. The diffuser regains some static pressure, although this leads to a loss of total pressure. The magnitude of this loss depends on the type and shape of the diffuser used. The losses in the diffuser (vaned or vanless) are due to work of friction force in the boundary layer on the solid surface of the diffuser. Static pressure is recovered by an increase in the cross-section area and the conservation of angular momentum.
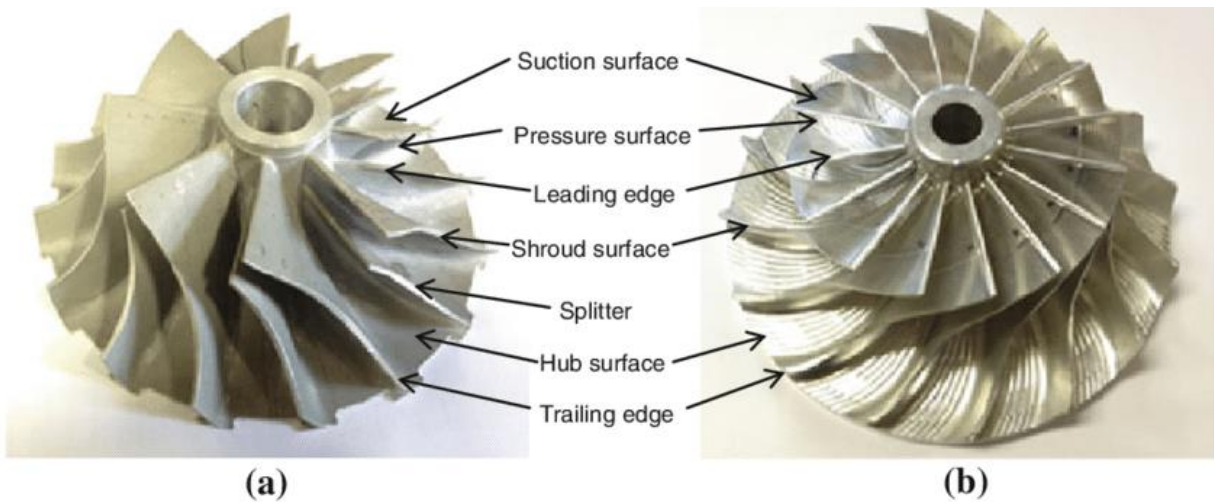
Figure 17: Terminology of surfaces at two types of centrifugal compressors [M. Suhaimi, et.al. 2013].

The most important parameter of a compressor is with no doubt its pressure ratio, which affects thrust, fuel consumption and engine's efficiency. The pressure ratio of a component is measured between its inlet and its exit. Worth mentioning that due to smaller blade heights, pressure ratio at micro jet engines is lower than conventional larger engines. For a centrifugal compressor, the pressure ratio is affected by both the diffusion of the relative velocity and the change in radius. This is why, for centrifugal compressors, a higher-pressure ratio can be achieved per stage than with axial flow compressors.

Pressure ratio is defined as:

$$\Pi_c = \frac{P_{t,exit}}{P_{t,inlet}}$$

(1.5.1)

Furthermore, for the design and the analysis of the centrifugal compressor and its performance, some dimensionless parameters are very useful. These parameters are defined as below:

a. Flow Coefficient *(φ)* is defined as the actual mass flow rate ($\dot{m}$) to the mass flow rate referred to the tip of the impeller. The value of the flow coefficient is usually between 0.28 and 0.32, with optimum value 0.3. The density, flow area and velocity at the denominator are at the tip of the impeller.

$$\varphi = \frac{\dot{m}}{\rho \cdot A \cdot u_{tip}}$$

(1.5.2)

b. Load coefficient *(λ)* is defined as the ratio of the increase in enthalpy in the compressor stage to the kinetic energy at the impeller tip.

$$\lambda = \frac{\Delta h_{stage}}{u_{tip}^2/2}$$

(1.5.3)

c. Pressure coefficient (Ψ) is the ratio of the isentropic enthalpy rise to the kinetic energy at the impeller tip.

$$\Psi = \frac{\Delta h_{is}}{u_{tip}^2/2}$$

(1.5.4)

d. Degree of Reaction (R) is defined as the ratio of enthalpy rise inside the rotor to the stagnation enthalpy rise inside the stage.

$$R = \frac{\Delta h_{rotor}}{\Delta h_{0,stage}} = \frac{\Delta h_{rotor}}{\Delta h_{0,rotor}}$$

(1.5.5)

e. Slip factor (σ) is defined as the ratio of the actual whirl (peripheral) velocity to the ideal whirl (peripheral) velocity. During design a slip factor have to be considered. Due to the finite number of impeller blades and the inertia of the fluid, there is a pressure difference across the blades, creating a relative velocity deficit. Fluid is said to have slipped with this relative velocity deficit, resulting to the definition of the slip factor. Slip factor depends on the number of the blades and is usually 0.9 for a number of 19 to 21 blades. An empirical formula by Stanitz is the following, where n is the number of blades:

$$\sigma = 1 - \frac{0,63\pi}{n}$$

(1.5.6)

The advantages of a centrifugal compressor make it ideal for micro jet engines. A centrifugal compressor has less sensitivity at foreign object damage (FOD) and stall, compared to an axial compressor, the design is more compact and reliable, with low maintenance cost, low weight and easy to design and manufacture. In addition, it has shorter overall length, when compared to the axial compressor for an equivalent pressure rise.

2. Market research for small/micro jet engines

2.1 Introduction

In this chapter market research for small/micro jet engines is presented. The market of small jet engines is highly developed nowadays and is expected to meet huge growth at the next decade. The unmanned aviation segment is projected to capture a large share in the aircraft micro turbine engines market by 2030. The research is focused on engines under 1000 N of thrust. Firstly, the current situation of the market is depicted, taking in consideration the progress of small jet engines throughout the years and presenting the market dynamics. Afterwards, the key player companies are presented, as well as engines with their characteristics, such as thrust, specific fuel consumption, weight, and pressure ratio. Finally, an effort is made to compare the presented engines, trying to analyze the trend that the market will follow the next years, the possible potentials, and the challenges that the market will face.

2.2 Market dynamics, scope and regional framework

Exploring the dynamics of the market, small aircraft turbine engines market is projected to reach USD 47.52 million, expanding at a CAGR of 9,8 % between 2020 and 2026 and up to USD 61 million by 2030 [*www.marketresearchfuture.com/reports/aircraft-micro-turbine-engines-market, 2021*]. CAGR (Compound Annual Growth Rate) is a measurement used by investors to calculate the rate at which a quantity grew over time. The demand for micro turbine engines has increased the last few years due to the increasing use of UAVs. Growth in the market can be also attributed to the focus on reducing carbon emissions and noise levels, through the adoption of smaller jet engines. Micro turbines provide many benefits, such as small size, compact design, lighter weight, etc., as has already been analyzed in Chapter 1. In recent years, as more and more drones are used to respond to global internal and external security threats, the aircraft micro turbine engine market has witnessed a rapid growth. In addition, low operating and maintenance costs and also the limited range and capacity of fully electric aircraft, are some of the factors driving market growth. However, the strict regulations and the high cost of micro/small turbine engines are expected to limit market growth to some extent [*www.marketresearchfuture.com/reports/aircraft-micro-turbine-engines-market, 2021*].

UAVs are considered to be the future in defense forces, combat missions, surveillance and reconnaissance missions by military forces; that is the main reason that the market invests at their propulsion systems. Although the military section is expected to witness the highest

growth, the commercial segment also is projected to steady increase its CAGR. In addition, the development of air taxis for urban air mobility is expected to drive the growth of the commercial market, as well as applications for faster delivery of cargo. The turbojet and turboshaft engine types are of greater interest and the first one is expected to observe substantial demand. It's also worth mentioning that the VTOL (Vertical Take Off & Landing) segment is expected to witness increased popularity, due to the demand for quick mobility in civil regions, while the small turbine engines are expected to see rapid adoption at VTOL applications [*www.marketsandmarkets.com/Market-Reports/aircraft-micro-turbine-engines-market, 2020*].

Looking at the regional framework, the market of micro turbines engines is expanding all over the developed world. The share of each continent is shown in Figure 18. Moreover, some additional information about the potentials of each region at the market are presented below [*www.marketsandmarkets.com/Market-Reports/aircraft-micro-turbine-engines-market ,2020*].
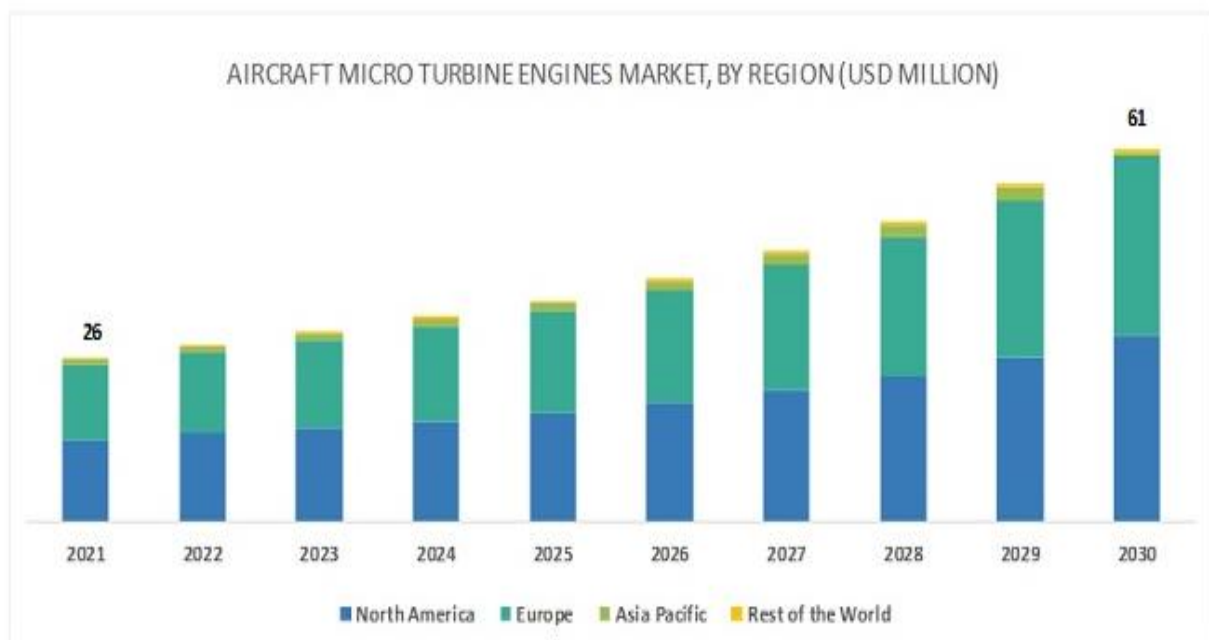
Figure 18: Share of global MTE market [www.marketsandmarkets.com/Market-Reports/aircraft-micro-turbine-engines-market, 2020].

Asia Pacific has exhibited a major potential in the aircraft micro turbine engines market. The market at this region is estimated to expand its CAGR, with countries such as **China**, Japan, India and Australia, by increasing defense expenditure on advanced UAVs. Moreover, China is expected to attract generally more investments, due to stable growth and important developments at the economy section, increasing the GDP (Gross Domestic Product) of the country at the next decade. The North America, with **USA** as the leader, surely dominates the market at present, as shown in Figure 18, and this trend is expected to keep growing at the forecast period 2021 to 2030, with prominent companies in the market such as General Electric Aviation, Williams International, Kratos Defense, Honeywell International and PBS Group investing at research and development of micro turbine engines for small aircraft

propulsion, for military and commercial use. Europe could not surely keep away of the small engines market, with the development of UAVs for both militaries, by air forces, and commercial reasons performing intelligence, surveillance, and reconnaissance missions. Main protagonist countries in Europe are **Germany** and the **UK**. At the rest of the world, Israel, UAE and Saudi Arabia are the most powerful competitors at the market [*www.marketresearchfuture.com/reports/aircraft-micro-turbine-engines-market, 2021*].
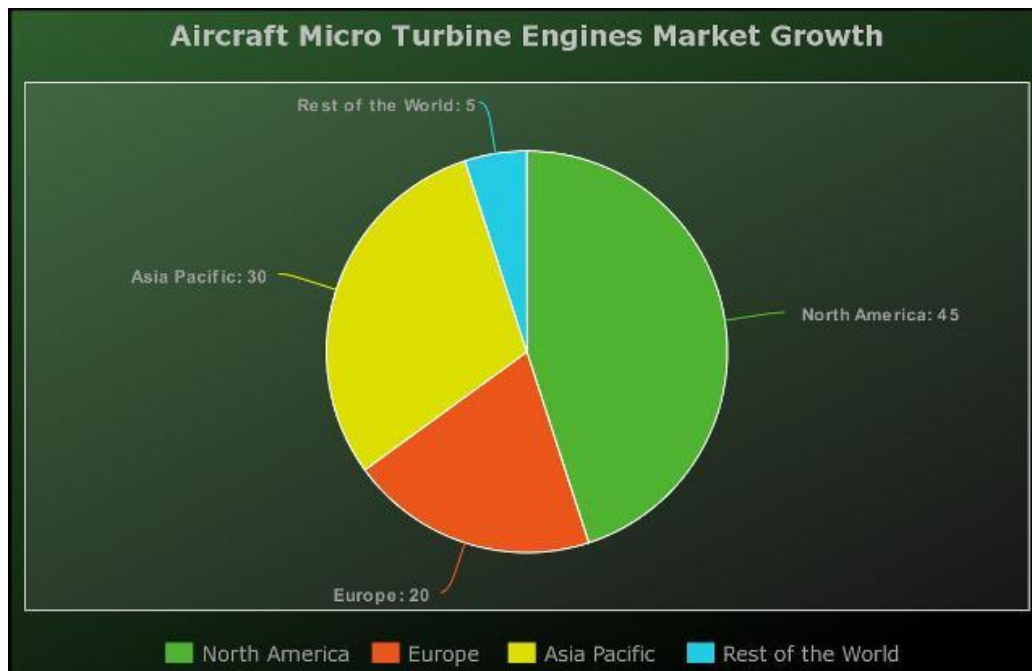
Figure 19: Global Aircraft Micro Turbine Engines Market Growth %
[www.openpr.com/news/2012622/aircraft-micro-turbine-engines-market-to-witness-huge-growth,
2020].

2.3 Key Market Players

This section is an overview of the most significant companies that are engaged with the design and production of micro turbine engines. Having already mentioned ***Kratos Defense & Security Solutions Inc***., it is also worth mentioning that this company plans to invest up to 725 $ million in research and development of jet turbines, through its Advanced Turbine Technologies for Affordable Mission (ATTAM) program, with much of that investment going to small jet engines. Kratos Turbine Technology division (KTT) is focused on the development and production of small, affordable, high performance jet engines for cruise missiles and UAVs. Kratos is active at this technology for over 20 years, based on the US, Florida, and is developing several types of small engines, including turbojets with 100 to 300 lbs thrust and turbofan engines in the 600 to 900 lbs thrust range [*www.kratosdefense.com*].

Another important company at this market is *JetCat* that develops and produces all its products in Germany, with a global supply chain. This company is designing small jet engines from 2000 and JetCat turbines are now used for the propulsion of model aircrafts, drones (X-56), industrial applications and for stationary use at universities (laboratory use). JetCat manufactures hobby engines up to 220 N thrust, engines for helicopters and more powerful engines for professional use. It is expected to be a strong player at the next period at the small turbines market [*https://www.jetcat.de/en*].

Williams International is one of the world leaders in the development, manufacture and support of small gas turbine engines. Williams produces jet engines for cruise missiles and small jet aircraft. A significant past achievement is the design of miniature turbofans that enabled the creation of long-range cruise missiles, the X-Jet flying platform, engines so small and inexpensive that navies around the world use drones powered by them to train their gunners. Beyond doubt Williams will play a substantial part in the market and the research for the development of small engines [*http://www.williams-int.com/*].

PBS Group is a Czech Republic company and *PBS Aerospace* is a subsidiary of the PBS Group that focuses on expanding business activity of the group in the United States at the aerospace field. The goal of PBS Aerospace is to become a major supplier of small jet engines for modern UAVs, having a long-term experience at the field, approximately 50 years in aviation. In the research and development field, during the past two years the company brought two turbojet engines to the market: the TJ80, manufactured using 3D measuring technology, and TJ150, with a thrust of 900 and 1500 N, respectively. Furthermore, through the ESPOSA project, PBS aims to develop propulsion technologies for small scale aircrafts, from design and production of engine parts up to the engine installation methodology in small aircrafts. PBS invests at innovation and development of small turbines, is a trustworthy and stable company with financial stability and will continue to be a leading company in this field [*https://www.pbsaerospace.com/*].

UAV Turbines Inc. is a company based in Florida, focused on the design, development and research of small, quiet, lightweight, with fuel efficiency engines, for the propulsion of UAVs as well as ground power applications. In 2011, an investment group took control of the initial parent company, Locust USA (rebranded UAVT AT 2014), and since then $16 million has been invested in the development of small turbine engines [*https://www.airframer.com*].

Brayton Energy, a small development company in UK, founded in 2004 is actively involved in both UAV and electrical vehicle market. The company, following the motive of the market, has cooperated with DOD, and US Air Force, to develop certain engine components for UAV engines, running also UAV projects for meteorological and geological research. These engines and their very small turbine components are a great candidate for additive manufacturing technology [*https://www.braytonenergy.net/gas-turbines/*].

Hawk Turbine AB is a high-tech Swedish company that designs and produces model jet engines. Hawk is providing engines with very low fuel consumption, a characteristic important to be competitive in the market. *BF-Turbines* in Germany is a manufacturer of small turbojet engines for model aircraft and military applications (B100F, B140F and B300F turbojet engine

series) and generally involved in the development of small gas turbines [*http://www.bf-turbines.de/*].

Other companies that is projected to take share of the market and generally in the UAV market are the giants Lockheed Martin Aero, and Rolls-Royce Holdings, with hybrid electrical propulsion systems, Honeywell International Inc., Lambert Microturbine in Germany, Stuttgart Engineering Propulsion Technologies UG, with turboprop engines for light, ultralight aircrafts and helicopters, JetsMunt SL (Spain), Sentient Blue Technologies (Italy), Micro Turbine Technology B.V. (Netherlands), Turbotech SAS (France), GE Aviation, KingTech Turbines and AMT Netherlands B.V..

2.4 Small jet engines existing in the market

At this section some of the most representative engines in the market are presented, with their technical parameters and features. The research is focused on engines at the range of 0 to 120 kg thrust. Figure 20 is a historical overview of engines under 100 kg thrust [*https://minijets.org/en/0-100*]. Engines of some key market player companies are shortly presented, as well as specification tables for the engines of interest.
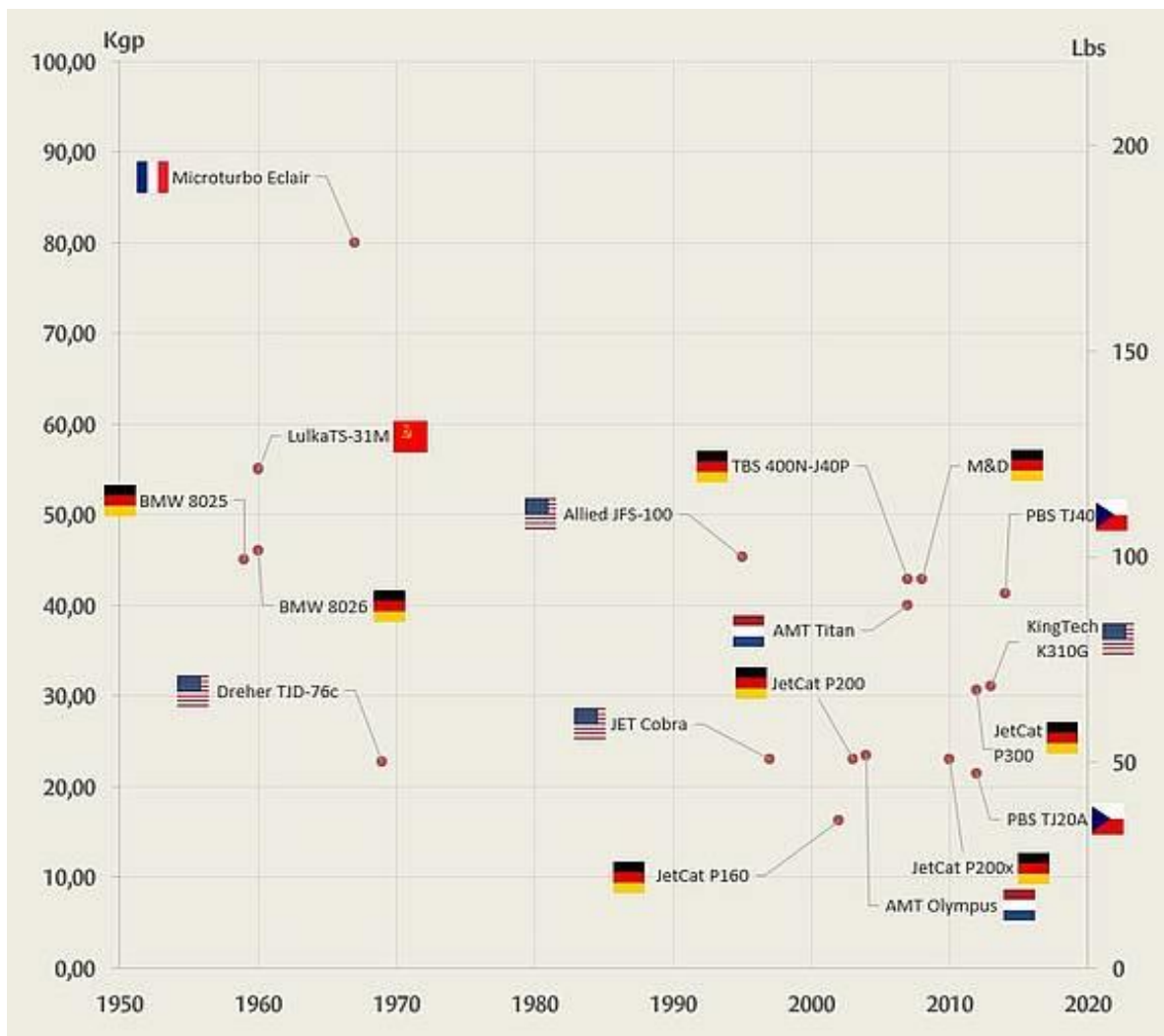
Figure 20: Turbojet engines sorted by thrust and year [https://minijets.org/en/0-100].

PBS TJ-40 (G1 and G2 versions) is a turbojet engine designed by PBS Aerospace for UAV systems, target drones, decoy and small reconnaissance drones. It can also equip gliders or ultra-light aircraft. Its advantage is its low weight of 3.8 kg and thrust at maximum rpm, of 395 N. The PBS TJ-40 jet engine is a single shaft engine with a one stage centrifugal compressor, radial and axial diffuser, annular combustion chamber, one stage axial turbine and an outlet nozzle. At the table beneath, the technical parameters of other engines that PBS designs are presented and are utilized for the same purposes [*https://www.pbsaerospace.com/aerospace-products/engines/turbojet-engines*].

Figure 21: PBS TJ 40 jet engine.

Engine	Diameter (mm)	Length (mm)	Weight (kg)	TSFC (kg/N/h)	Max Thrust (N)
PBS TJ80	235	514	12.5	0.123	900
PBS 23-U	121	316	1.98	0.165	230
PBS TJ40-G2	147	373	3.8	0.147	395
TJ100	272	625	19.5	0.118	1250
TJ100P	272	636	17.6	0.126	1250

JetCat designs a variety of engine series and the name of the engine usually specifies the thrust that produces in Newtons. This company has a series of engines for hobby and modelers, as well as more professional engines. The technical parameters of JetCat engines are shown at the table below. The price of the engines with thrust under 500 N are from 2,000 € to 11,000 € [*https://www.jetcat.de/en/products/*].

Figure 22: P200-RX jet engine, produced by JetCat.

Engine	Diameter (mm)	Length (mm)	Weight (kg)	TSFC (kg/N/h)	Max Thrust (N)	Max Ex Gas temp °C
P-20 SX	60	171	0.350	0.188	24	690
P-60 SE	83	243	0.845	0.183	63	650
P-80 SE	112	286	1.315	0.15	97	650
P 100-RX	97	241	1.08	0.187	100	720
P 130-RX	99	284	1.326	0.185	130	720
P 200-RX	132	355	2.53	0.15	210	750
P 220-Rxi	116.8	307	1.85	0.158	220	750
P180-NX	112	283	1.71	0.16	175	750
P-250 Pro s	121	322	2.155	0.158	250	750
P-300 Pro	132	380	2.73	0.157	300	750
P-400 Pro	148.4	353	3.65	0.157	400	750
P-500 Pro-GL	175	419	4.9	0.151	500	740
P-550 Pro-GL	175	419	4.9	0.144	550	750

Other engines of the same category, designed and manufactured by several companies, are also presented in the table below. Some parameters that are not openly available are described as N/A (Not Available).

Engine	Diameter (mm)	Length (mm)	Weight (kg)	TSFC (kg/N/h)	Max Thrust (N)	Ex Gas temp °C
Mercury AMT	100	292	1.55	0.193	90	750
Pegasus	120	342	2.255	0.174	167	675
Olympus AMT	130	374	2.9	0.167	230	750
Titan	147	385	3.645	0.156	392	850
Hawk 240 R	N/A	N/A	2.8	0.129	240	760
B300F	133	390	2.65	0.196	300	760
K-310 G	132.5	270	2.7	0.136	310	700
Locust H195	207	455	13	N/A	736	N/A
Tarantula H140	165	345	7.5	N/A	500	N/A

Figure 23: KingTech K-310G jet engine.

3. Design of the compressor components

3.1 Introduction

The benchmark engine chosen for this project is AMT Olympus (Figures 25, 26). This engine is designed by AMT Netherlands a company that designs and manufactures small turbojets for propulsion of target vehicles and drones, radio-controlled aircrafts and experimental aircrafts. The Olympus HP engine is in production since middle of 2004. In 2010 the engine converted to a direct kerosene starting system. It is mainly used by the community of radio modelers, but also by certain professionals, universities and research institutes. It is a single flow turbojet engine which is built around a centrifugal compressor and an axial turbine and produces a thrust up to 230 N. The engine has the ability to operate with different fuels, such as kerosene and paraffin oil, while the fuel is premixed with lubrication oil to lubricate the bearings of the engine. The Olympus jet engine is controlled and protected from improper use by a microprocessor controller, a fully automatic ECU. The basic engine data is presented in Figure 24.

Specifications			All data at STP +/- 2%
Engine diameter	130 mm	/	5.1 Inch
Engine length	374 mm	/	14.7 Inch
Engine weight	2900 gram	/	6.4 Lbs
System airborne weight *	3845 gram	/	8,5 Lbs
Thrust at S.T.P. **	230 N	/	51.7 Lbf
Maximum RPM	108.500	/	108.500
Thrust at Idle RPM	13 N	/	2.9 Lbf
Pressure ratio	3.5:1	/	3.5:1
Mass flow	450 Gr/sec	/	0.99 Lb/Sec
Max continues EGT	750 Deg C	/	1380 Deg F
Fuel consumption	640 Gr/min	/	22,5 oz/min
Specific fuel consumption	46,4 gr/(Kn*sec)	/	1,64 lb/(lbf*hr)
Starting method	Direct kerosene starting gas turbine, on request propane start.		
* Total weight of; Engine,ECU,pump,battery,thermosensor, valves, mounting straps.			
** On request the RPM can be raised to 110.000 RPM giving 10 Newton additional thrust.			

Figure 24: Specifications of AMT Olympus [www.amtjets.com].
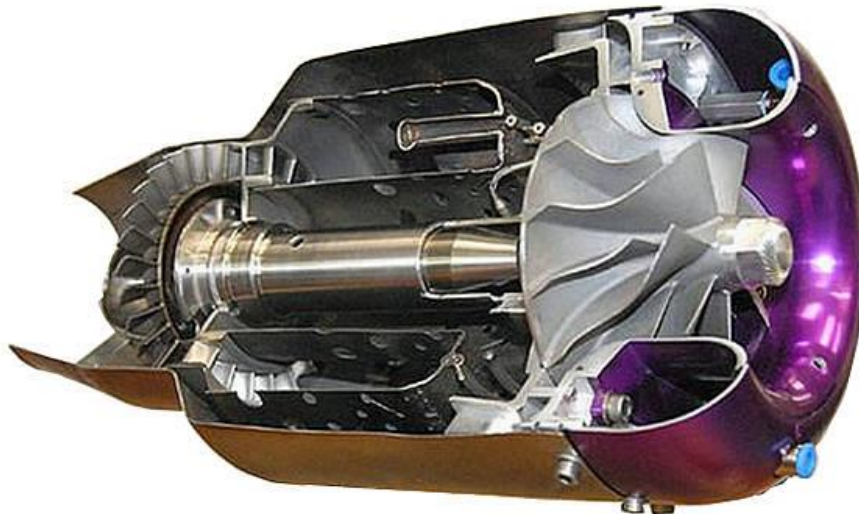
Figure 25: AMT Olympus sectional view [Minijets.org].

Existing components of **AMT Olympus** were firstly measured using a **CMM** (Coordinate Measuring Machine) (Figure 27); the related work was performed by Mr. P. Zografos, as part of his M.Sc. Thesis. In order to perform a CFD analysis of the centrifugal compressor, an accurate digital model of the compressor parts needs to be developed, using a CAD software. Afterwards, the corresponding flow domains will be defined from the assembly of these digital models. For the digital modelling process the SOLIDWORKS CAD&CAE software was used. After creating each individual part, the full assembly was built. Then, the flow domain was defined, using Boolean Operations.
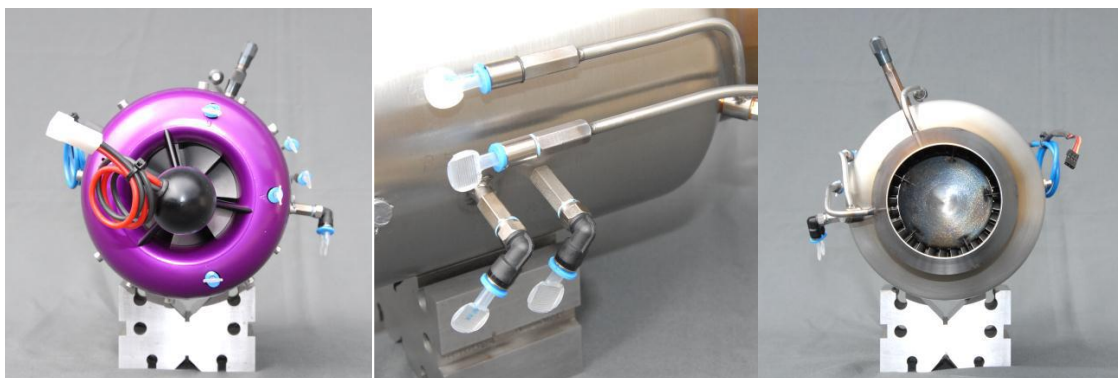
Figure 26: Front, Side and Rear Engine View.
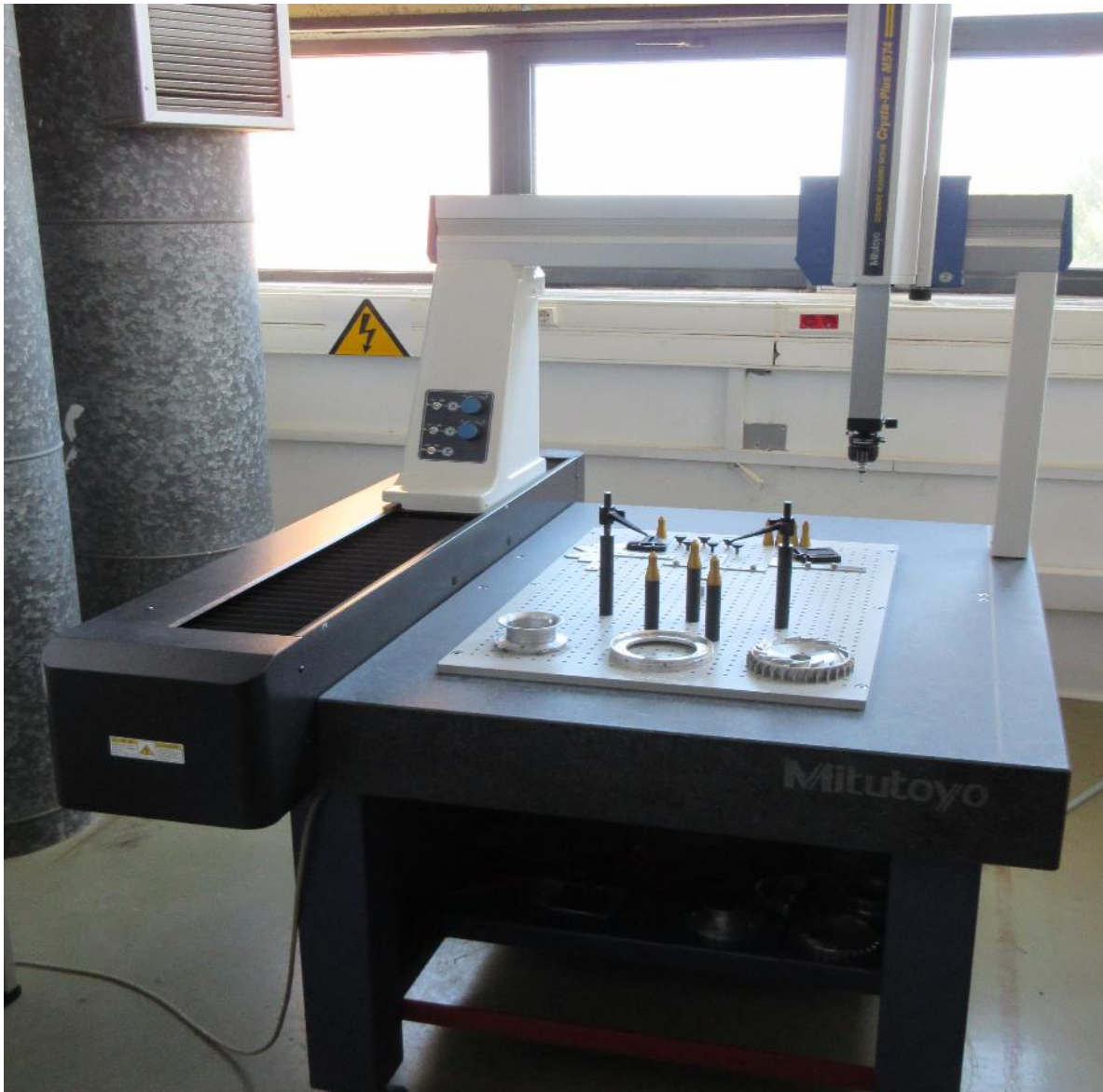
Figure 27: The CMM with the parts ready to be measured.

The CMM uses a probe to measure points on a workpiece. Each point on the workpiece is unique to the machine's coordinate system. The machine allows the probe angle to be controlled to enable the measurement of complex surfaces that may otherwise be unreachable with very high accuracy. About the measuring process, the spherical contact point attached to the tip of the probe is applied to the object on the stage and the coordinate values in three dimensions (X, Y, Z) are specified and measured *[https://en.wikipedia.org/wiki/Coordinate-measuring_machine]*.

3.2 Inlet Duct

Following the process described above, the spherical contact point attached to the tip of the probe is applied to the inlet duct surfaces, as shown in Figure 28, to measure and specify the coordinates for this part.
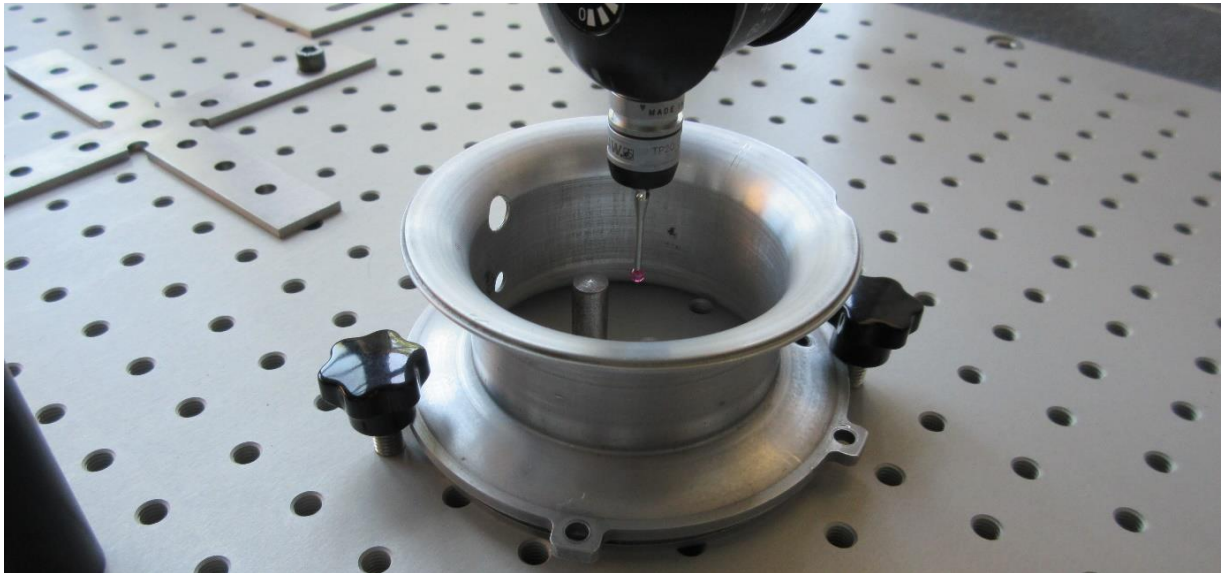
Figure 28: Duct measuring using the CMM.

After completing this task, the next step is to design the duct at SOLIDWORKS. Firstly, the design of the sketch (blue line curves) takes place and then with the command "Revolve" around the axis in the center, the part of the inlet duct is generated (Figure 29).
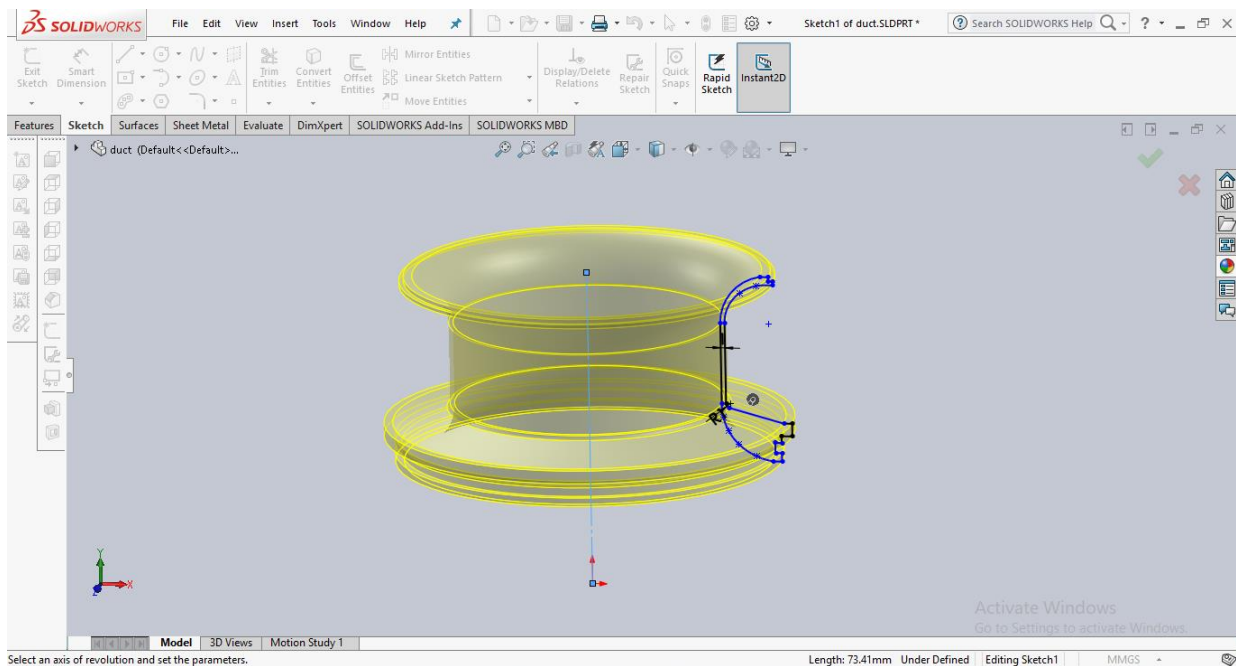
Figure 29: Design of the duct at SW.
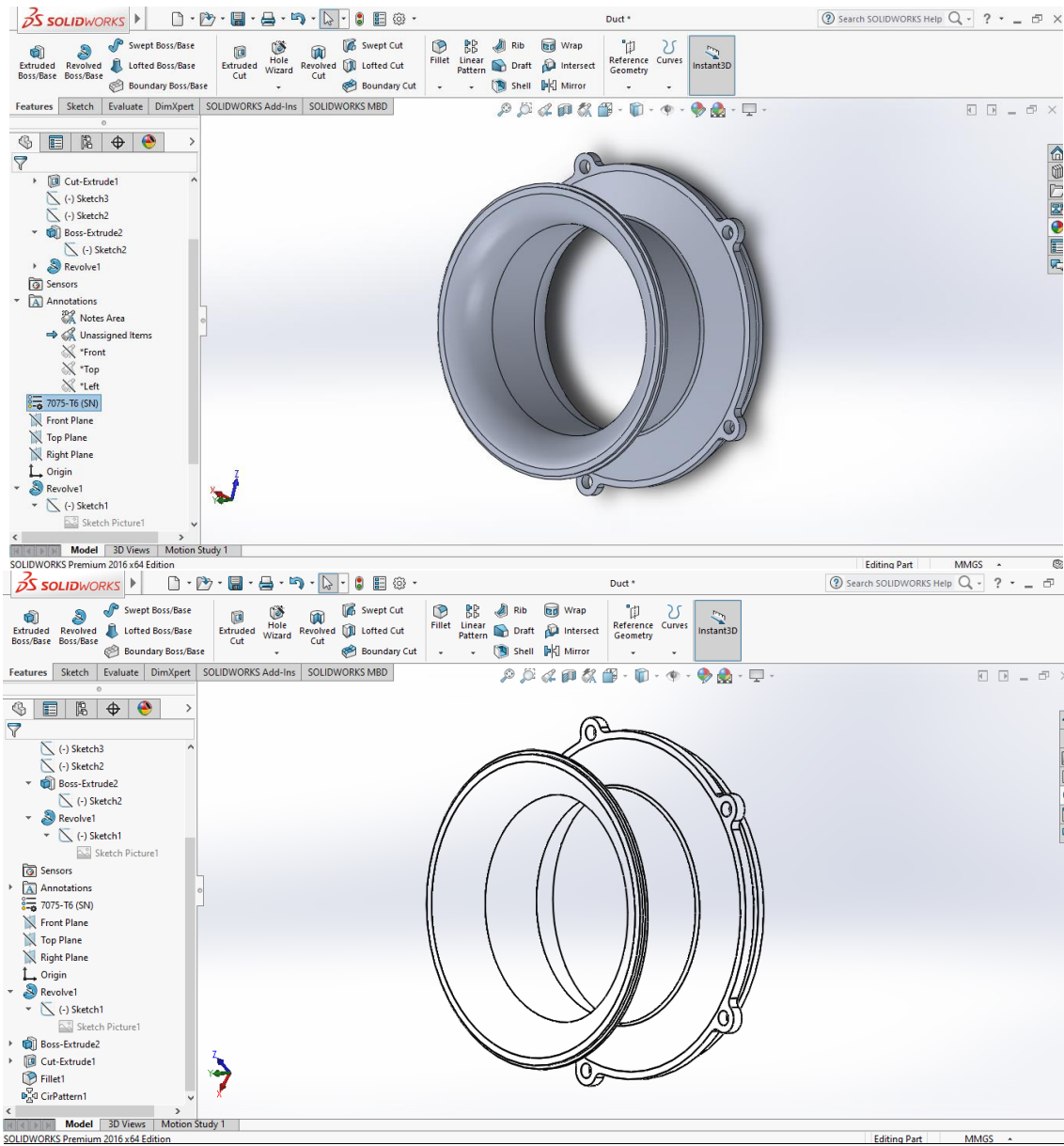
Figure 30: Complete depiction of the part.

3.3 Duct Casing

The next part to be designed is the duct casing. In the same way as the duct, the coordinates of the component are measured using the CMM (Figure 31).
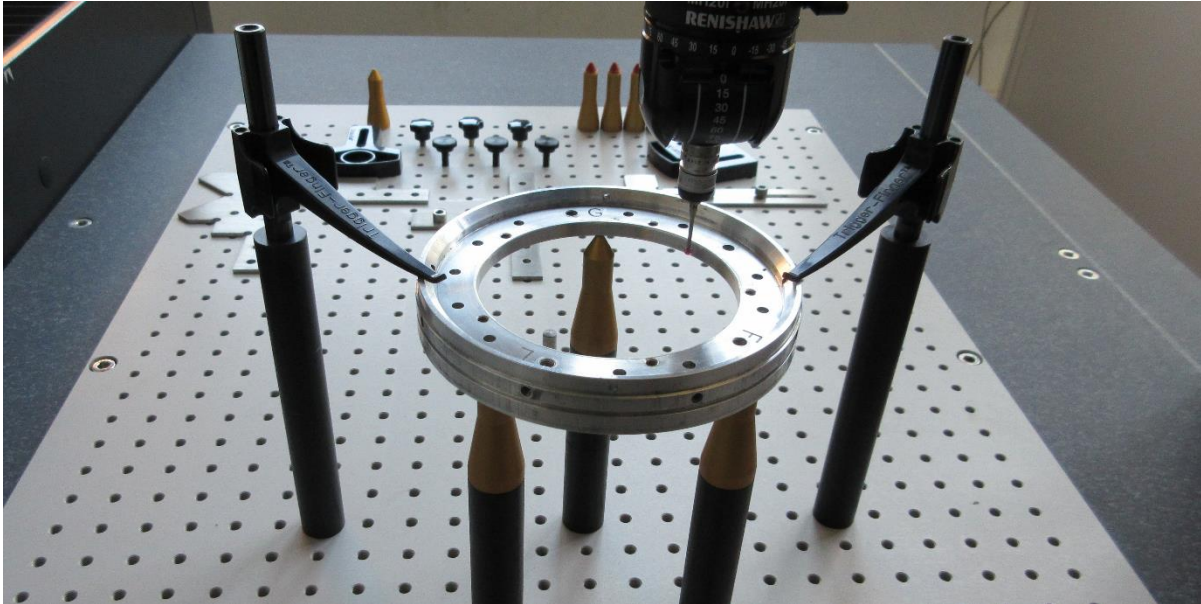
Figure 31: Casing measurement at CMM.

Afterwards, the part design using SOLIDWORDS, was performed (Figures 32, 33).
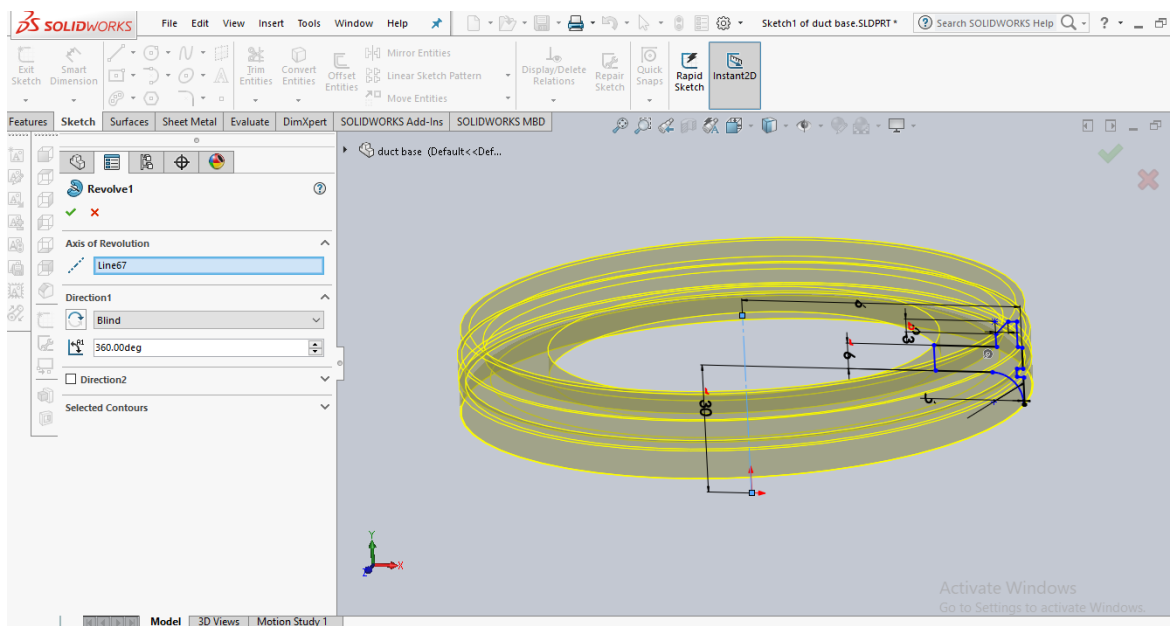
Figure 32: Design of the casing using SW.
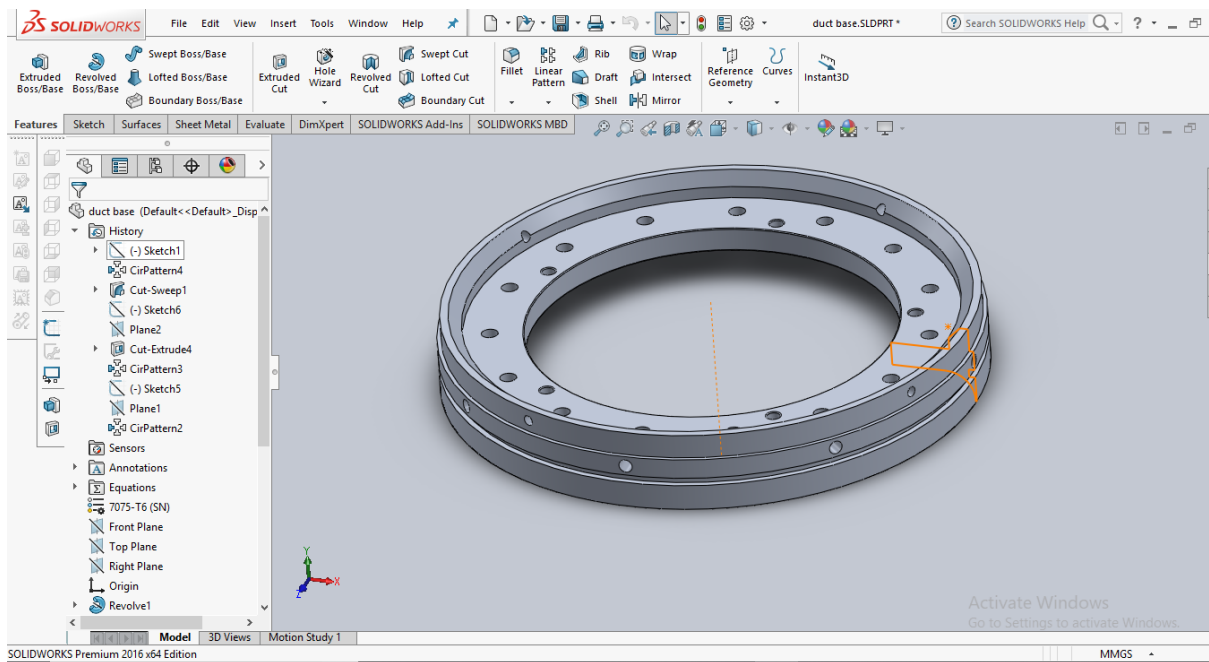
Figure 33: Complete depiction of the duct casing.

3.4 Impeller

The impeller was the most complicated component to measure and model. The small size of the impeller made it difficult to obtain accurate measurements in the CMM, while small inaccuracies may have a higher impact to the CFD results. For the design of the blades, the curves had to be generated as a set of points. The measurement of the impeller (using the CMM) was performed by Mr. G. Bilalis, during his Diploma Thesis (Figures 34, 35).
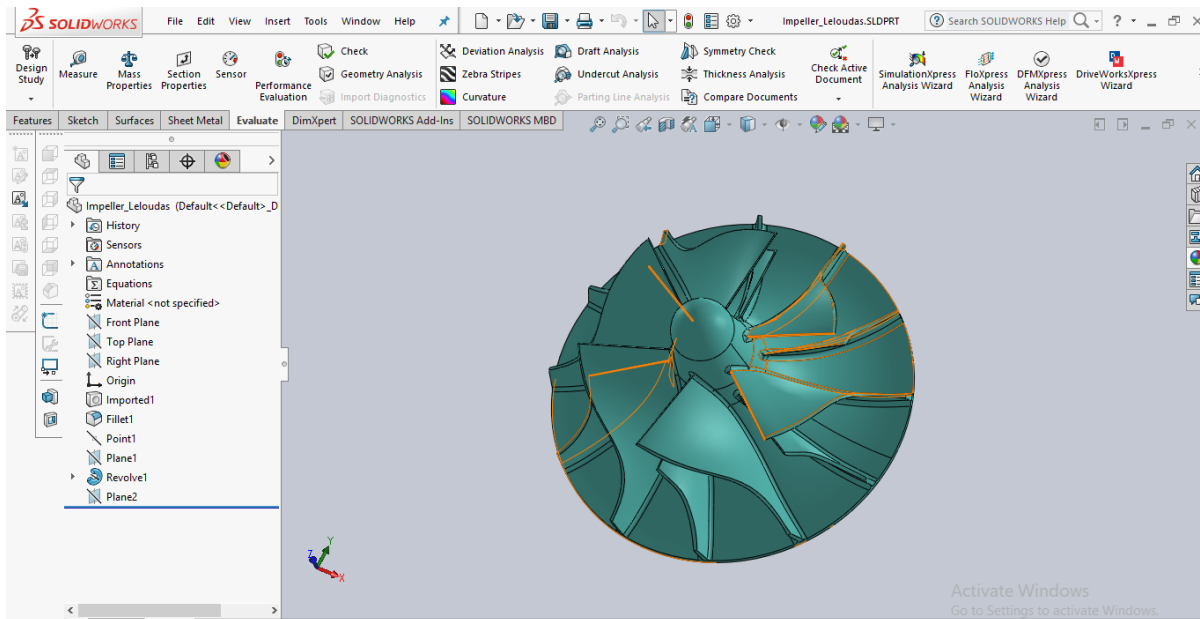
Figure 34: Impeller and blades.
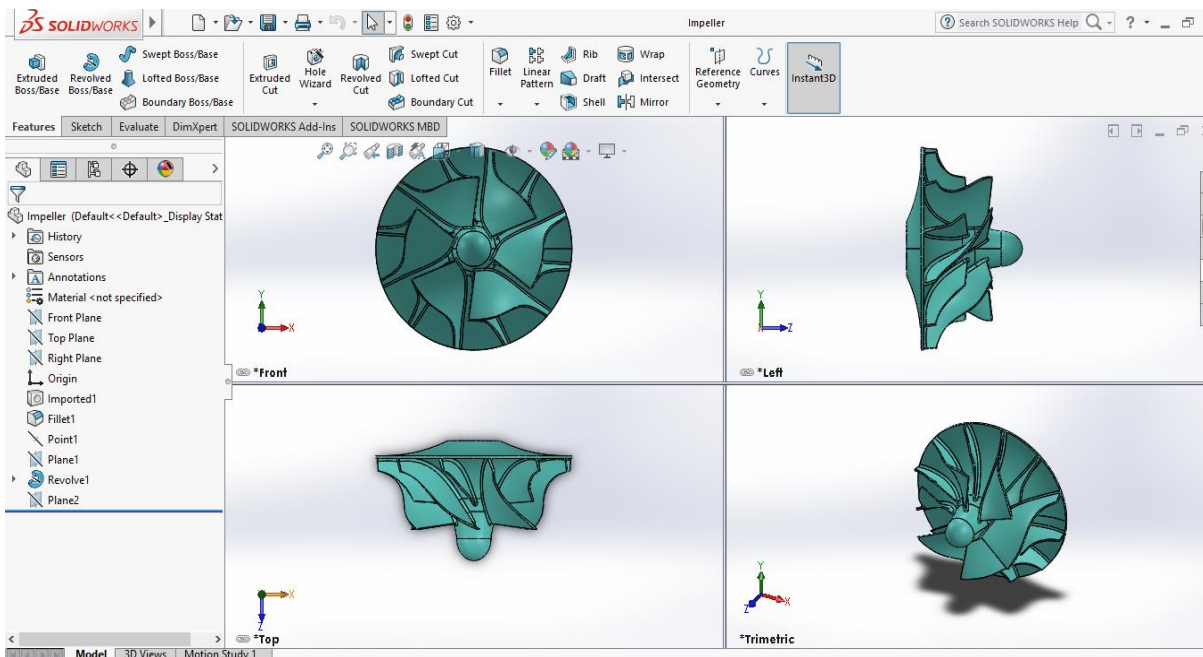
Figure 35: Four view depiction of the impeller.

3.5 Diffuser

The last part is the bladed diffuser. Following the same steps, the diffuser with its blades was first measured at the CCM (Figure 36) and then the digital model was produced in the CAD software (Figures 37, 38).
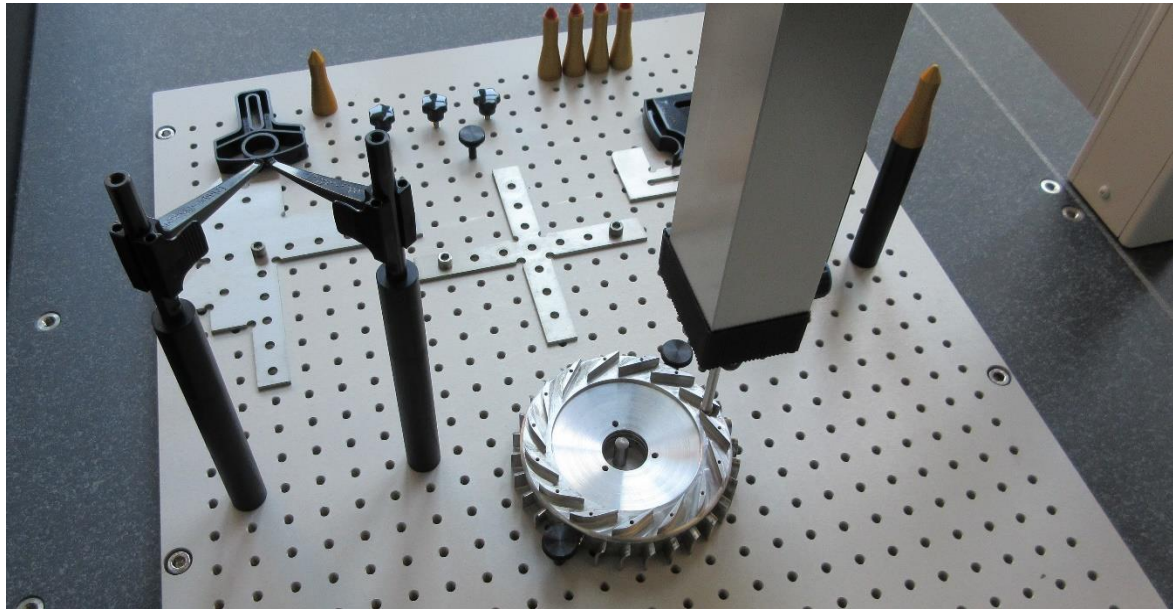
Figure 36: Diffuser measurement at CMM.
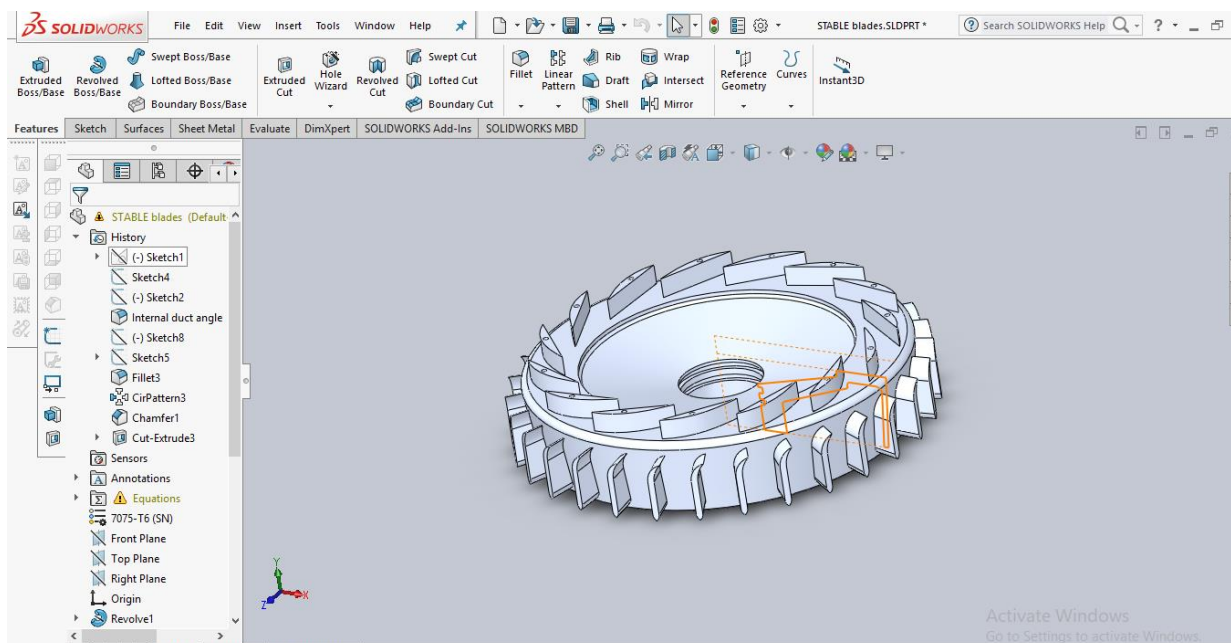
Figure 37: Generation of the diffuser's digital model.
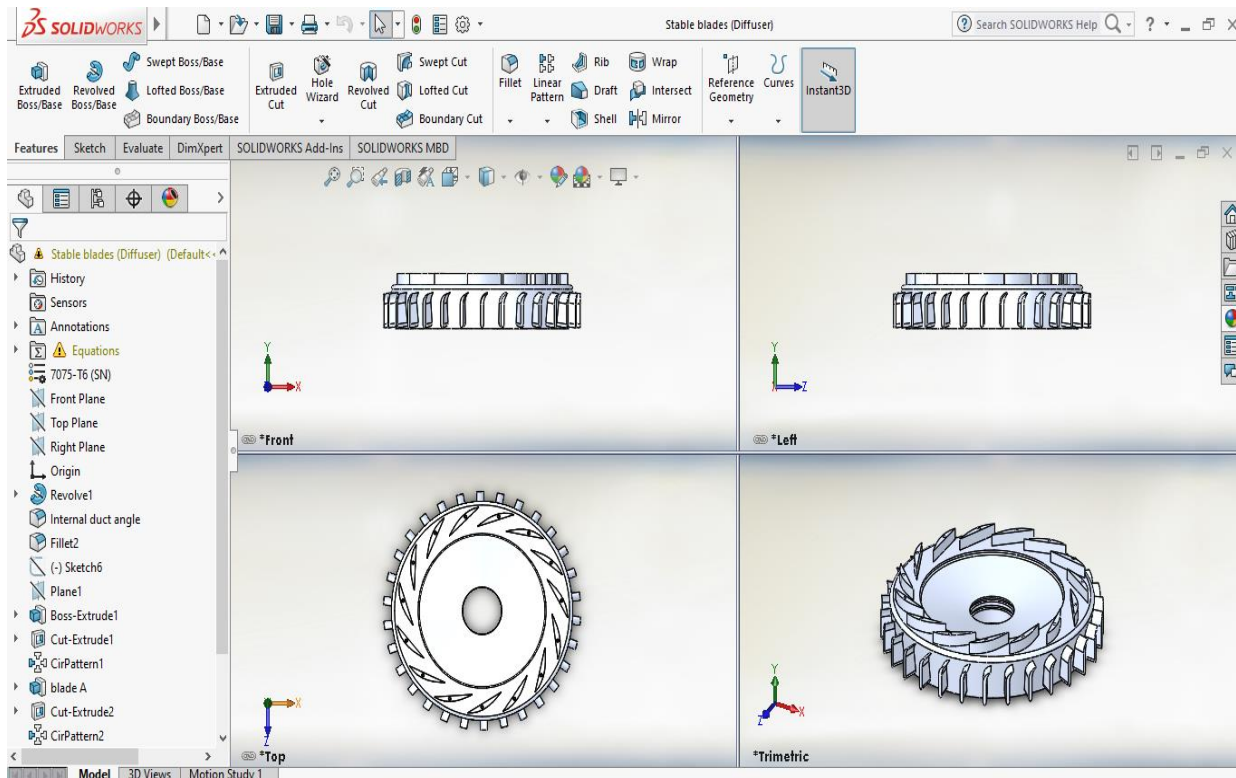
Figure 38: Four-view depiction of the diffuser's digital model.

3.6 Assembly

With the appropriate mates between the parts, an assembly was produced, as shown in Figures 39, 40.
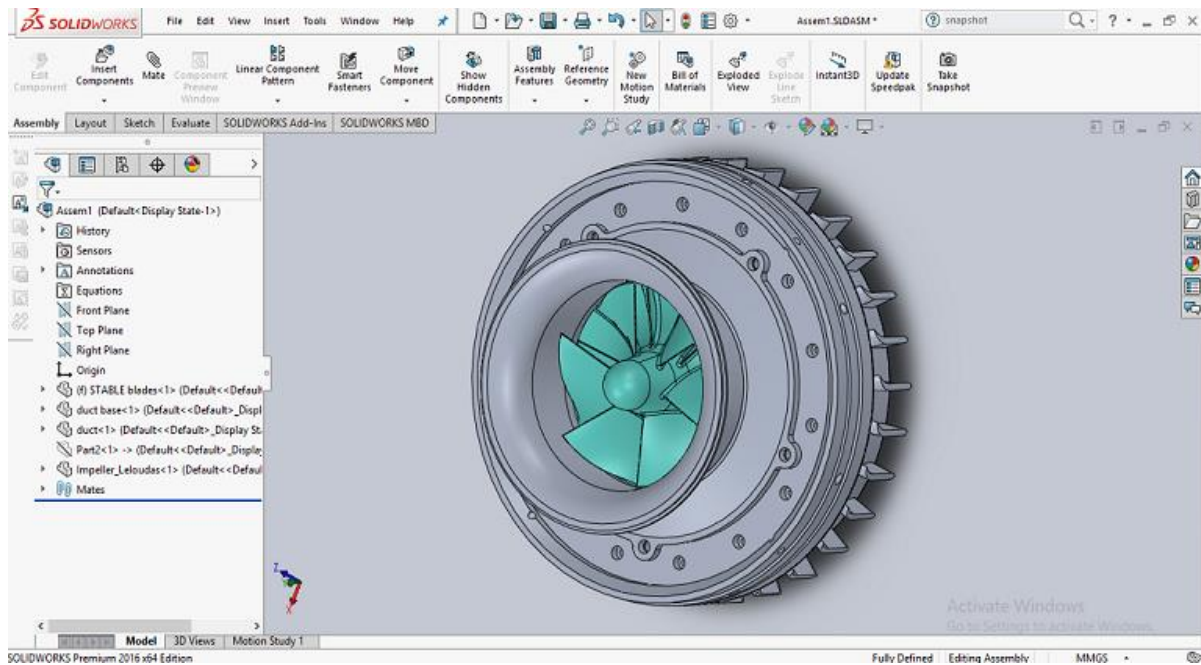
Figure 39: The assembly of all parts.
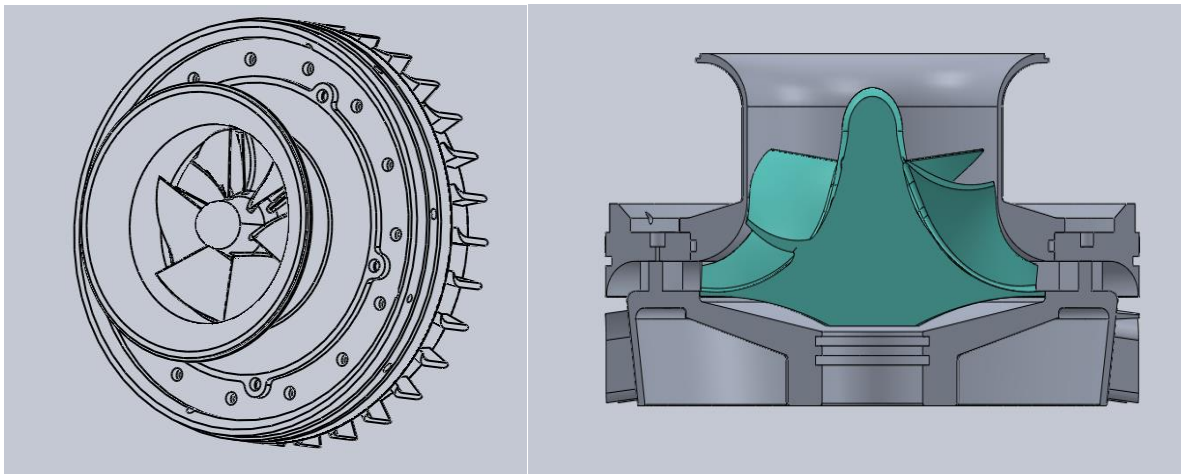
Figure 40: Sectional view of the assembly.

The next step after completing the assembly is to create the fluid domain. The fluid domain is defined using Boolean subtraction. The fluid domain is shown in Figures 41 - 45.
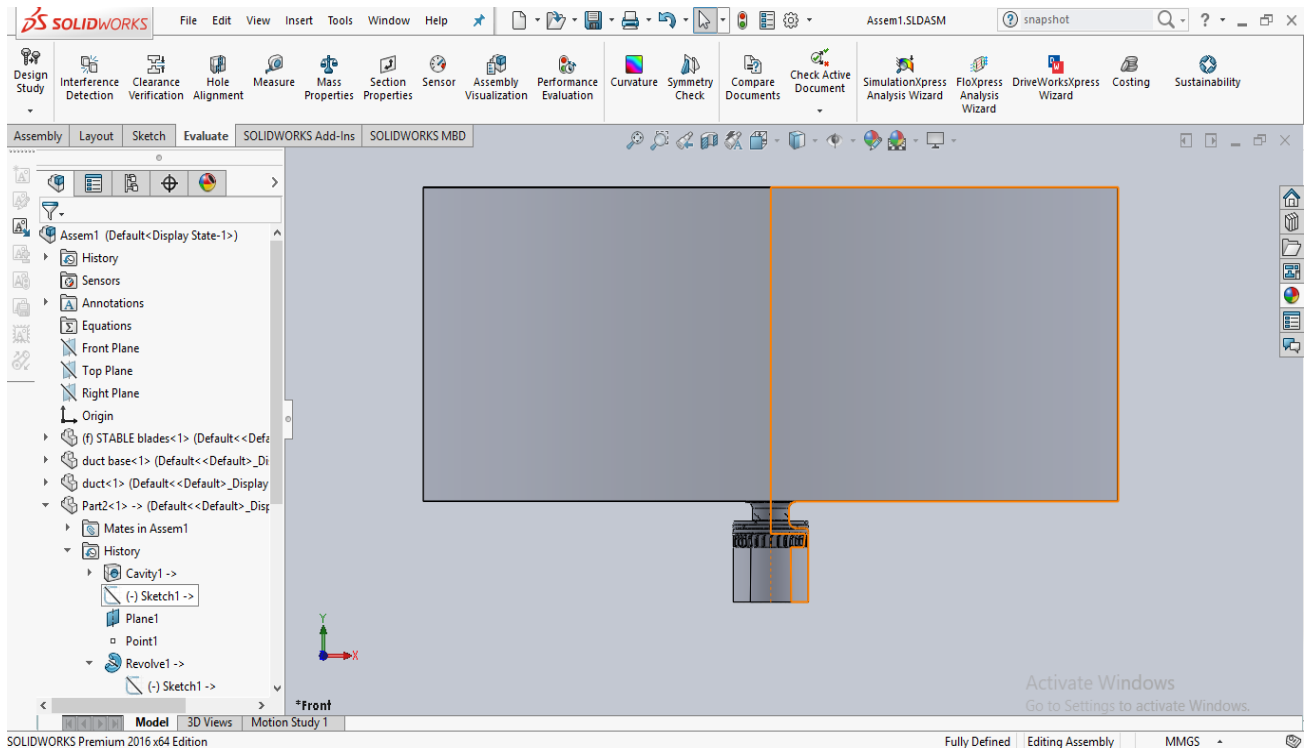
Figure 41: Illustration of the flow domain.
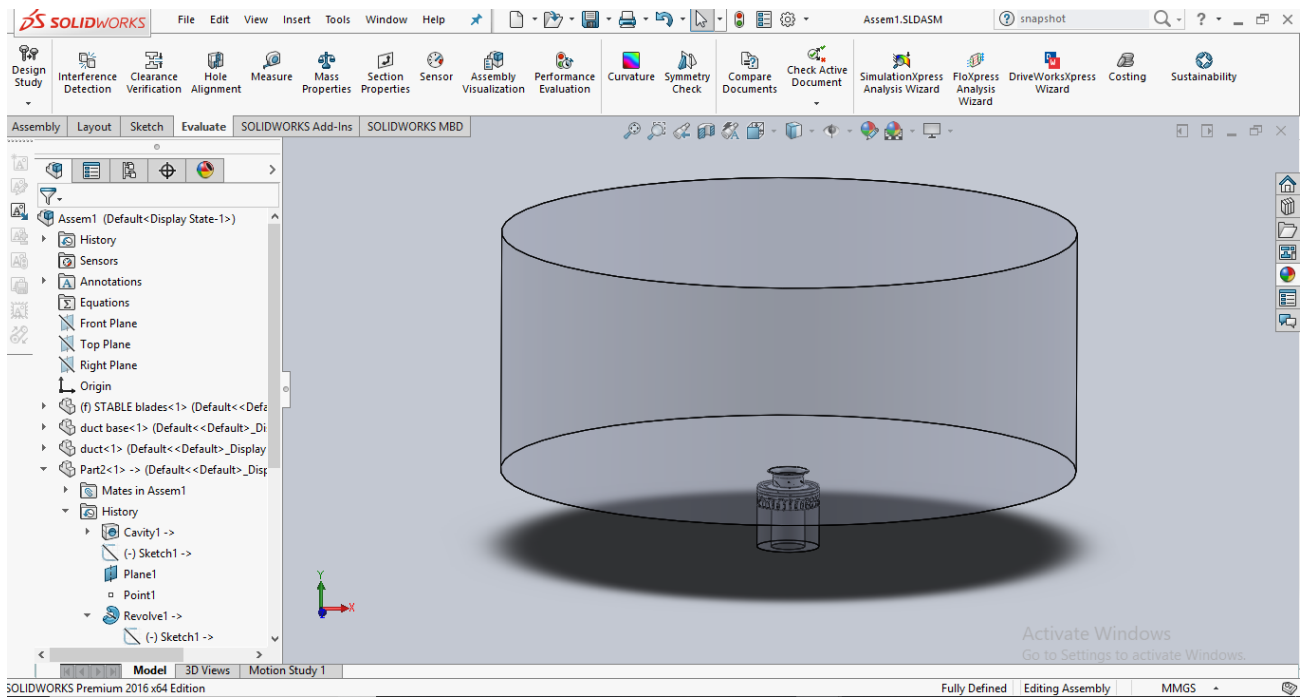
Figure 42: General view of the flow domain.
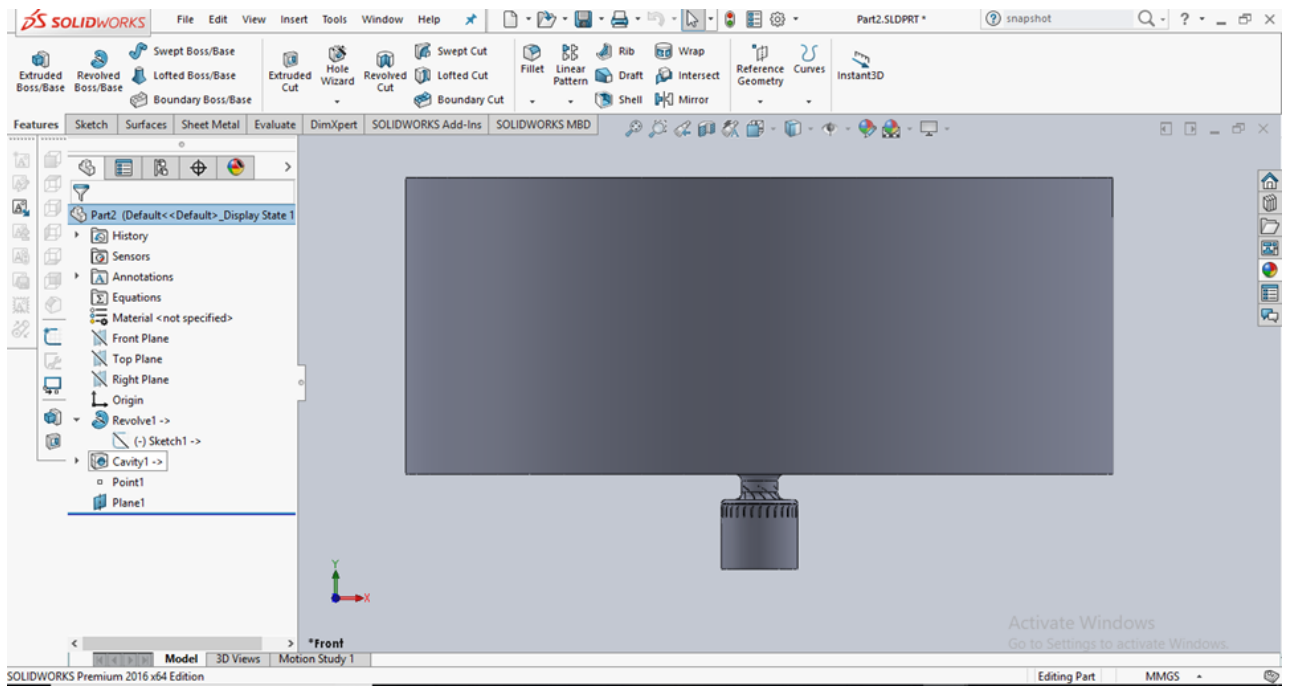
Figure 43: Creation of the flow domain.
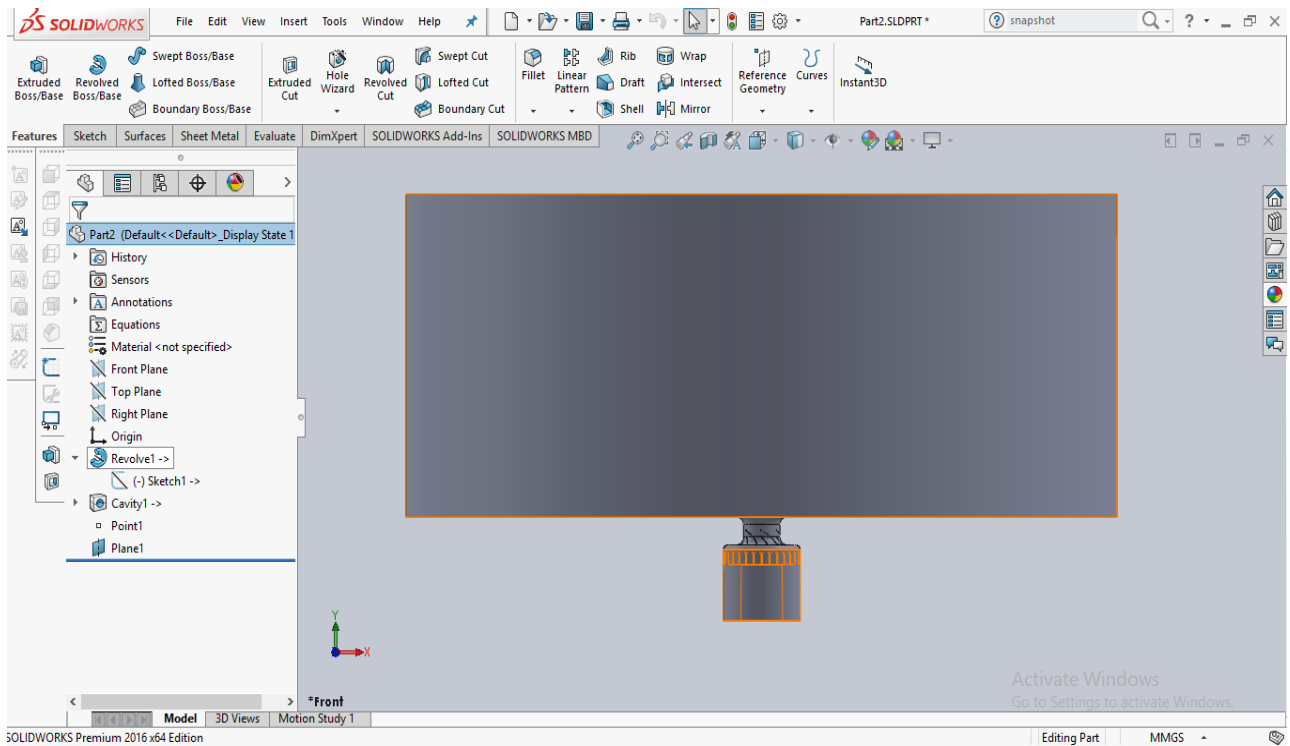
Figure 44: The flow domain.
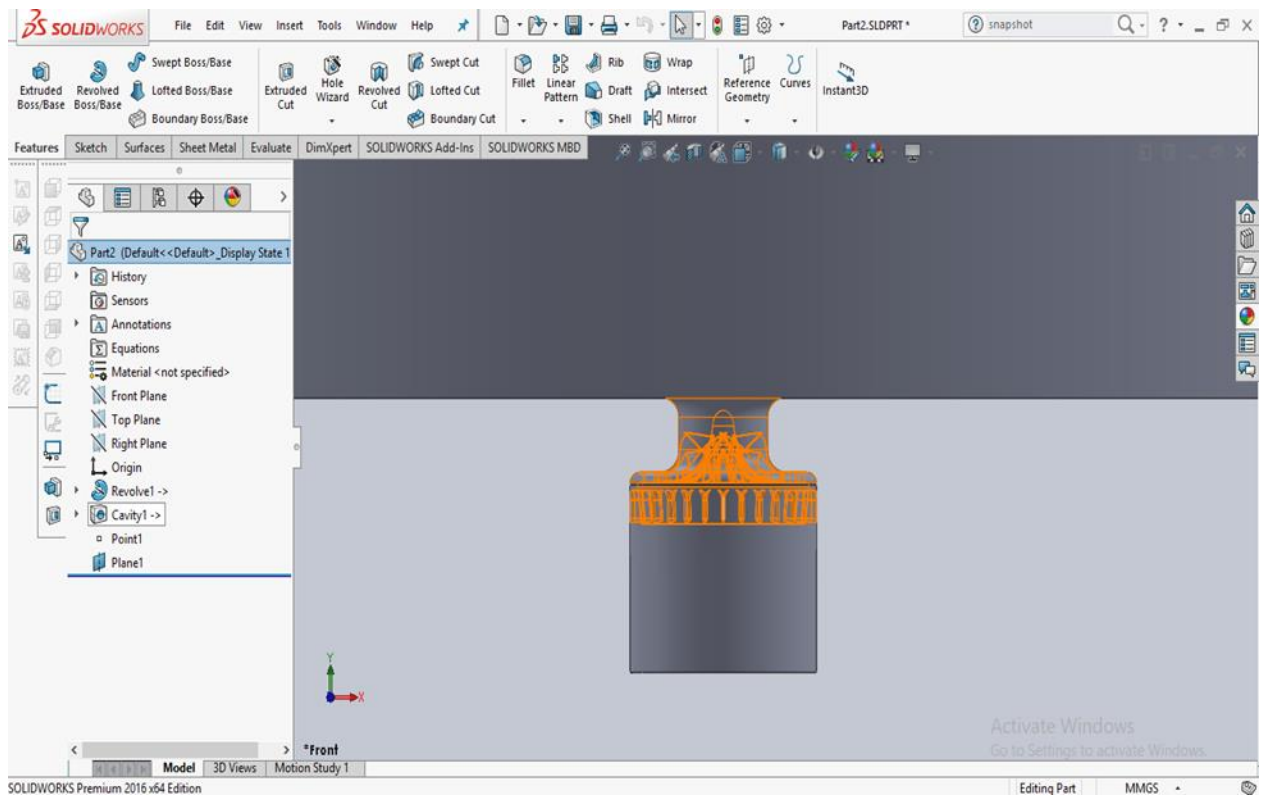
Figure 45: Close view of the flow domain, where the details of the impeller and the diffuser are shown.

4. Geometry import and meshing

4.1 Geometry import

The .stp file of the flow domain was imported to ANSA mesh-generation software (Figure 46). The ANSA environment consists of several different modules: "Topo" is used for geometry clean up; "Mesh" is used to generate surface mesh; "Volume Mesh" is used for the generation of solid and 3D mesh; "Decks" (Solver) includes different solvers; "Morph" module is an advanced tool to manipulate geometry.

Clicking on the first module the user is transferred to the **"Topology"** interface. This interface (Topo menu) offers the ability to change and improve the geometry of the surfaces, the curves and the connection of points. A properly cleaned up geometry is the key prerequisite for a well-defined mesh model. The following figures demonstrate the steps that should be taken in order to prepare the imported geometry for further analysis.
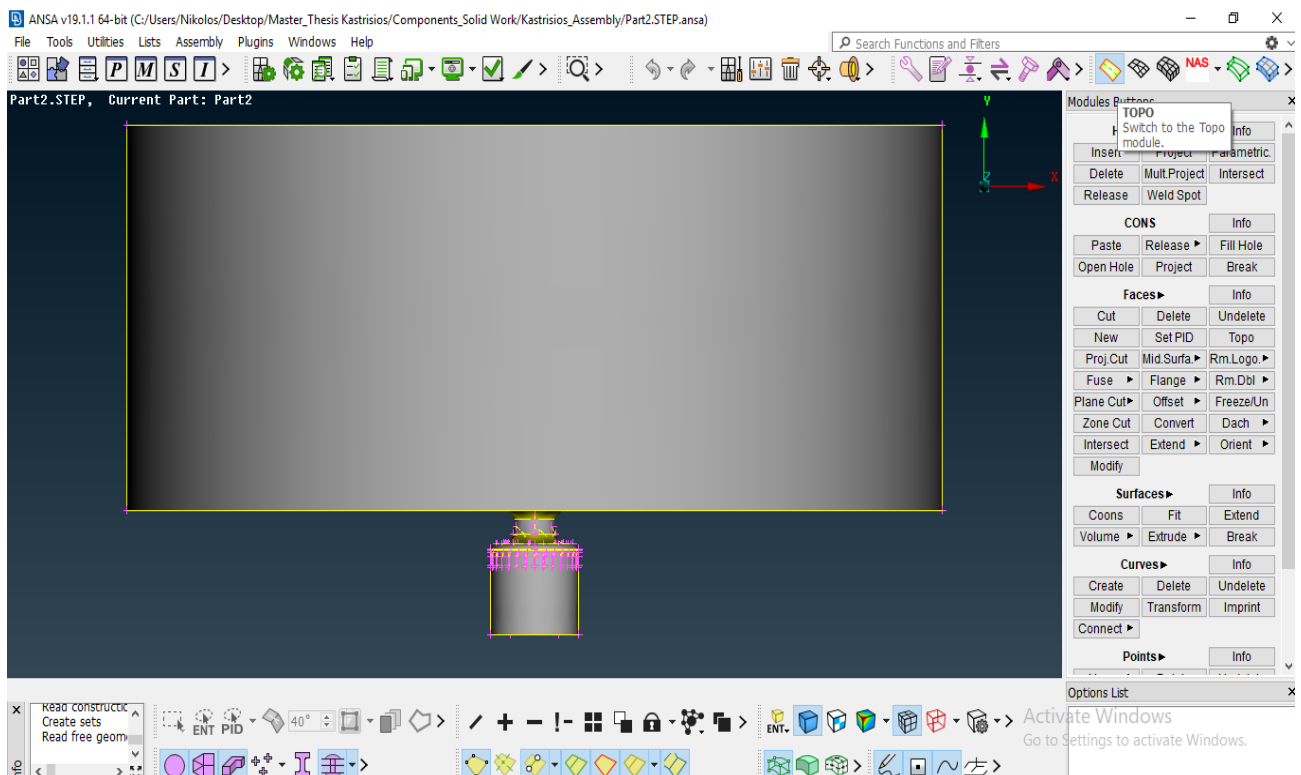
Figure 46: Ansa-Topo menu.

At the "Topo" module the first step is to modify the orientation of the faces with the command "Orient". Selecting this command is for identifying which side of the faces is the positive (front) and which the negative (back) one. The software depicts the front side with a

gray color and the back with a yellow one (Figure 47). These colors can be changed from the software settings.
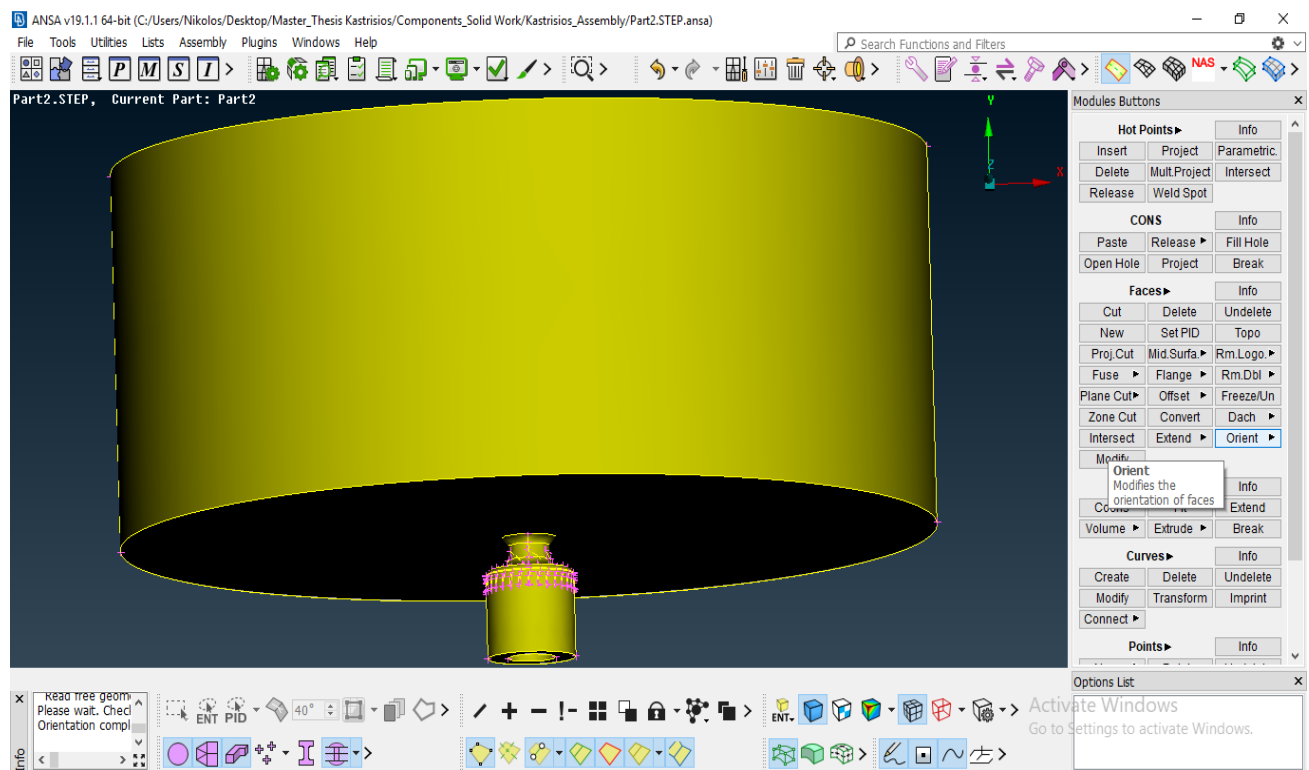
Figure 47: Orientation of the faces.

4.2 Surface mesh

Switching to the **"Mesh"** module the model is ready to be meshed. The first step is to fix the perimeters of the geometry before meshing. The model consists of 430 surfaces that will be meshed. Each surface has to be meshed properly to take the best results during the analysis. An appropriate mesh is the key for an effective and accurate simulation of the flow and determines the cost of the simulation. The meshing of flow domains is a tricky procedure in turbomachinery, because of the edges of blades and the corners in the flow channels.

The main step is to define the distance and the spacing of the elements. With the command "Perimeters/Length" or "Spacing" the definition of the elements' size is achieved, as well as the definition of the distance between points that produce the elements. Furthermore, during this process the minimum and the maximum size of the elements are defined, either using Length or Spacing.
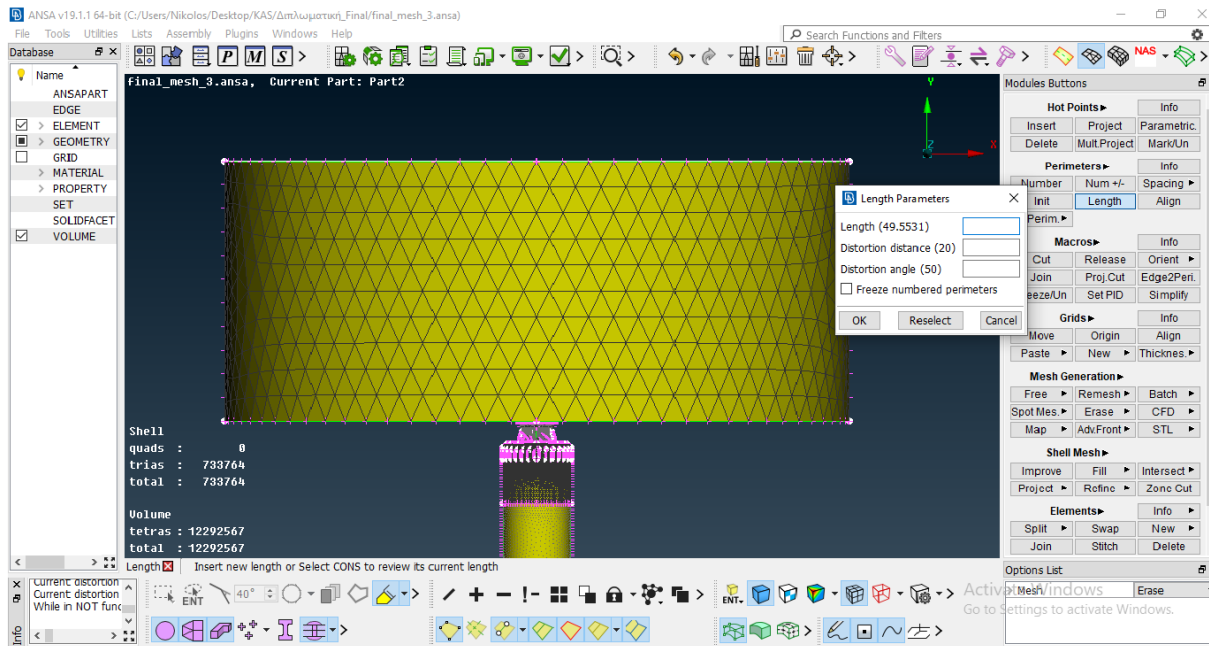
Figure 48: Perimeters/Length or Spacing process.

Selecting the "Length" command a window of "Length Parameters" definition is shown (Figure 48), where the user defines Length, Distortion distance and Distortion angle of the elements. Choosing Spacing/Auto CFD the distribution of the elements depends on the geometry of the selected curve and the elements are not necessarily at the same distance. It is possible to select either a specific curve or a macro section. During this mesh procedure both of these techniques were used, to achieve sufficient spacing at the curves of the flow domain. It is worth mentioning that this step is of high importance to build a satisfactory and qualitative mesh of the surfaces.

After completing this step, the next one is to create the elements through the CFD Command, (Figure 49). Selecting CFD, it is possible to select the surface or the macro, in which mesh will be created. To accomplish that, few parameters are required to be defined at the options list menu. The element type for this analysis is the triangle. In addition, interior growth rate, distortion angle, minimum and maximum target length are defined. The definition of the said parameters at the option list is different at the curves or/and the parts of the assembly, depending on the thickness of the mesh that is required. For example, the mesh at the impeller blades is required to be very thick, due to the complexity of the flow across the blades.
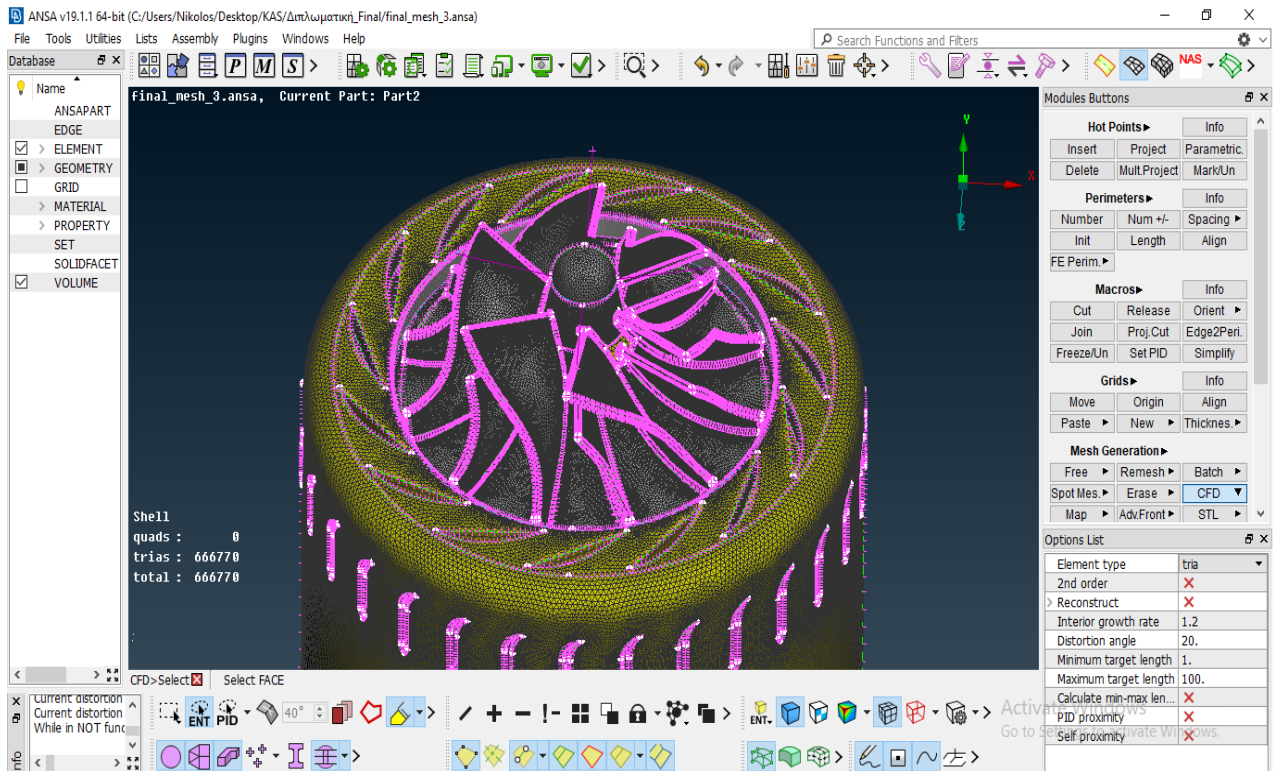
Figure 49: Creation of the triangles- CFD Command.
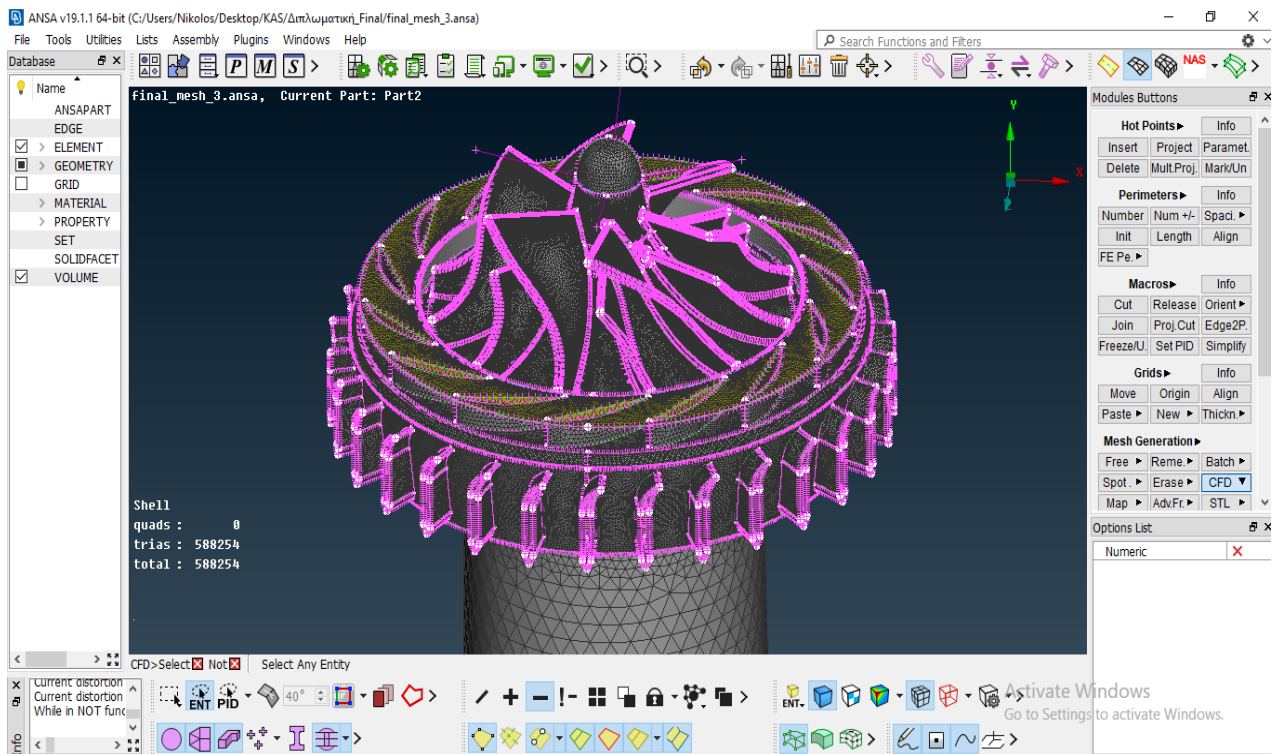
Figure 50: Thick mesh definition inside the impeller and the diffuser.

The final mesh of the surfaces consists of 733,764 triangles and the satisfactory quality of the mesh leads to the next step, namely the **"Volume Mesh".**
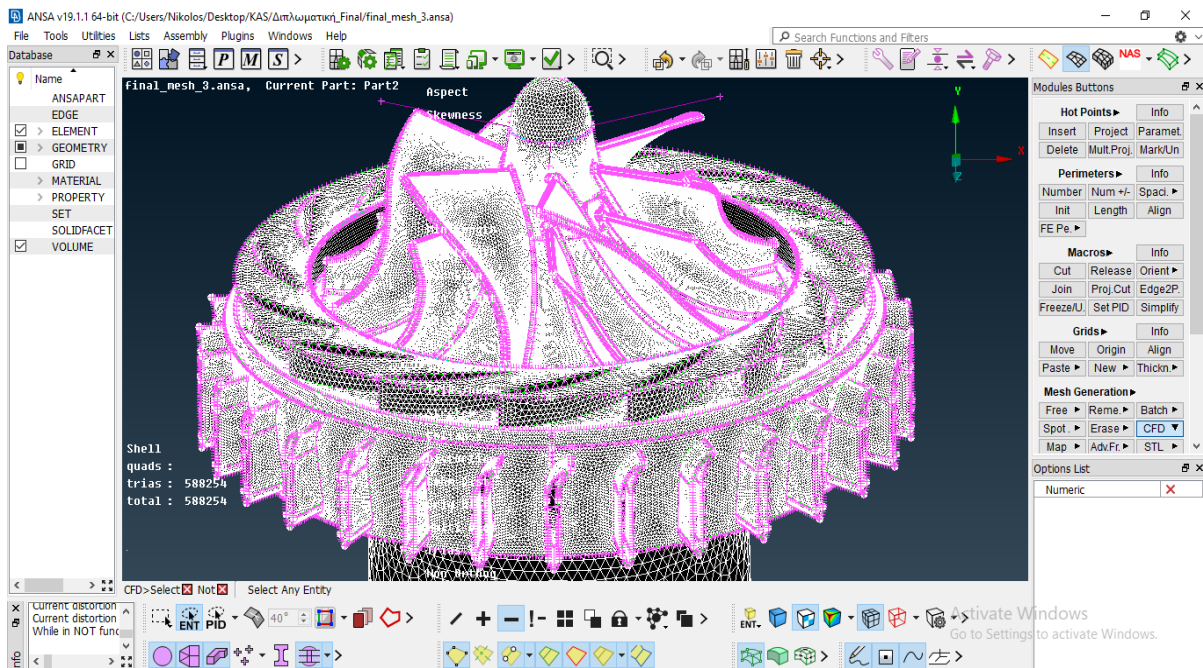
Figure 51: Overview of the surface mesh.

4.3 Volume mesh

Switching to the "Volume mesh", this module is used to create tetra elements based on the surface mesh. From the "Unstructured Mesh" options, "Tetra Rapid" is selected to mesh the volume with tetrahedral elements. Before creating the volume mesh a few additional modifications are to be accomplished. For the analysis of the flow inside the centrifugal compressor, three different volumes are created. The first one is the volume until the inlet of the impeller, where the flow domain is stationary, the second one is the flow domain inside the impeller that will be a rotating one, while the last one is from the outlet of the impeller to the outlet of the assembly, which is also stationary. To achieve the separation of these domains-volumes some extra surfaces are designed using the "Topo" module and depicted at Figures below.
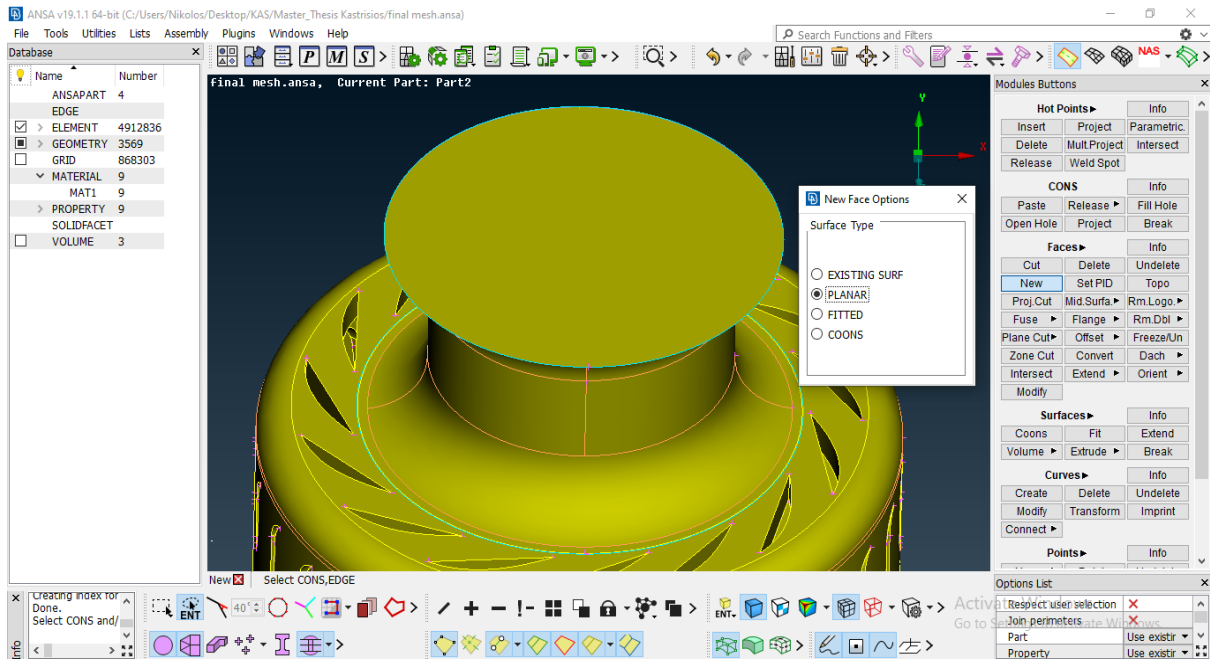
Figure 52: New surface creation for volume separation.

The cylindrical surface that is used for separation of the rotating domain is depicted in Figure 53. The final mesh with tetrahedrals is depicted in Figures 54 and 55. The number of the resulting tetrahedral elements is 12,292,567.
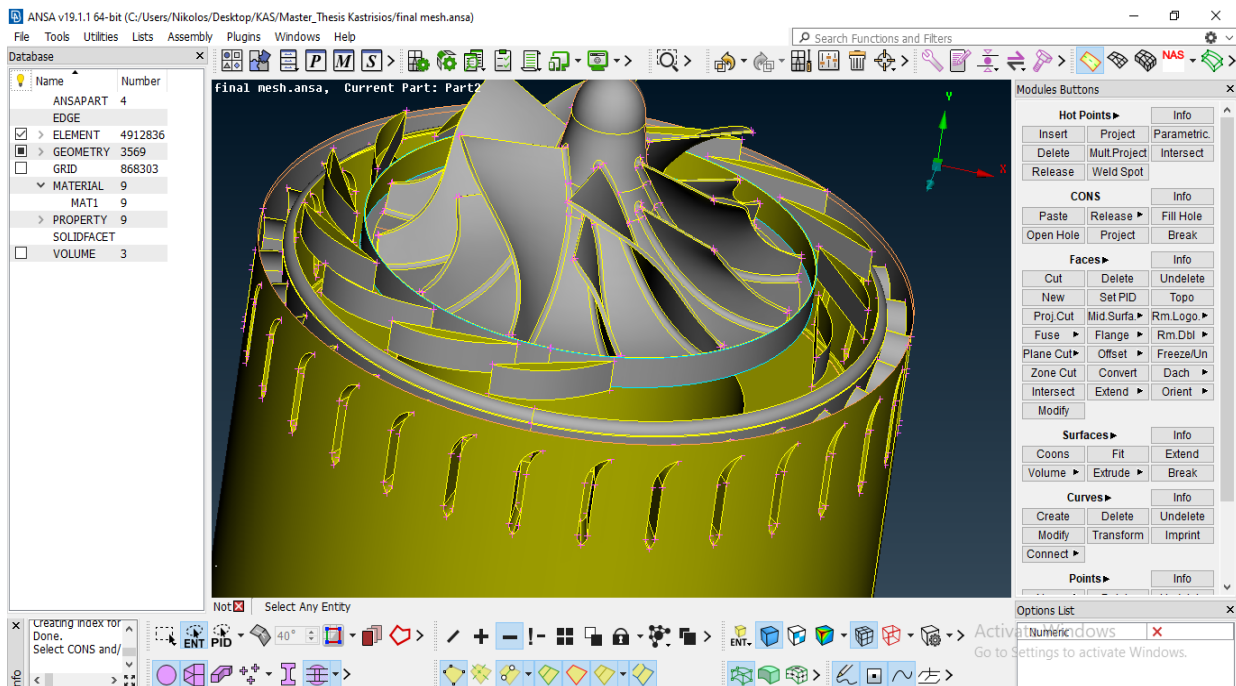
Figure 53: New circular surface for separation of the rotating domain.
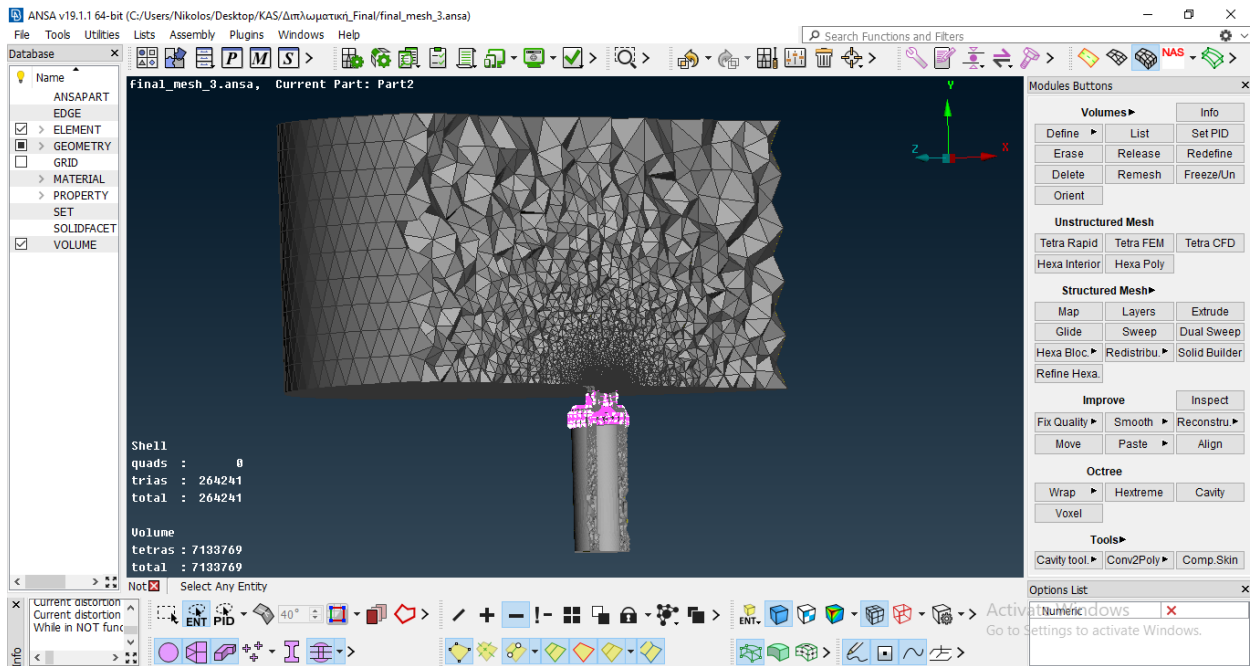
Figure 54: Final mesh-intersection of the entity.
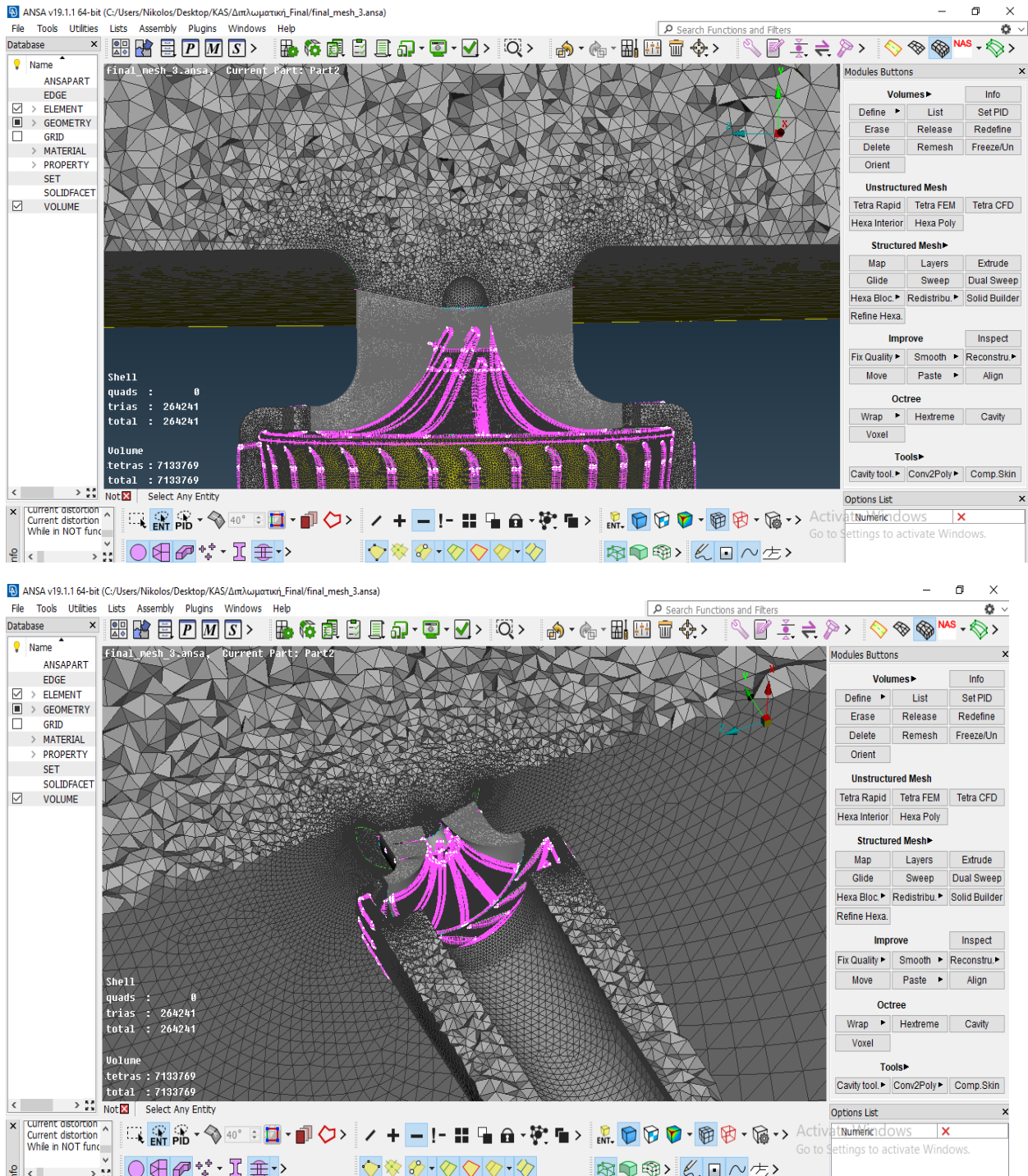
Figure 55: Closer view of the volume mesh.

An additional procedure is setting PIDS. Mainly, this step is about giving names to specific entities, in order to be identified by the CFX solver (Figure 56).
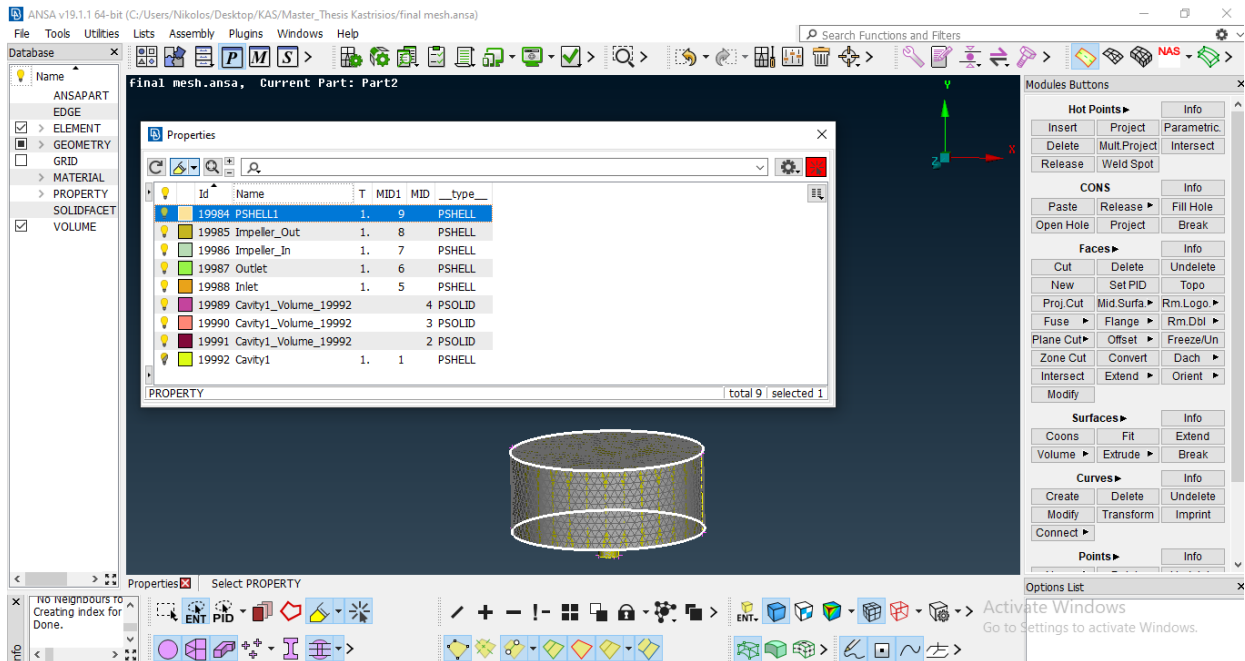
Figure 56: Setting PIDS.

The entities with PIDS are (Figure 56):

- Impeller inlet,
- Impeller outlet,
- Inlet of the assembly,
- Outlet of the assembly,
- The free flow.

Completing the above procedure in ANSA, the file, has to be extracted as a CFX file, as shown in Figure 57, ("File", "Output", "More", "CFX") in order to be recognized from the ANSYS CFX solver.
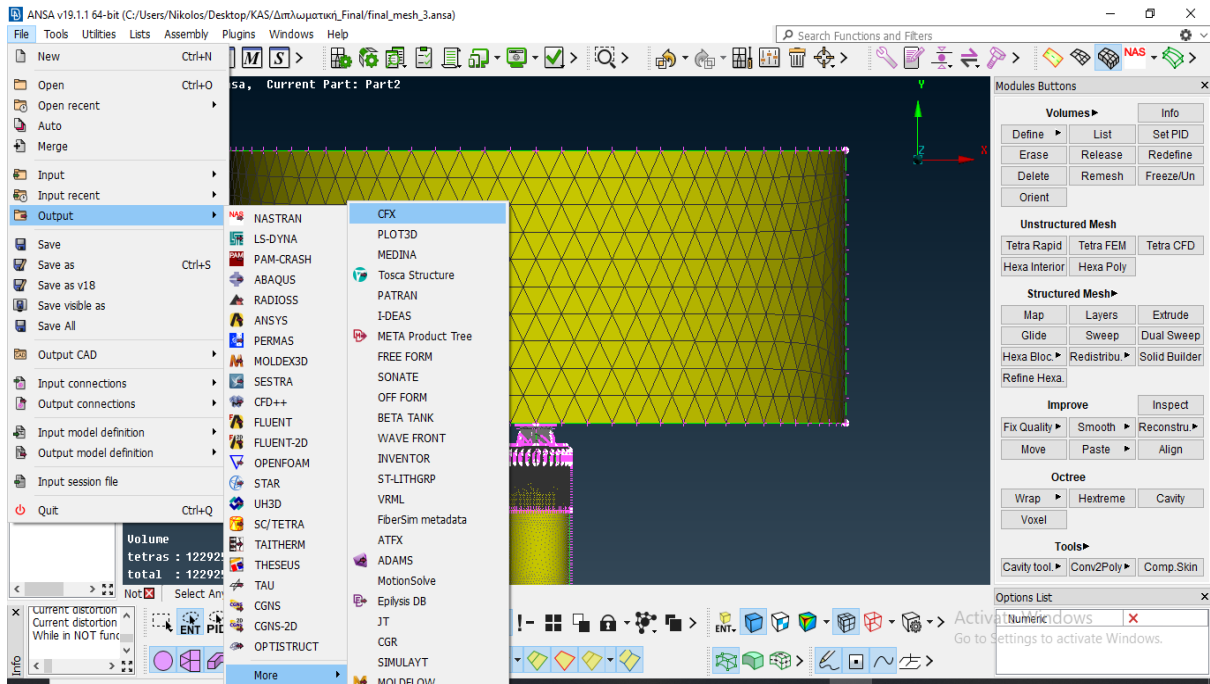
Figure 57: Output of the mesh as a CFX file.

5. Simulation setup

Simulation process is carried out using CFD Software ANSYS CFX. The simulation setup is described at this chapter and is defined as a steady state one. The computational domain is partitioned into the stationary inlet, the rotating impeller and the stationary diffuser with frozen rotor interfaces. The definition of these domains, the interfaces between them and the boundary conditions will help to achieve the flow domain analysis. First step is to insert the three (3) domains and name them properly as (Figures 58, 59):

- Impeller-Rotating Domain,
- Inlet-Stationary Domain,
- Outlet-Stationary Domain.
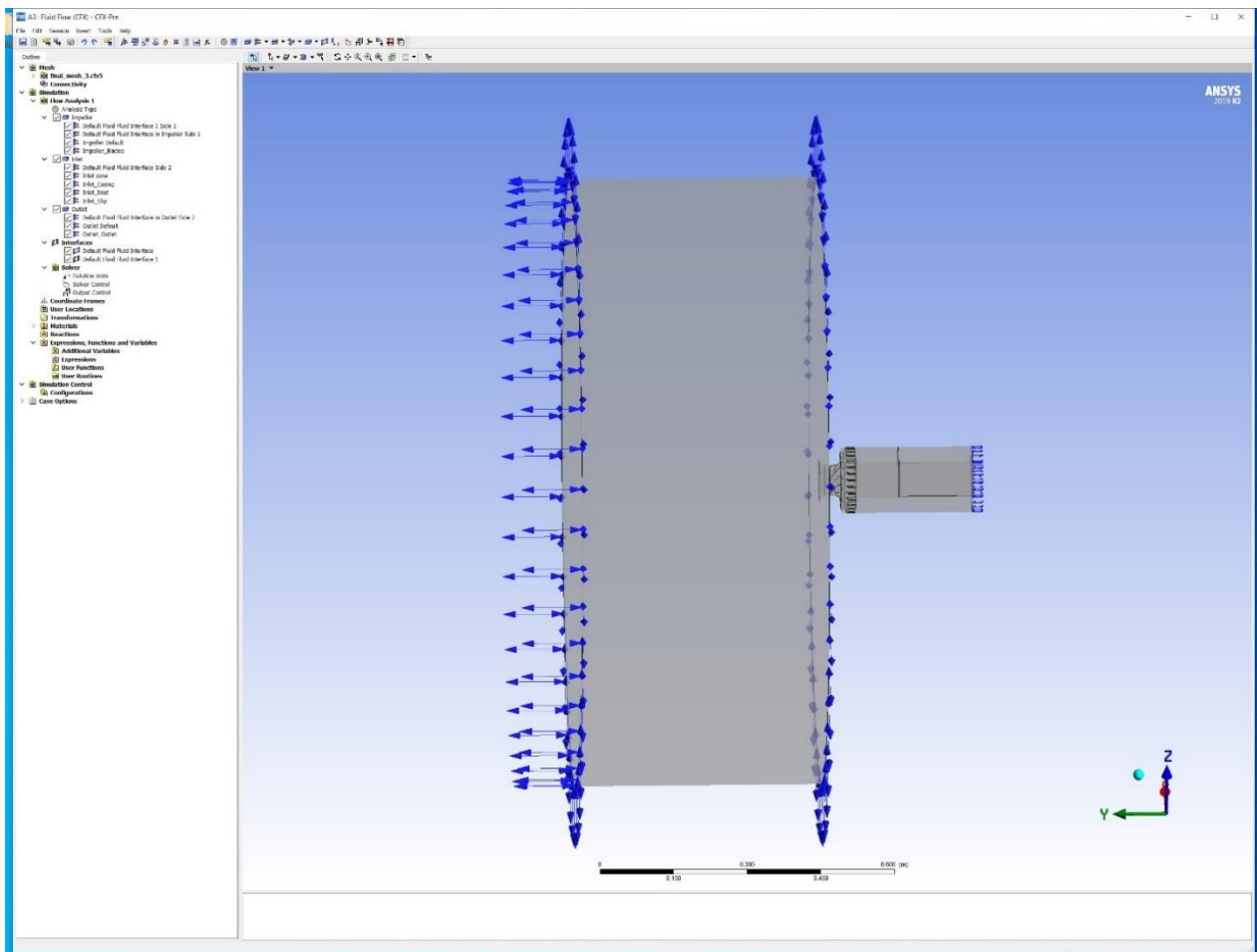
Figure 58: Domain's setup.
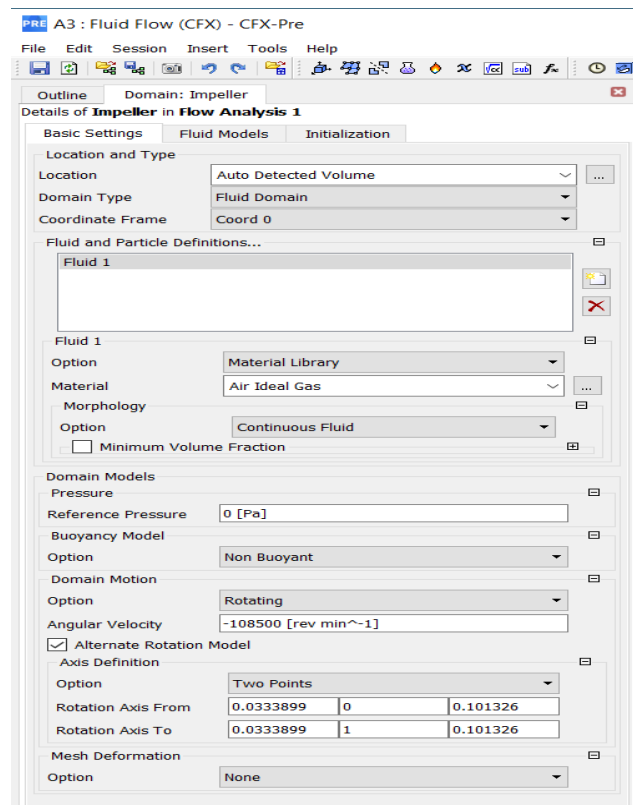
Figure 59: Setting Impeller as Rotating Domain.

Air is considered to be an ideal gas. The domain motion for the impeller is set as rotating and the velocity for the rotor is 108,500 rpm (Figure 24 - Specifications of AMT Olympus). For all domains, the SST (Shear Stress Transport) turbulence model was selected (Figure 60).
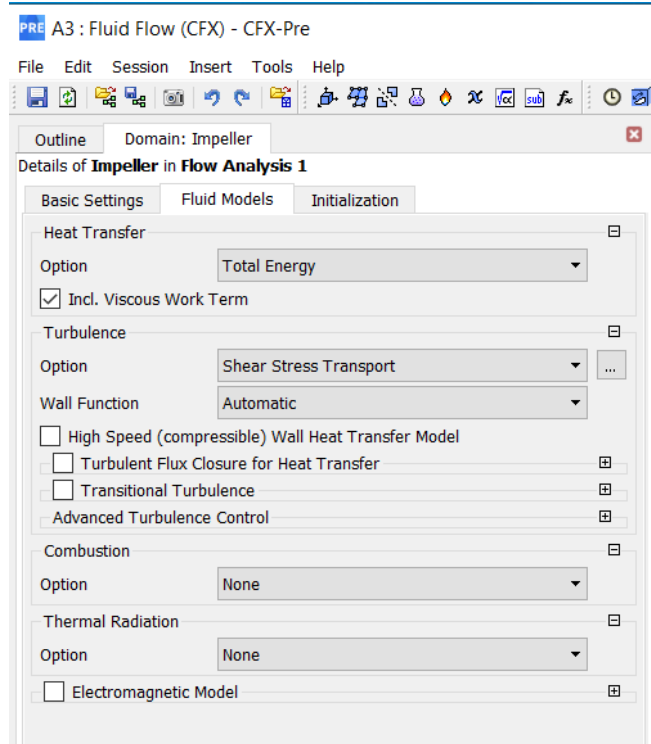
Figure 60: SST Turbulence Model for Impeller.
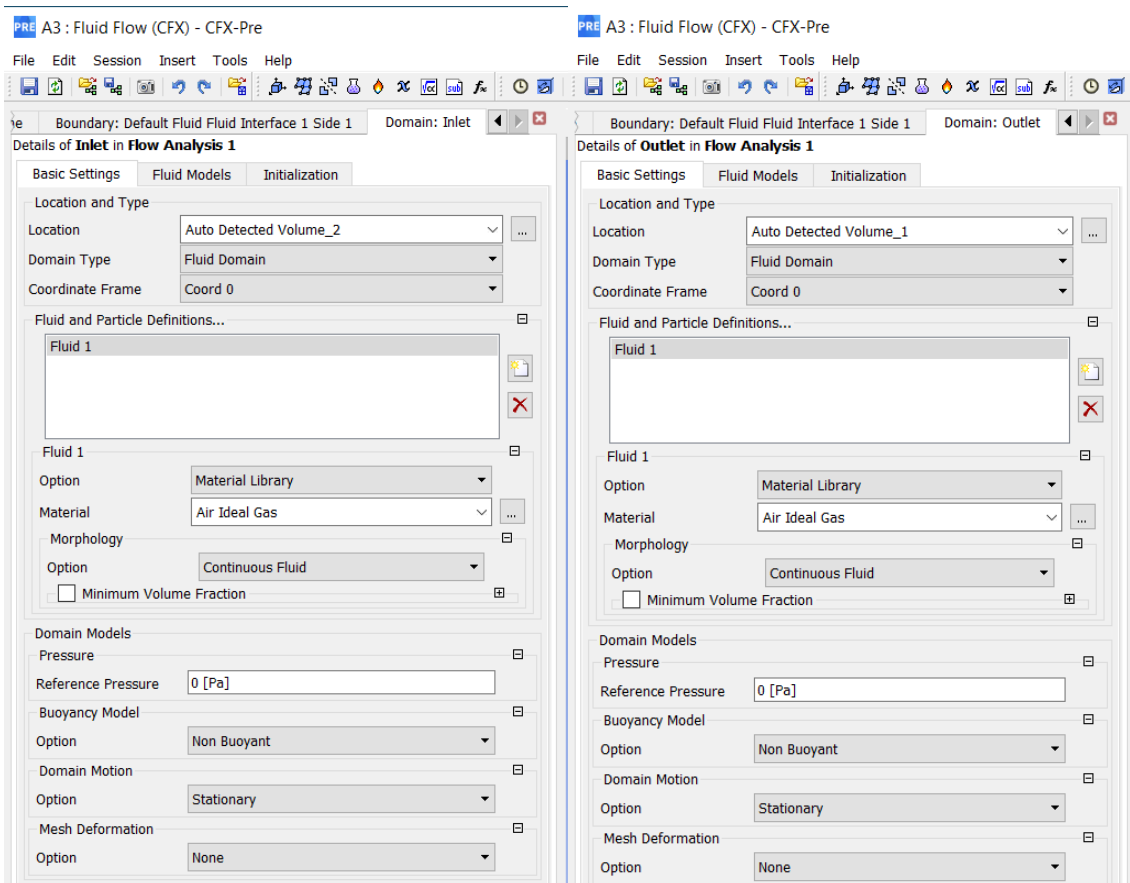
Figure 61: Inlet and Outlet domain settings.
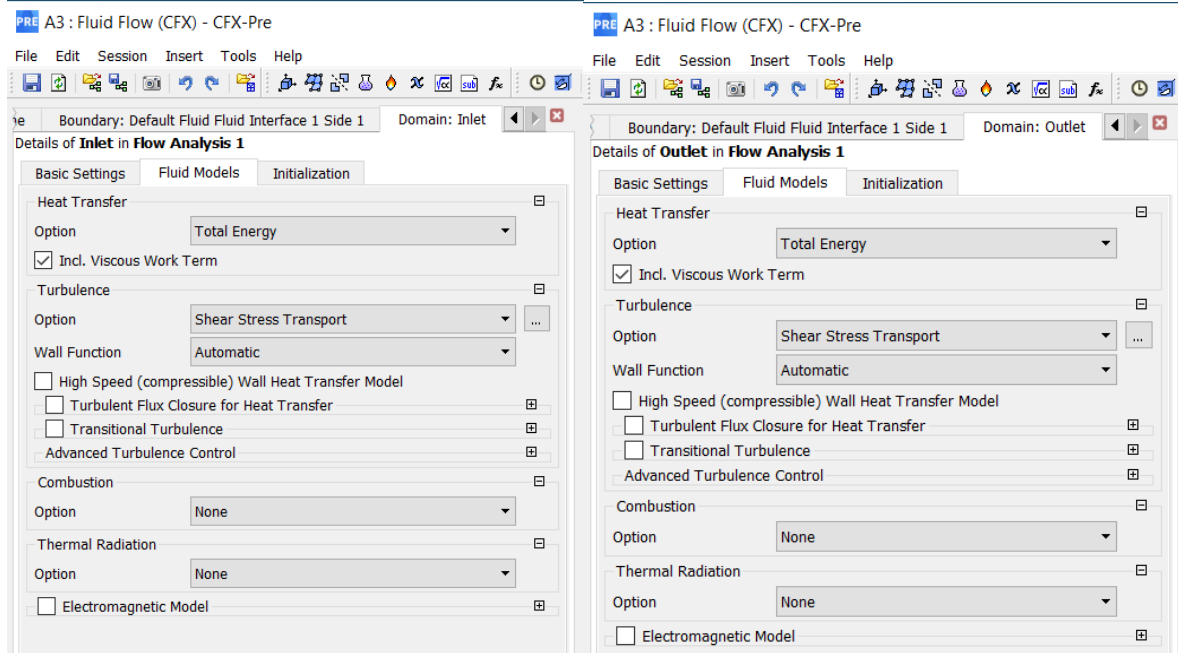
Figure 62: SST Turbulence Model for Inlet and Outlet domains.

The chosen SST model is widely used and has been validated for turbomachinery applications. It takes into account the transfer of shear stresses of the turbulence and gives accurate results around the detachment of the flow under adverse pressure gradients.

The model is robust to predict the basic local flow phenomena in a centrifugal compressor [*Gibson et al., 2017*]. The interface models between the rotating-Impeller and the stationary-Inlet and Outlet domains are set as "General Connection" and the mixing model as "Frozen Rotor" as shown in figures below.
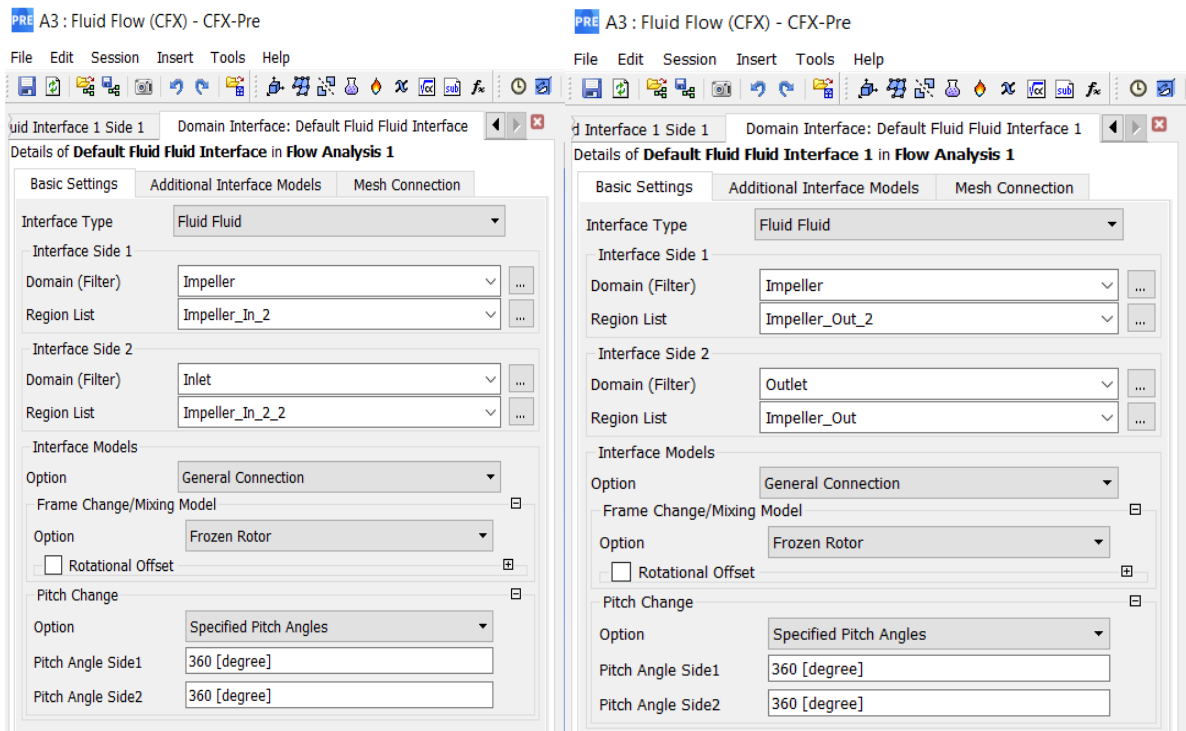
Figure 63: Interface models between domains.

The iteration number at the "Solver Control" was set to 5000 iterations, while the convergence criteria are of "Residual Type-RMS" with a residual target value of 1e-05 (Figure 64).
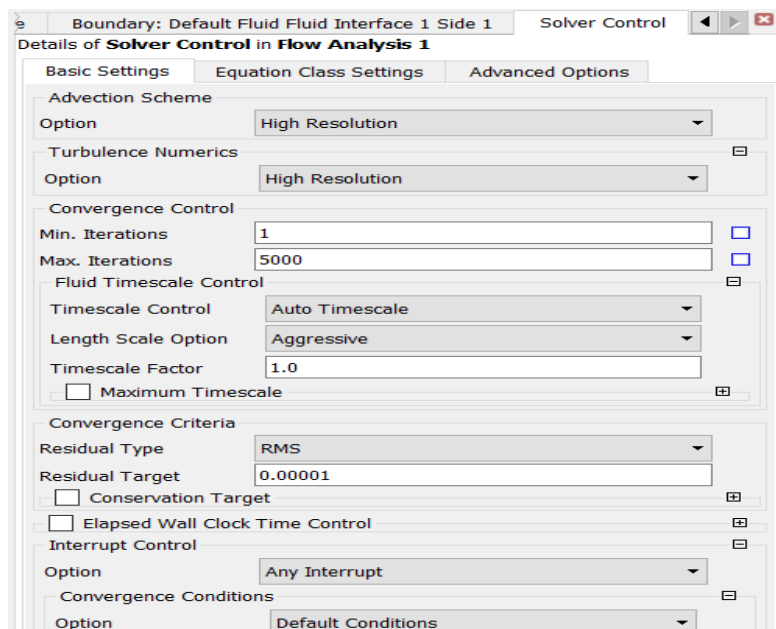
Figure 64: Solver Control Settings.

The following figures depict the interfaces between the inlet domain, the impeller domain and the outlet domain, along with the corresponding boundary conditions. These interfaces are used to separate the domains with each other. The blue and green vectors show that the corresponding boundary conditions have been applied.
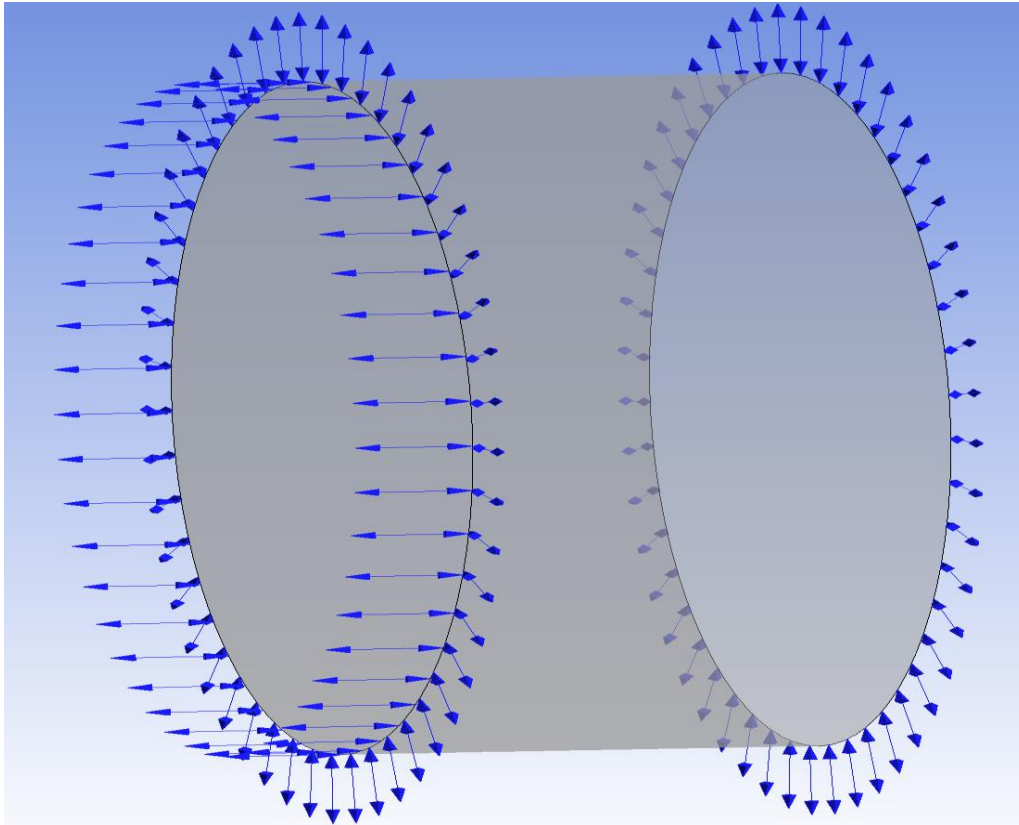
Figure 65: Inlet domain.
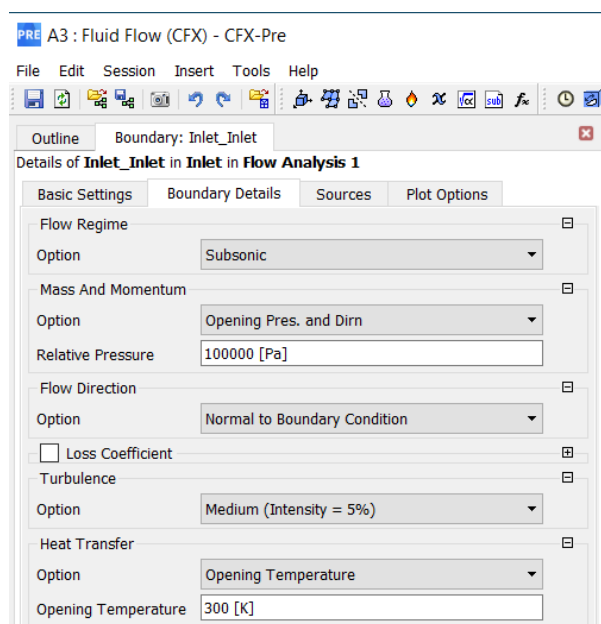
Figure 66: Inlet Boundary Conditions.

For the boundary conditions at the inlet, the flow regime option is subsonic and the Pressure and Temperature are set as 100000 Pa and 300 K, respectively, as well as a medium value of 5% turbulence intensity is selected (Figure 66).
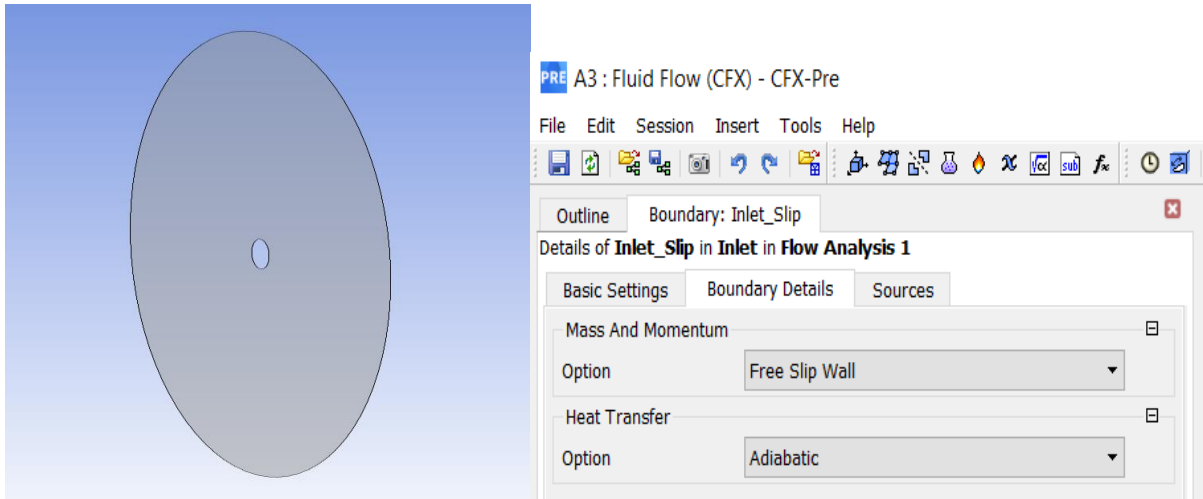
Figure 67: Inlet Slip Interface and Boundary Conditions.
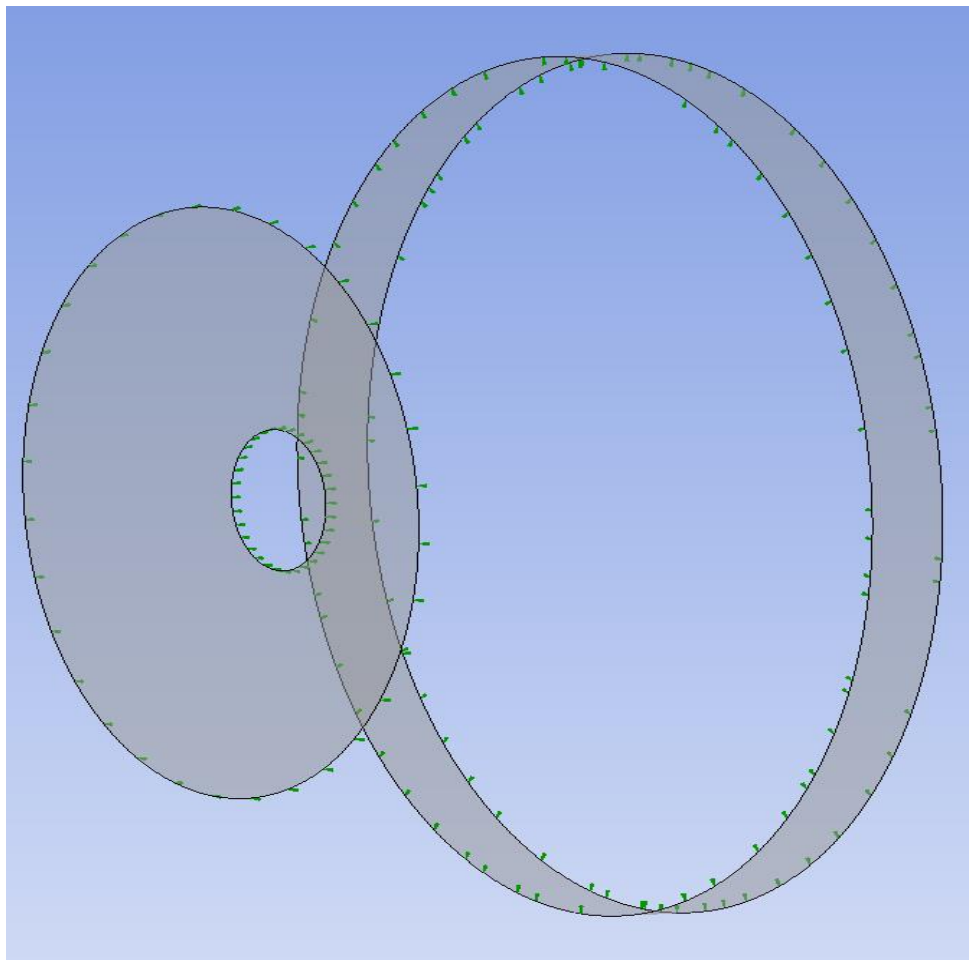
Figure 68: Impeller Interfaces.
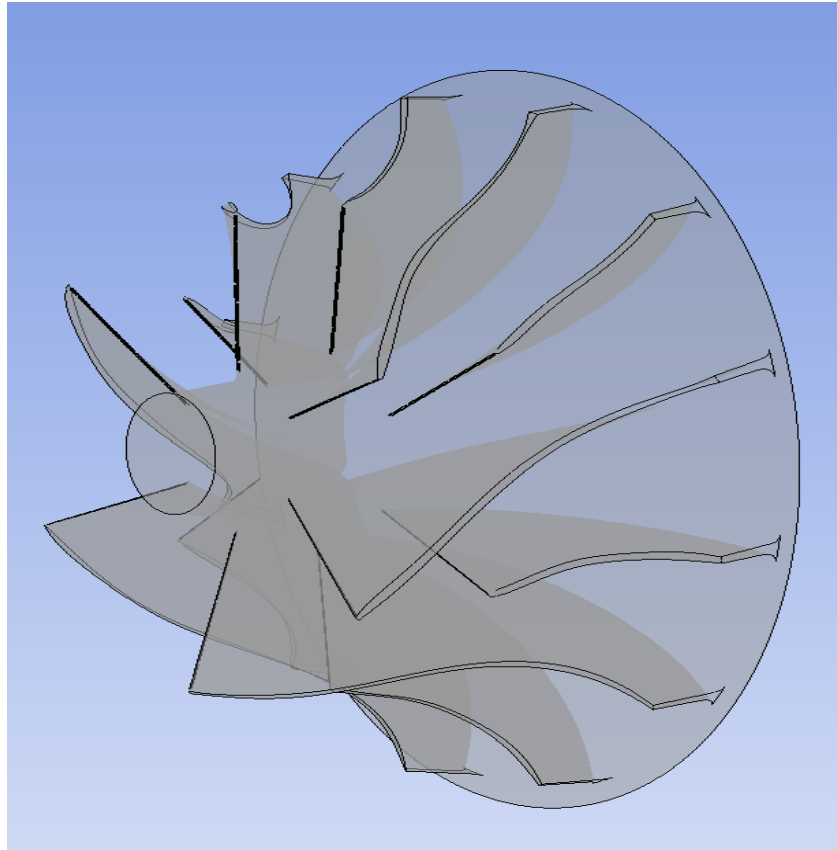
Figure 69: Impeller's solid surface.
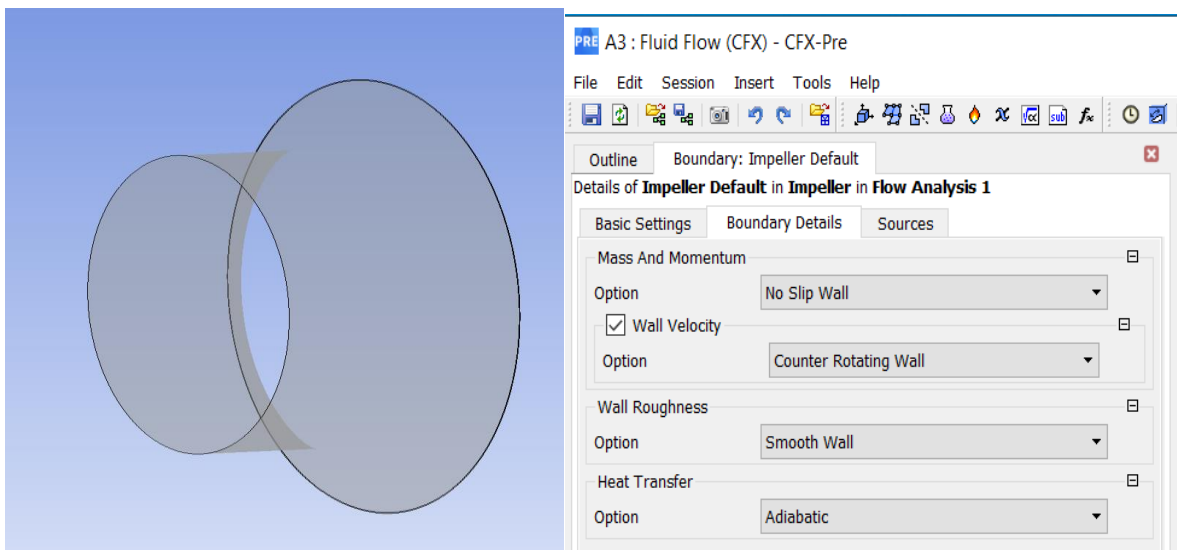
Figure 70: Impeller Default Boundary.

Adiabatic, smooth wall and no slip boundary conditions were applied at the impeller and counter rotating wall, for the wall velocity option.
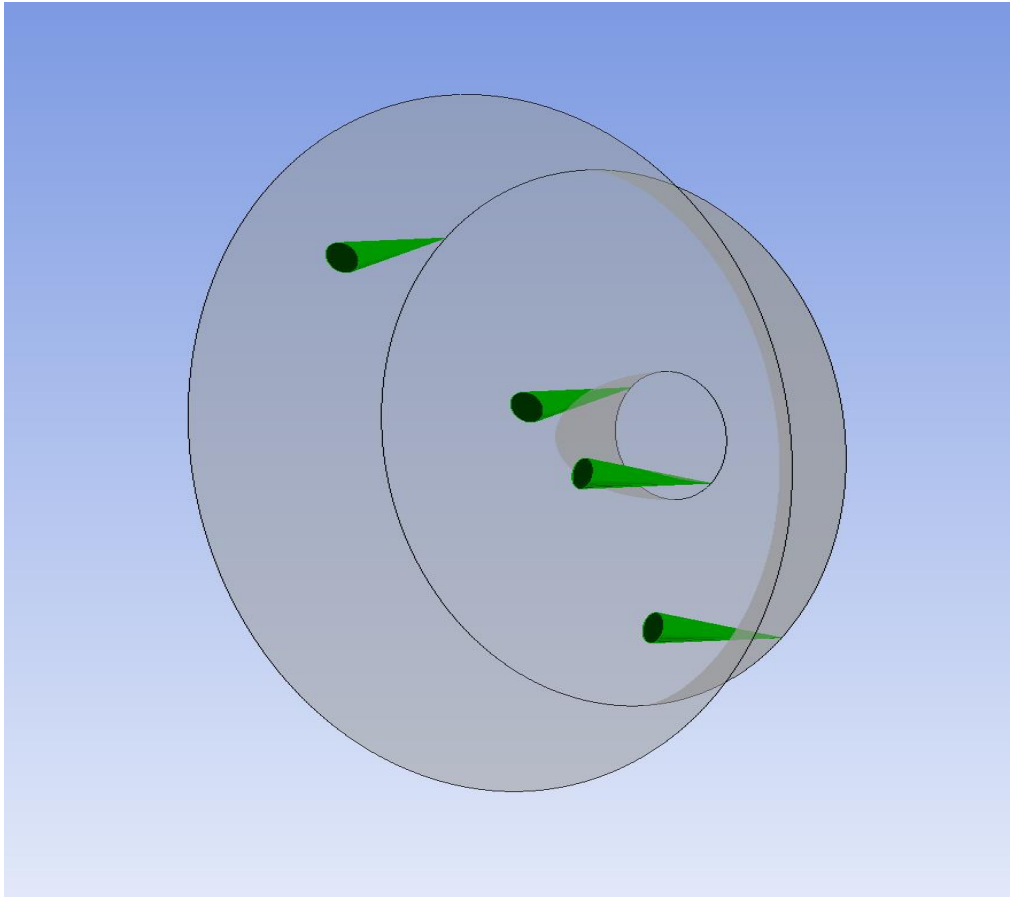
Figure 71: Inlet Casing, Cone and Interface.
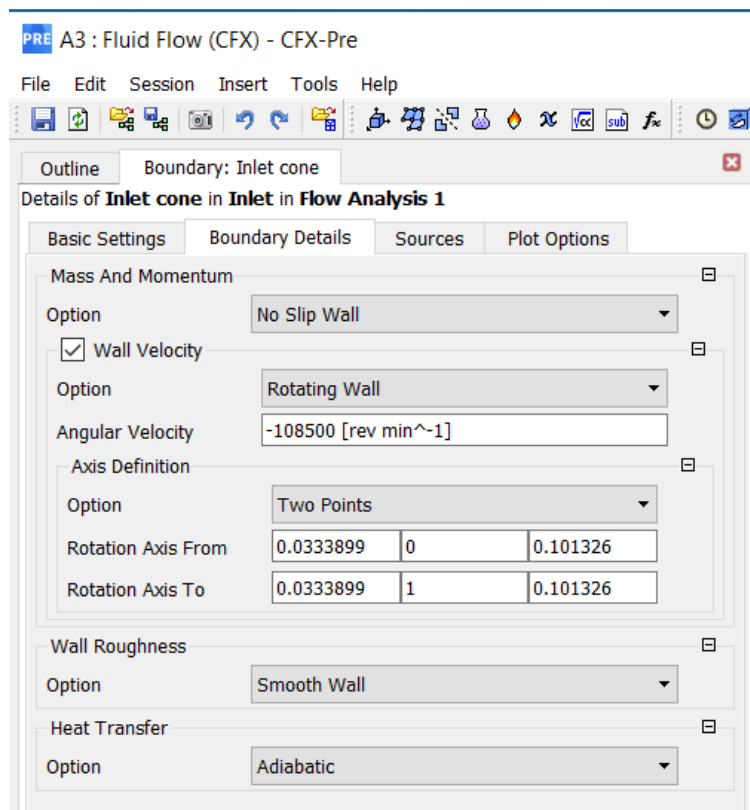
Figure 72: Inlet Cone Boundary Conditions.

At the inlet cone, rotating wall regime is applied and a velocity of 108,500 rpm.
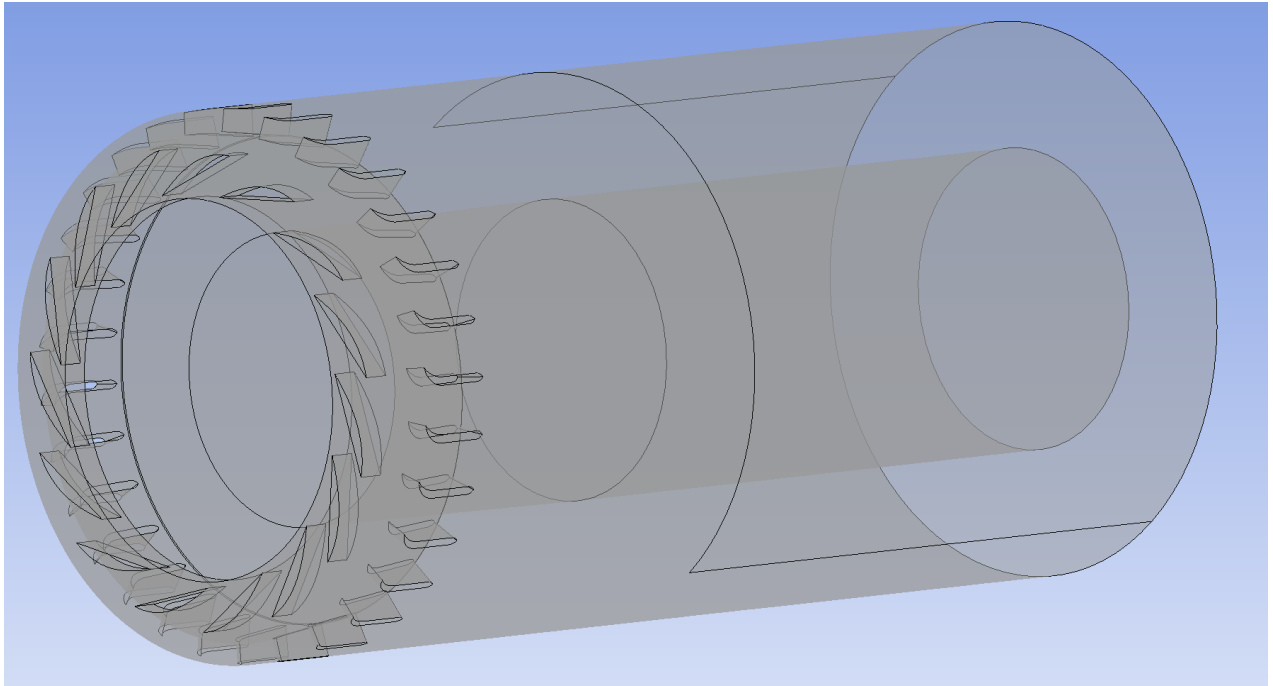
Figure 73: Outlet domain.
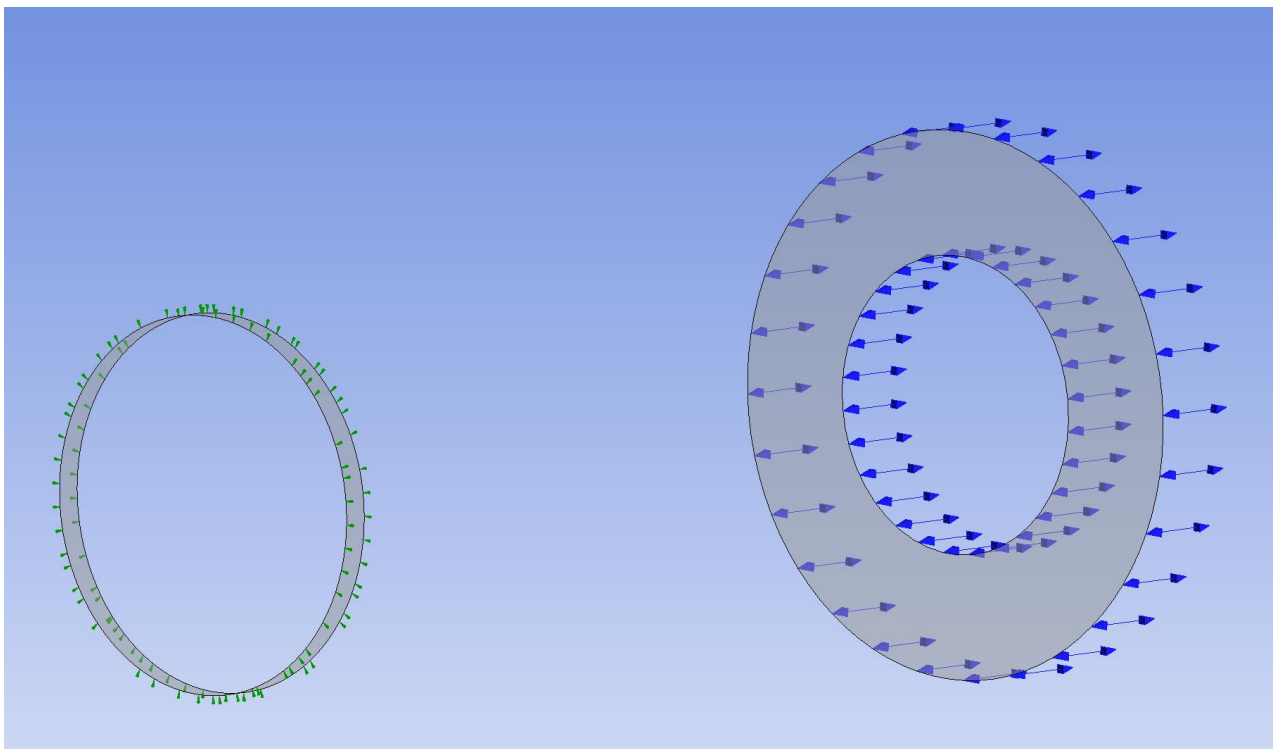
Figure 74: Outlet domain Interfaces.
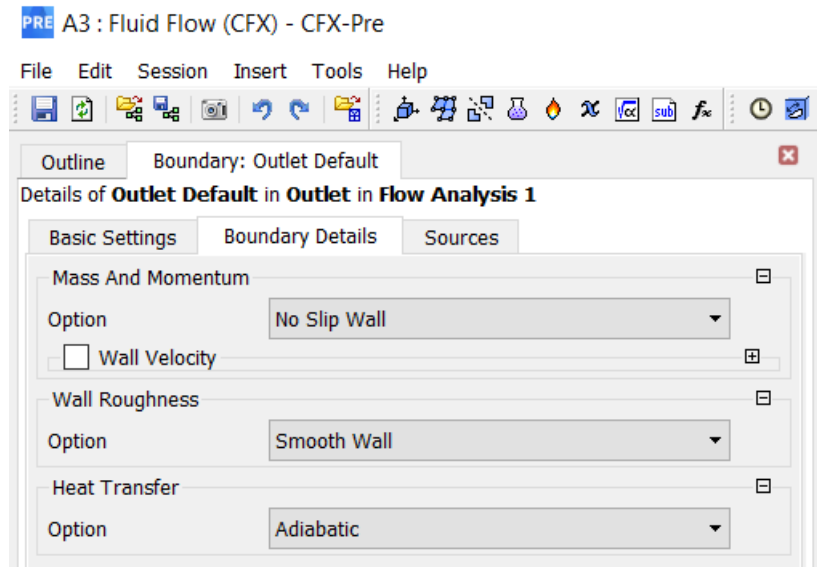
Figure 75: Outlet boundary conditions.
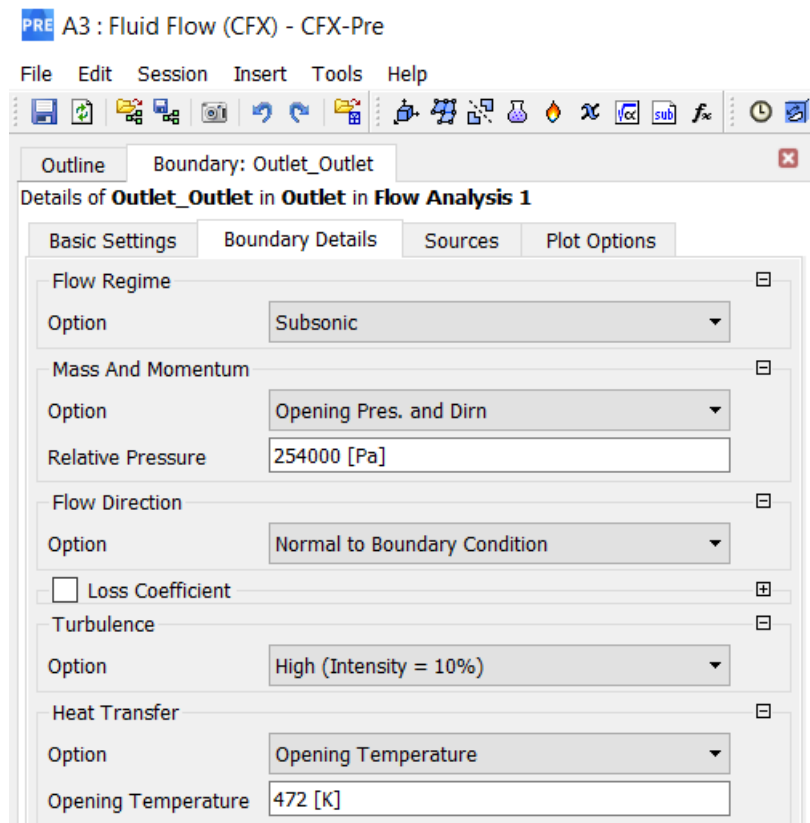
Figure 76: Outlet boundary conditions.

For the boundary conditions at the outlet, subsonic flow regime is selected, 254,000 Pa pressure and 472 K temperature and a higher turbulence intensity of 10%.

6. Simulation results and discussion

After completing the simulation at ANSYS CFX, the iso-contours of basic thermodynamic quantities are produced. The following figures depict the velocity streamlines, the distribution of static and total pressure at the casing and the impeller, as well as the correspondingly contours for the temperature. In addition, contours with distribution of pressure, temperature and Mach number are presented at sectional views.
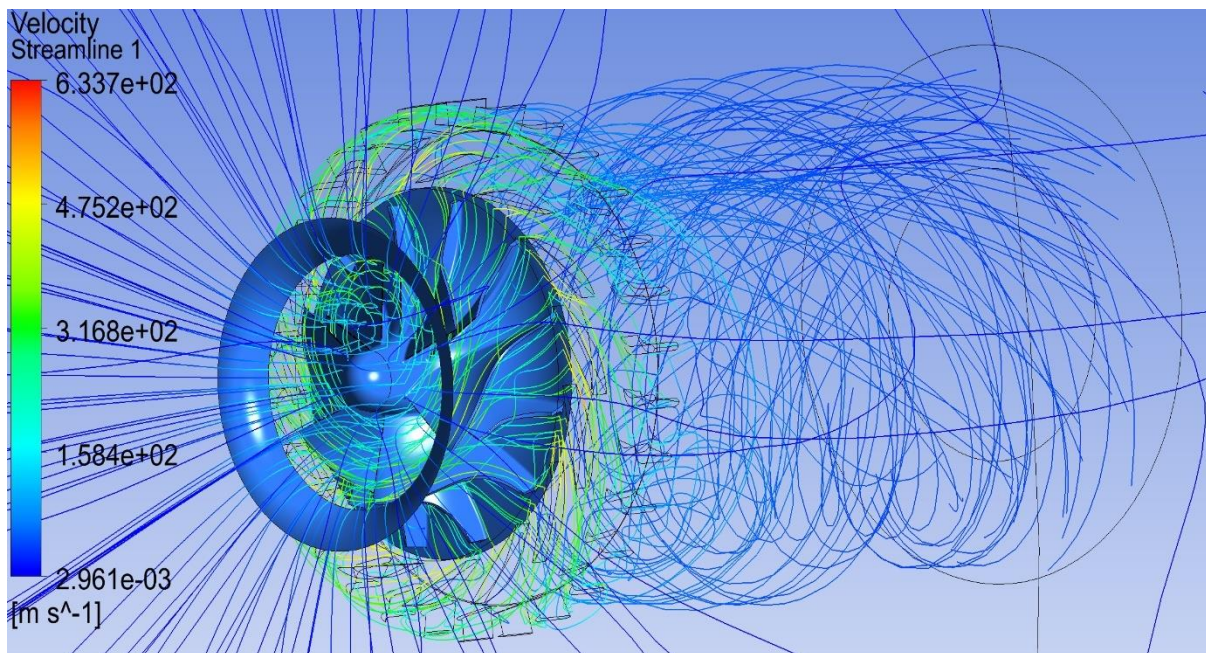
Figure 77: Velocity Streamlines inside the flow domain.

A streamline is defined as a line which is everywhere parallel to the local velocity vector. It can be seen that the streamlines follow a proper path without any backflow. Observing Figures 77 and 78 it is interesting how the impeller centrifuges the streamlines at the outlet, reducing the velocity and increasing the pressure of the flow. The streamlines follow the relative frame of reference inside the impeller.
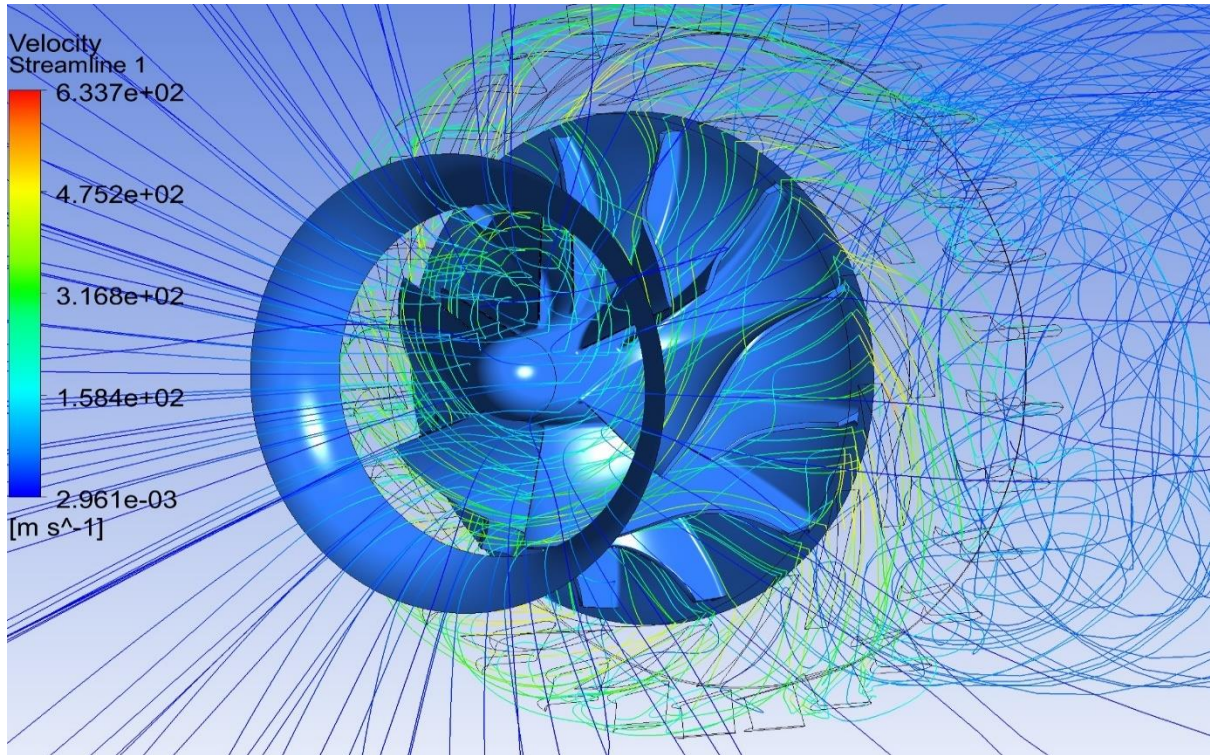
*Figure 78: Closer view of velocity streamlines at the impeller.*
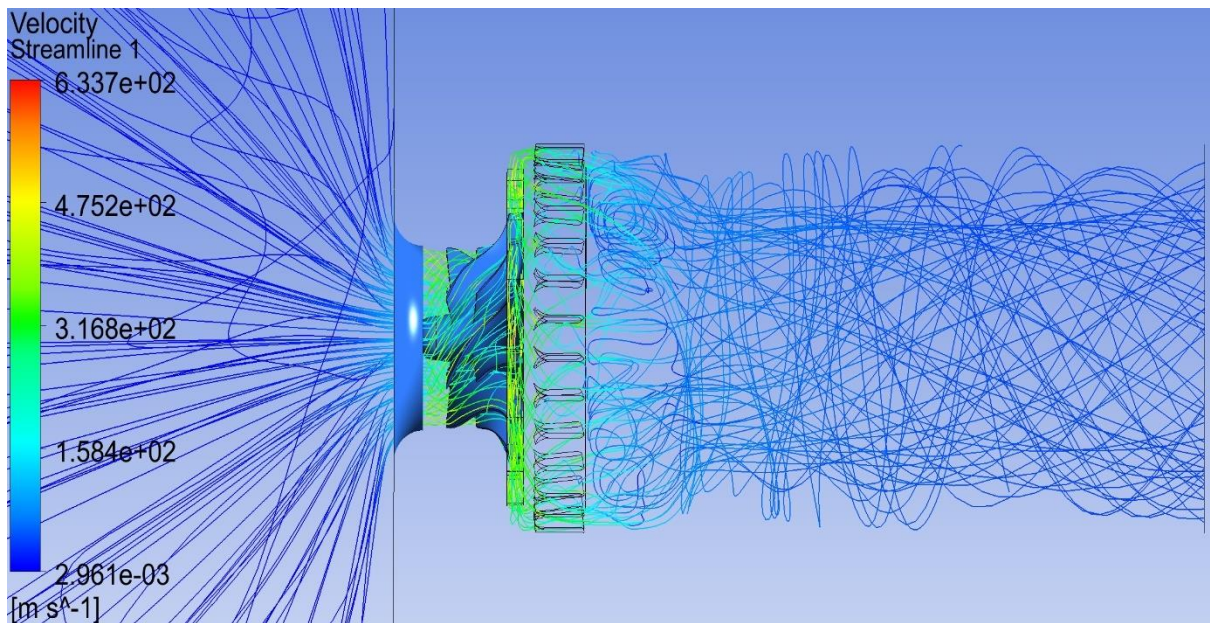
*Figure 79: Velocity streamlines, side view.*
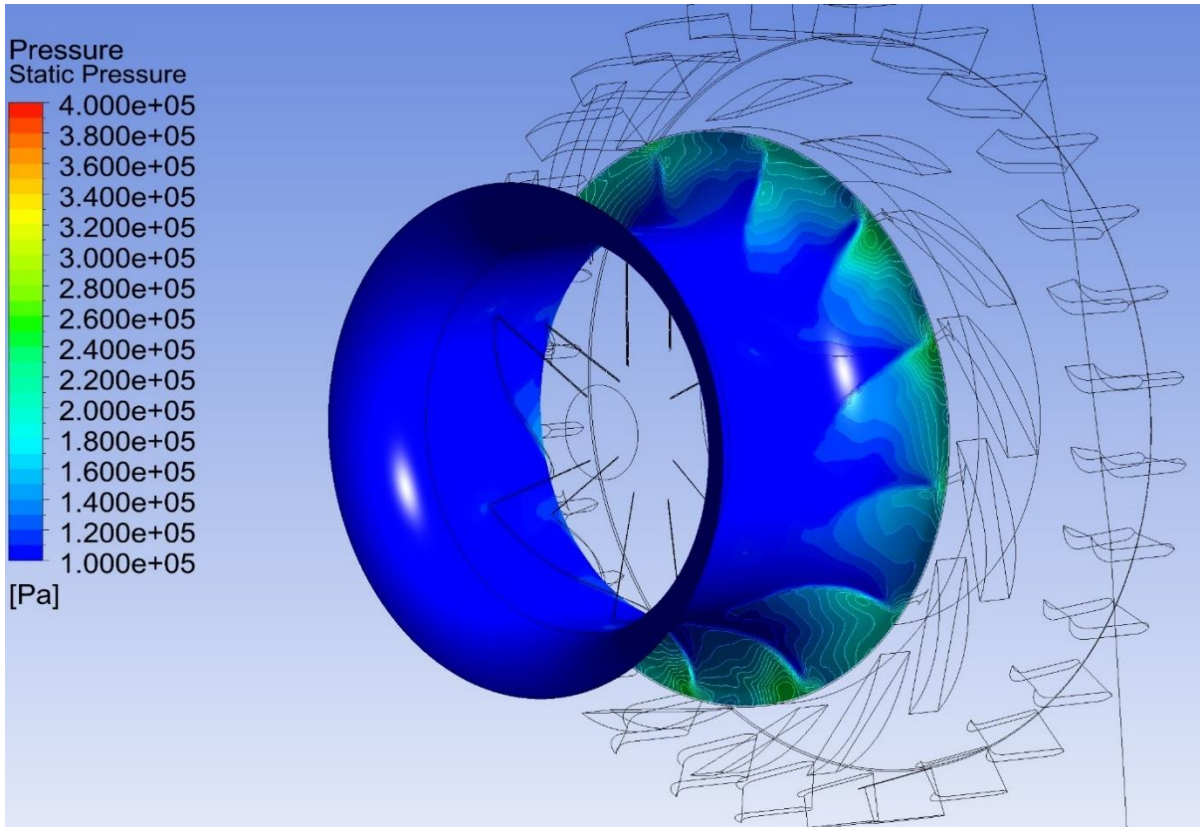
*Figure 80: Static Pressure distribution at the casing of the impeller.*
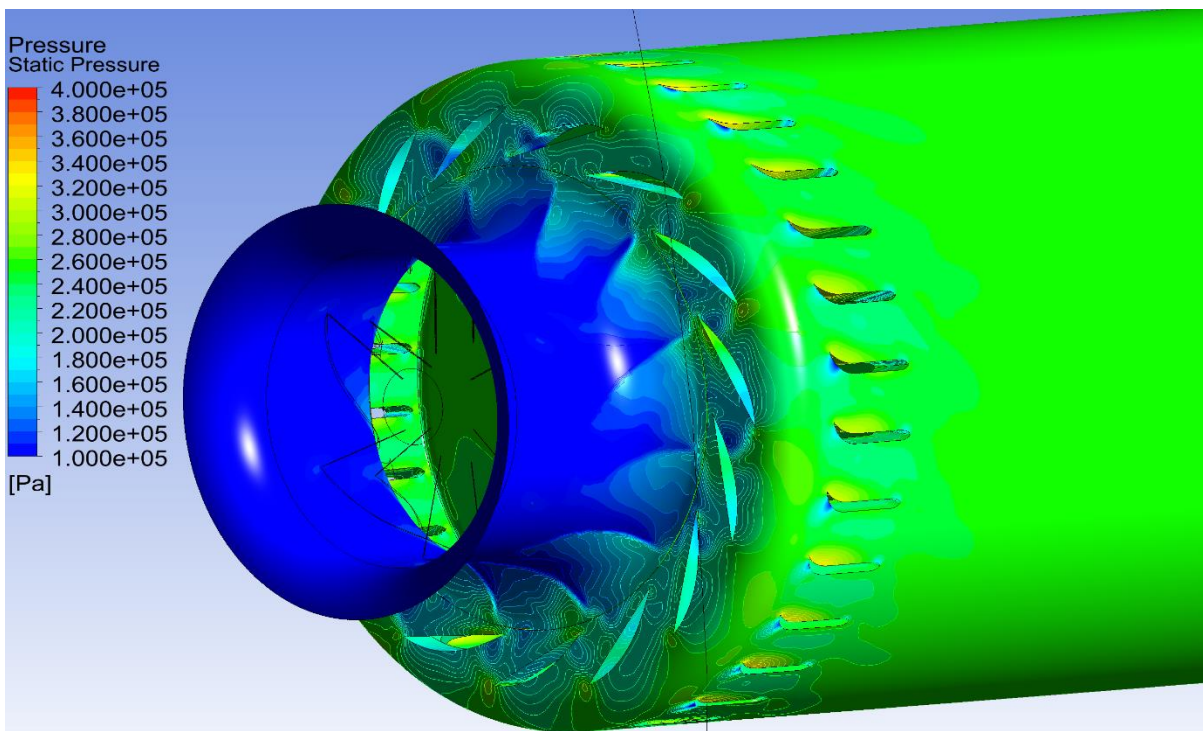

Figure 81: Casing Static Pressure distribution.
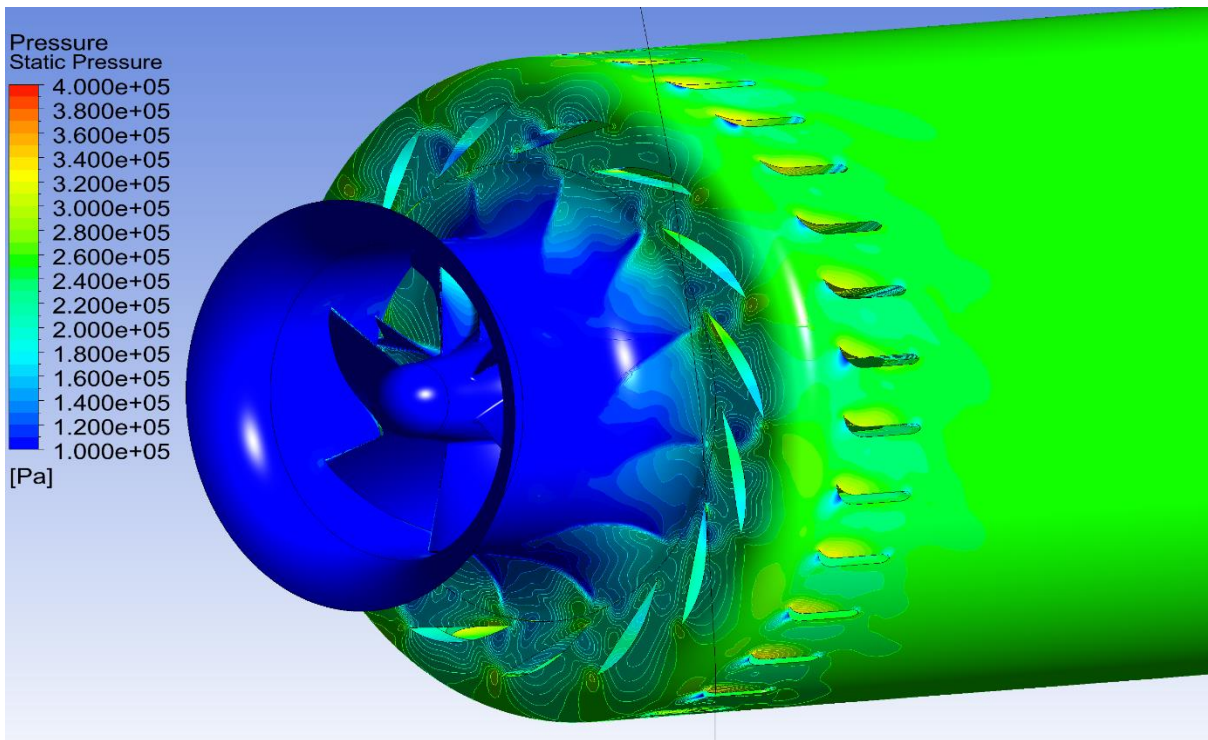
*Figure 82: Static pressure distribution at the casing.*
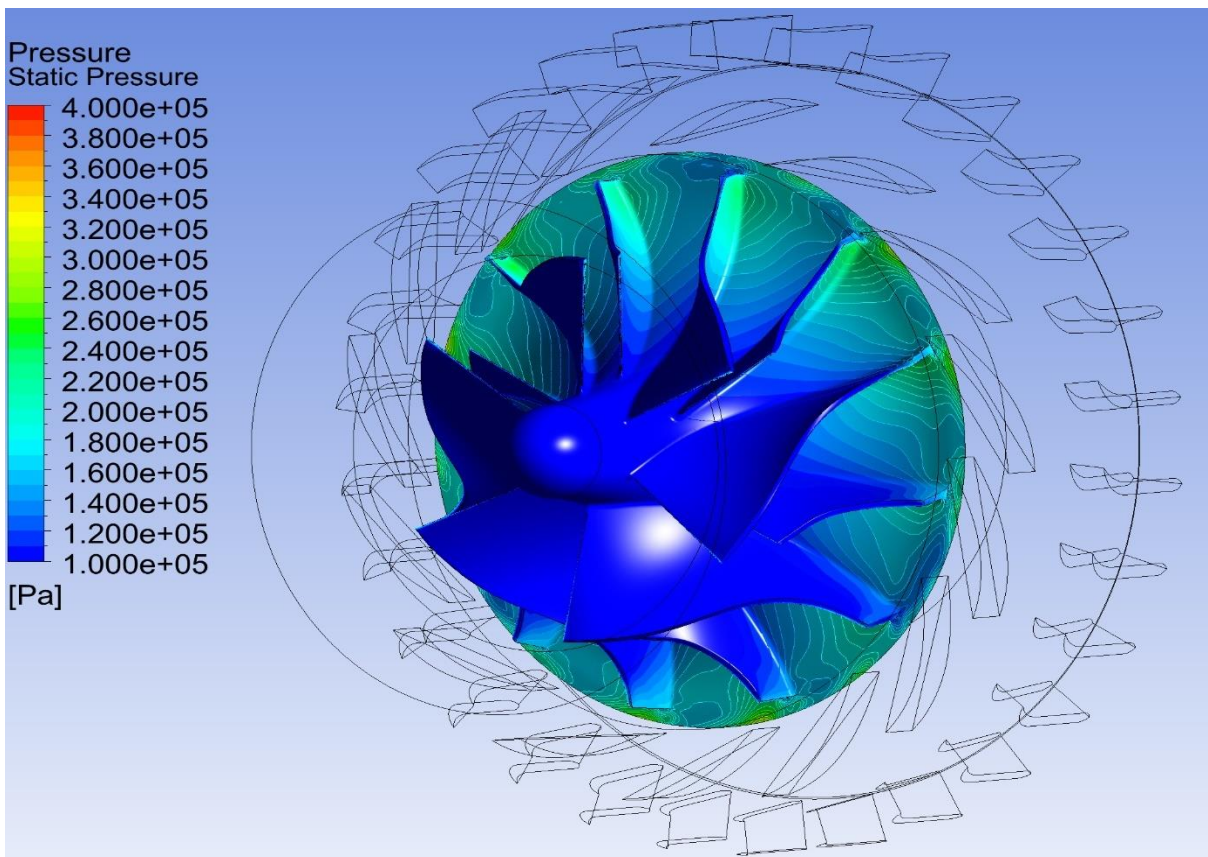
*Figure 83: Impeller static pressure contours.*
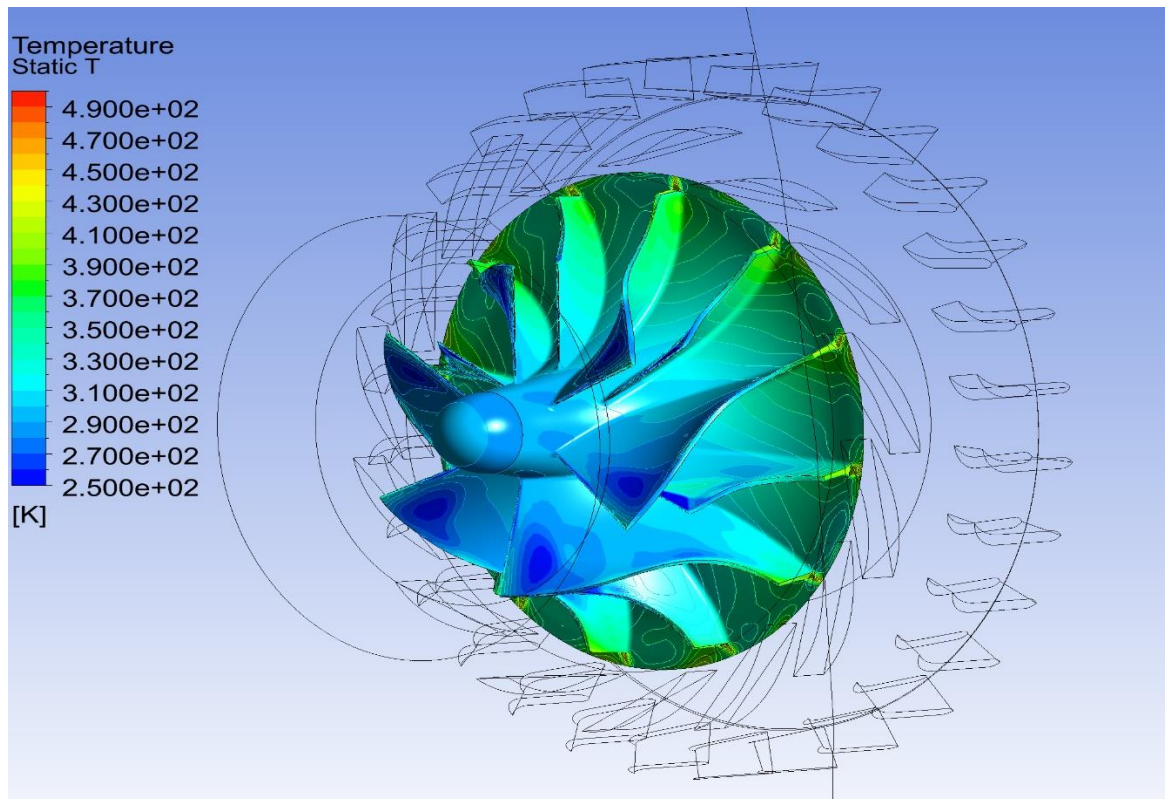
*Figure 84: Static Temperature distribution at the surface of the impeller.*
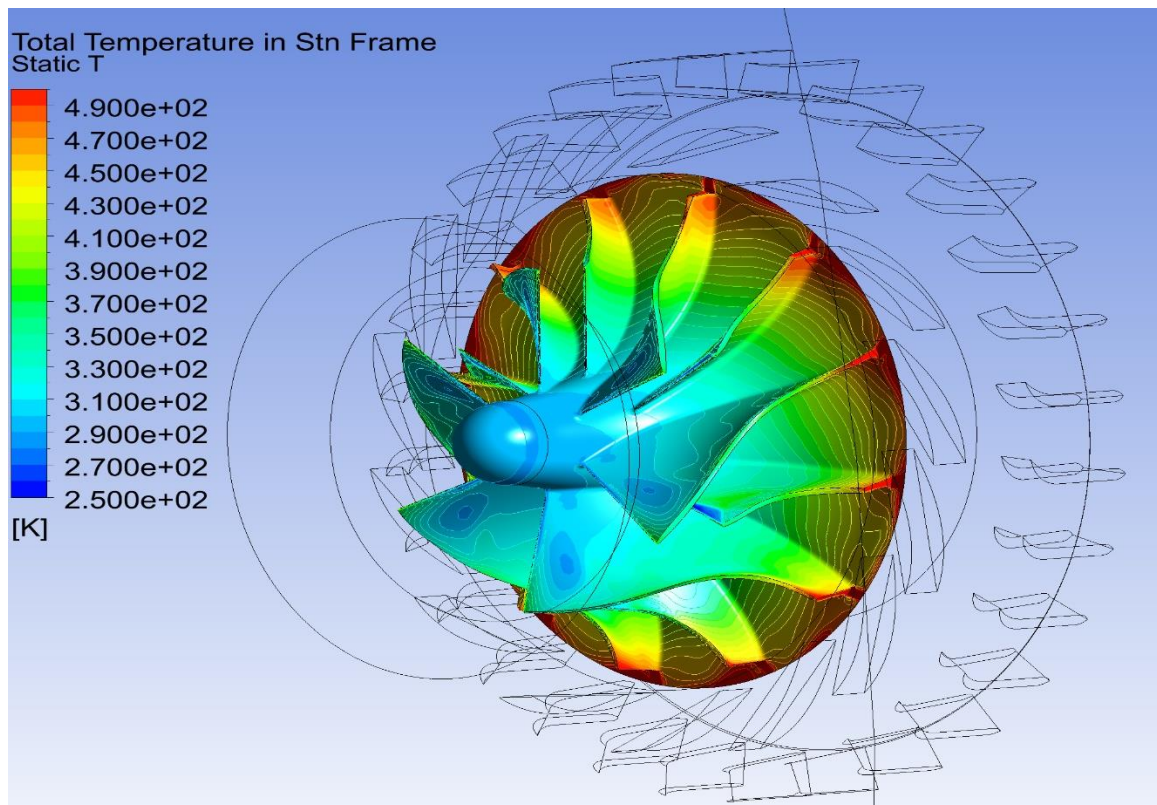
*Figure 85: Total Temperature distribution in the stationary frame of reference.*
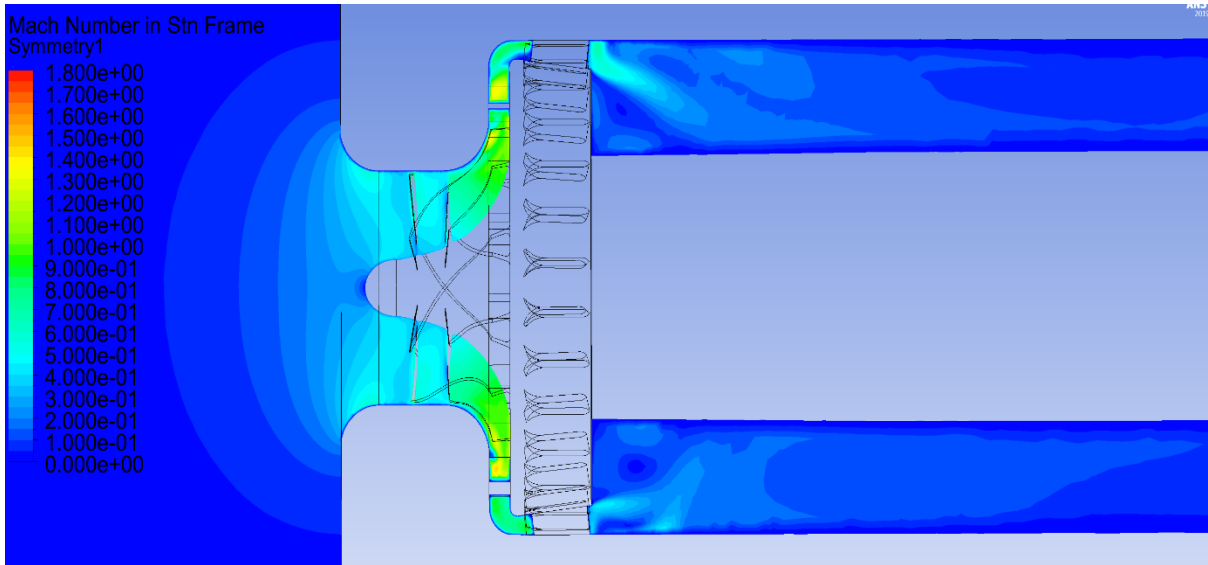
*Figure 86: Mach number contours (Meridional Plane).*
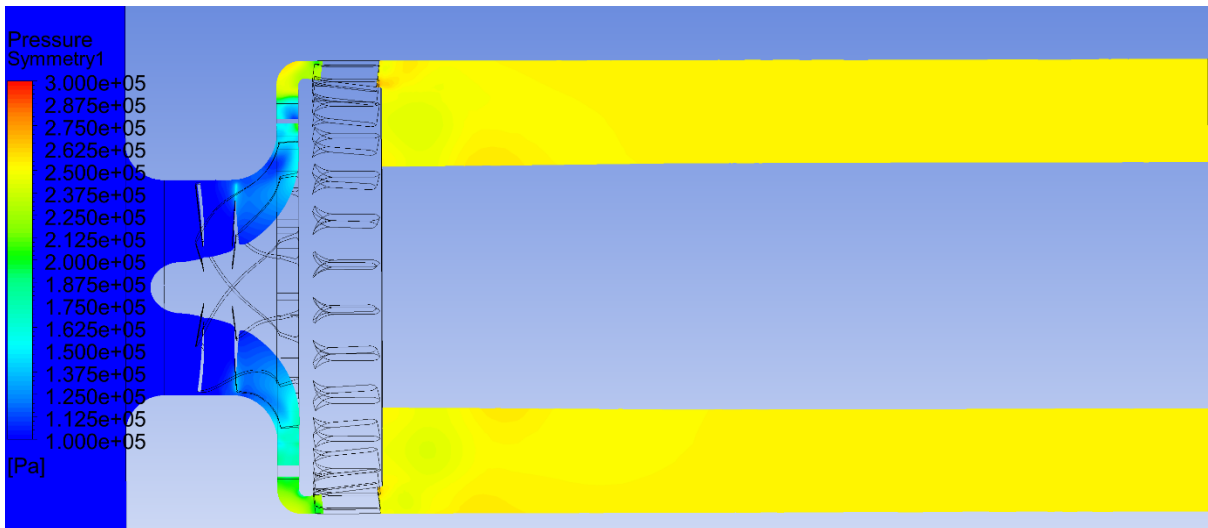
*Figure 87: Pressure distribution (side view – Meridional Plane).*
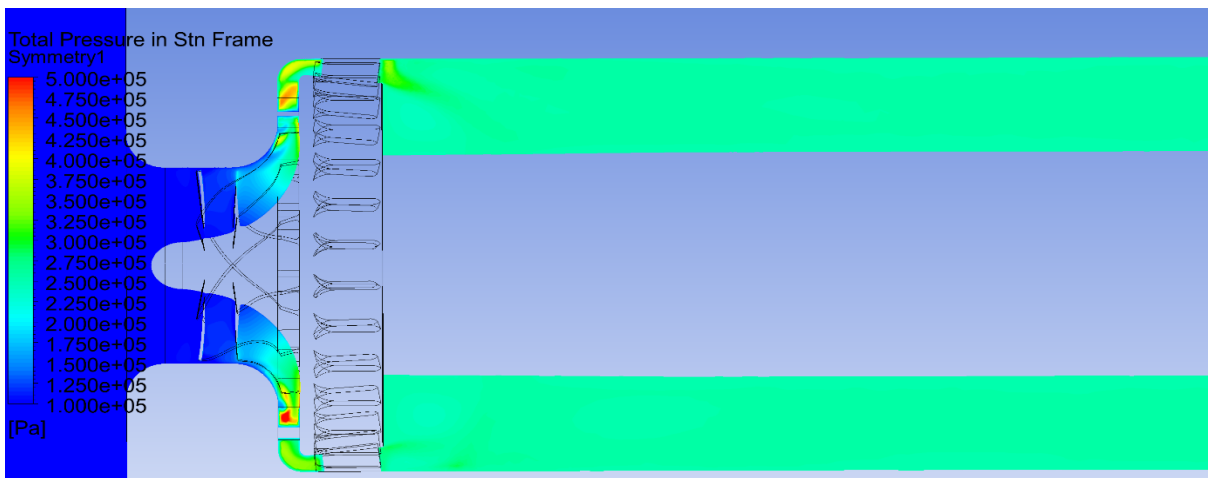
*Figure 88: Total pressure contours (Meridional Plane).*
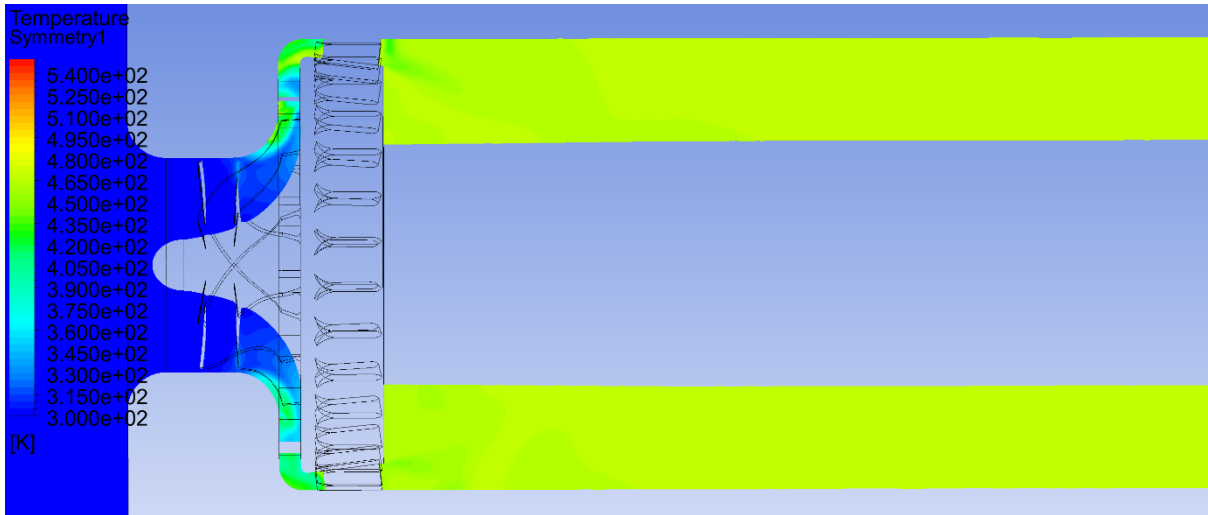
Figure 89: Temperature contours (Meridional Plane).
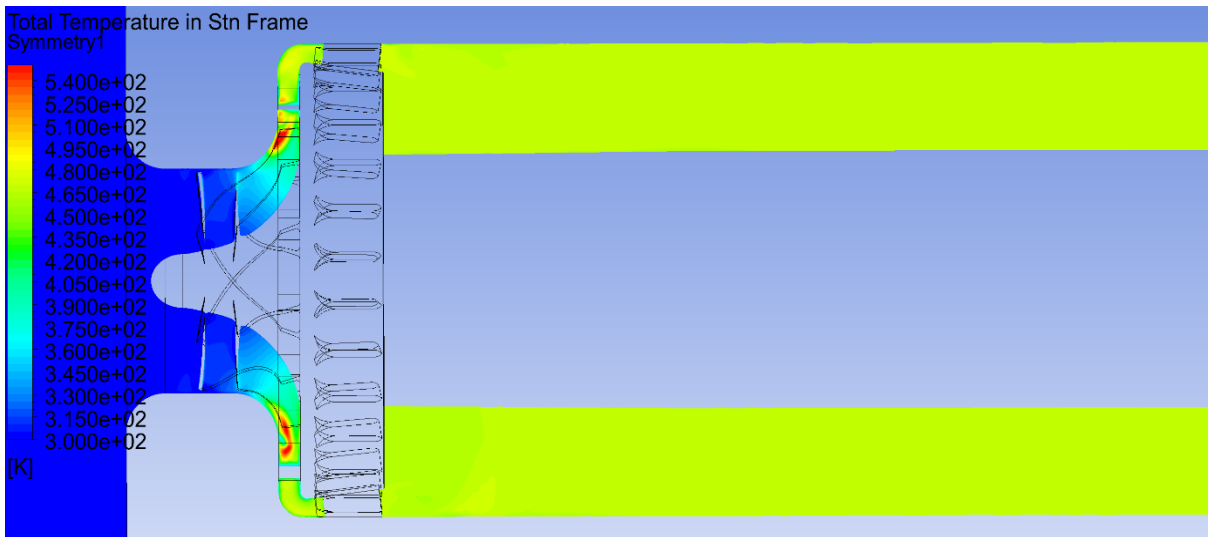

Figure 90: Total temperature contours (Meridional Plane).

In order to show the distribution of pressure and temperature between the hub and the shroud of the diffuser, a cylinder was created with an intermediate radius; the corresponding contours are shown below.
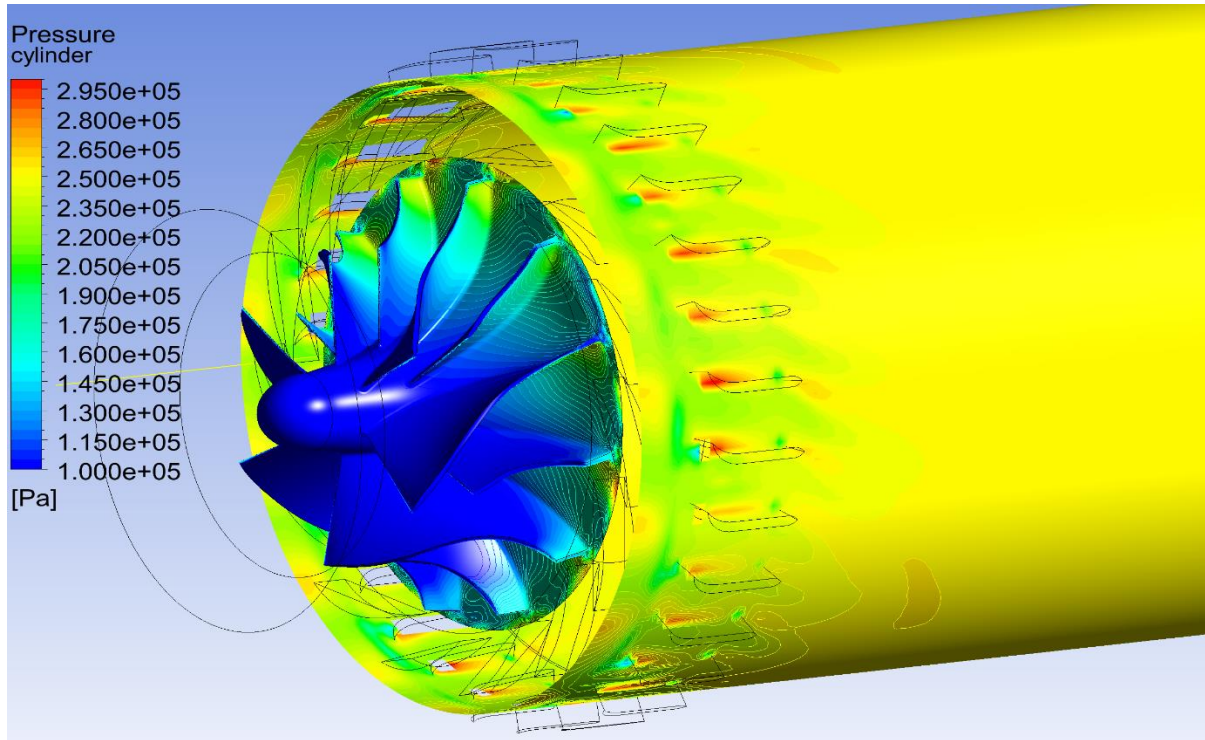

*Figure 91: Static pressure contours (Cylinder).*
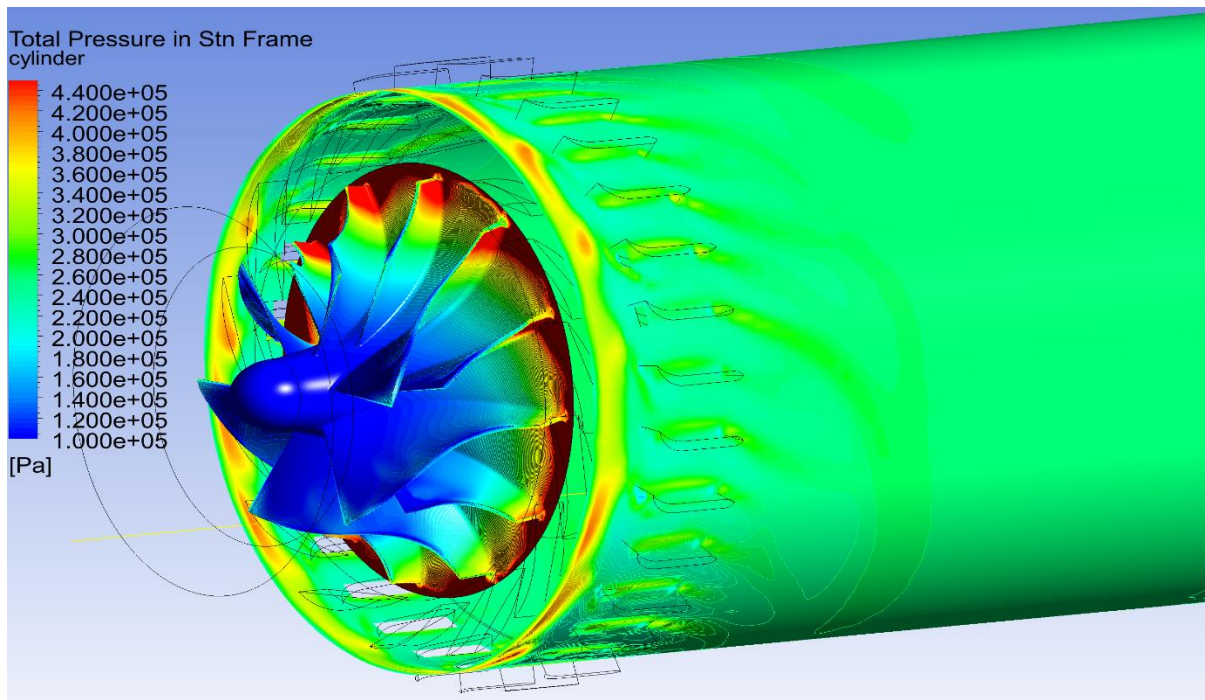
Figure 92: Total pressure contours (Cylinder).
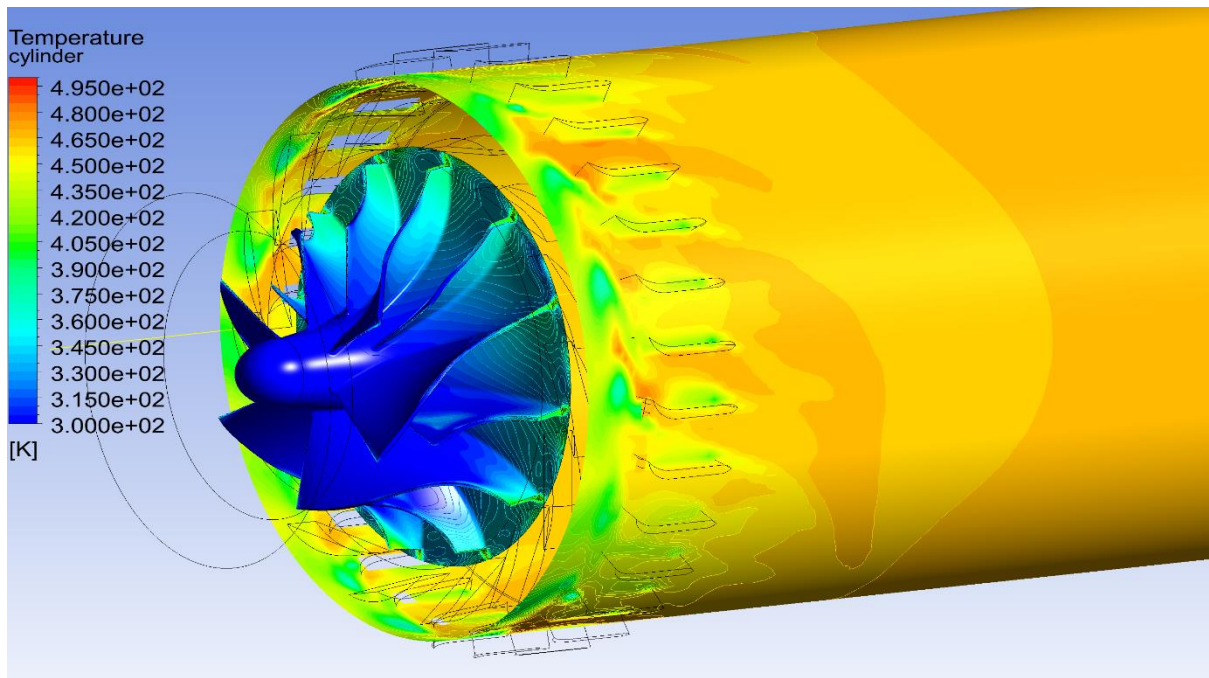
Figure 93: Static temperature contours (Cylinder).
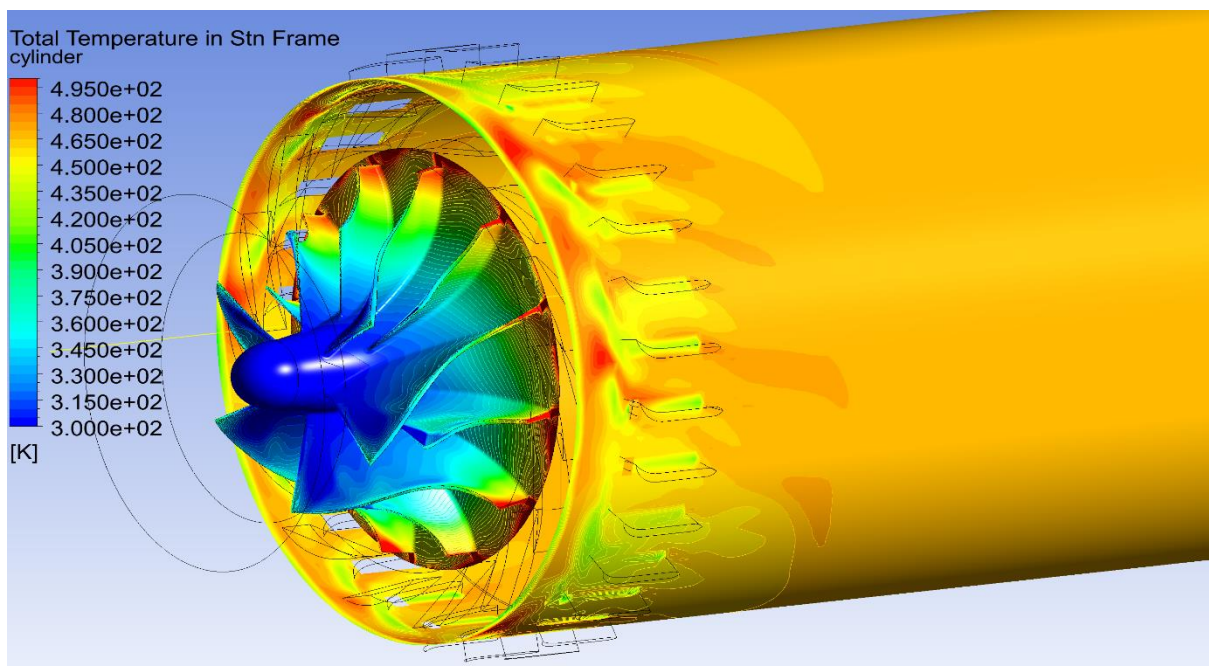
Figure 94: Total temperature contours (Cylinder).

The corresponding results are very rational. The streamlines follow the geometries of the blades (inside the impeller in the rotating reference frame – inside the diffuser in the stationary reference frame). The static and total pressures rise gradually inside the impeller, as it was expected. Increased total pressure losses are observed downstream of the stationary blades inside the diffuser, due to the corresponding boundary layers. The most crucial observation, resulting from the above simulation results is the fact that the diffuser fails to

minimize the swirling flow, downstream to its exit. As a result, the flow enters the combustion chamber with a considerable swirl, which corresponds to lost static pressure and probable problems with the flame in the combustion chamber.

This observation leads to the main outcome of this work; the diffuser should be redesigned, so as to obtain less swirl at its exit. Further investigation is required though, in different rotational speeds, to quantify the extent of the problem.

References

1. J.D. Mattingly, "Elements of Gas Turbine Propulsion", Mc-Graw-Hill, 1996.
2. K. Hünecke, "Jet Engines Fundamentals of Theory, Design and Operation", Zenith Press, 1997.
3. Bakalis D., "Turbomachinery Analysis and Design for Hybrid SOFC-GT Systems-Optimized Performance", Ph.D. Thesis, 2014.
4. Francis Oppong, Sybrand Johan van der Spuy, Theo von Backström, Abdullatif Lacina Diaby, "An Overview of micro gas turbine engine performance investigation", 2017.
5. Garrett Reim, "USAF eyes revolution in small jet turbines", 2019
6. Fabian Fuchs, Vitus Meidinger, Nicolas Neuburger, Thorsten Reiter, Magnus Zündel, Andreas Hupfer, "Challenges in designing very small jet engines – fuel distribution and atomization", 2016
7. E. Benini and S. Giacometti, "Design, manufacturing and operation of a small turbojet-engine for research purposes," Appl. Energy, vol. 84, pp. 1102–1116, 2007.
8. V.Raviteja, T.Kashivishwanath, V.Ashok kumar, N.Venugopal, R.Pavan Kumar, "Design and Fabrication of a Model Jet Engine", vol.5-2015
9. ANSA BETA CAE-Solver Theory Guide
10. Daniel Alonzo, Alex Crocker, Eric James, John Kingston, "Design and Manufacturing of a Miniature Turbojet Engine", MQP 2018.
11. Tatiana Trebunskikh, Andrey Ivanov, Gennady Dumnov, "Small but Mighty Powerful"
12. J. Dutczak, "Micro turbine engines for drones' propulsion", 2016
13. Junting Xiang, Jorg Schluter, "Study of KJ-66 micro gas turbine compressor: Steady and unsteady Reynolds averaged Navier-Stokes approach", 2016
14. Bosman Botha van der Merwe, "Design of a Centrifugal Compressor Impeller for Micro Gas Turbine Application", Faculty of Mechanical and Mechatronic Engineering at Stellenbosch University, 2012.
15. https://www.jetcat.de/de
16. https://minijets.org/en/0-100
17. https://www.marketresearchfuture.com/reports/aircraft-micro-turbine-engines-market-9635
18. https://www.marketsandmarkets.com/Market-Reports/aircraft-micro-turbine-engines-market-248924999.html
19. https://www.braytonenergy.net/our-projects/uav-turbojets-turboprops/
20. http://www.amtjets.com/index.php
21. https://www.kratosdefense.com/
22. https://www.pbs.cz/en/
23. http://www.williams-int.com/
24. http://www.hawkturbine.com/
25. http://www.bf-turbines.de/
26. Joshua A. Hartman, "Design and Fabrication of a Low-Cost Turbine Engine Component Testbed (TECT)", University of Tennessee – Knoxville, 2014.

27. Tamer S. Fathy, Aly M. Elzahaby, and Mohamed K. Khalil, "Micro TJE centrifugal compressor performance prediction", Volume 2_Issue 4_Pages 185-203, 2018.

28. J Dutczak, "Micro turbine engines for drones' propulsion", Institute of Automobiles and Internal Combustion Engines, Cracow University of Technology, 2016.

29. James Large and Apostolos Pesyridis, "Investigation of Micro Gas Turbine Systems for High Speed Long Loiter Tactical Unmanned Air Systems", Department of Mechanical and Aerospace Engineering, Brunel University London, 2019.

30. Description of the AMT Netherlands Olympus HP gas turbine, 2014.

31. Mohseni, A., Goldhahn, E., Van den Braembussche, R., Seume, J.R., "Novel IGV Designs for Centrifugal Compressors and Their Interaction with the Impeller", 2012.

32. http://dma.ing.uniroma1.it/users/paciorri/ansa_for_cfd_brief_user_guide.pdf

33. L. Gibson, L. Galloway, S. I. Kim, and S. Spence, "Assessment of turbulence model predictions for a centrifugal compressor simulation," *Journal of the Global Power and Propulsion Society"*, vol. 1, pp. 142–256, 2017

34. CFD Modelling of a Centrifugal Compressor with Experimental Validation through Radial Diffuser Static Pressure Measurement, Ryoichi Samuel Amano, 2019.